

# JDAT



**Journal of The Dental Association of Thailand**

Volume 75 Number 4 October - December 2025

**[www.jdat.org](http://www.jdat.org)**

ISSN 2730-4280

300um



SCHOOL OF  
DENTISTRY,  
KMITL

The 22<sup>nd</sup> International Scientific Conference  
of The Dental Faculty Consortium of Thailand (DFCT 2025)





วิทยาสารทันตแพทยศาสตร์

ปีที่ 75 ฉบับที่ 4 ตุลาคม - ธันวาคม พ.ศ. 2568 | e-ISSN 2730-4280

# ทันตแพทยสมาคมแห่งประเทศไทย ในพระบรมราชูปถัมภ์

## THE DENTAL ASSOCIATION OF THAILAND

### Advisory Board

Asst. Prof. Anonknart	Bhakdinaronk
Dr. Charmary	Reanamporn
Assoc. Prof. Porjai	Ruangsi
Lt. Gen. Nawarut	Soonthornwit
Dr. Werawat	Satayanurug
Assoc. Prof. Wacharaporn	Tasachan
Dr. Anuchar	Jitjaturunt
Dr. Prinya	Pathomkulmai

### Board of Directors 2025 - 2027

President	Assoc. Prof. Dr. Sirivimol	Srisawasdi
President Elect	Dr. Adirek	Sriwatanawongsa
1 <sup>st</sup> Vice-President	Assoc. Prof. Dr. Nirada	Dhanesuan
2 <sup>nd</sup> Vice-President	Asst. Prof. Dr. Sutee	Suksudaj
Treasurer	Assoc. Prof. Poranee	Berananda
Secretary General	Dr. Chavalit	Karnjanaopaswong
Deputy Secretary General and National Liaison Officer	Lt. Col. Thanasak	Thumbuntu
Chairman of the Foreign Affairs Committee	Asst. Prof. Ekachai	Chunhacheevachaloke
Editor	Dr. Ekamon	Mahapoka
Executive Committee	Clinical Prof. Pusadee	Yotnuengnit
	Assist. Prof. Suchit	Poolthong
	Clinical Prof. Dr. Sirichai	Kiattavorncharoen
	Clinical Prof. Dr. Siriruk	Nakornchai
	Asst. Prof. Piriya	Cherdsatirakul
	Dr. Terdsak	Utasri
	Prof. Dr. Thanaphum	Osathanon
	Dr. Thornkanok	Pruksamas
	Asst. Prof. Taksid	Charasseangpaisarn
	Dr. Adisa	Suthirathikul

# วิทยาสารทันตแพทยศาสตร์

## JOURNAL OF THE DENTAL ASSOCIATION OF THAILAND

**Advisory Board**      Assoc. Prof. Porjai Ruangsri      Assist. Prof. Phanomporn Vanichanon  
                                 Assoc. Prof. Dr. Patita Bhuridej      Prof. Dr. Teerasak Damrongrungruang

**Editor**      Dr. Ekamon Mahapoka

**Associate Editors**      Prof. Dr. Waranun Buajeeb  
                                 Assoc. Prof. Dr. Siriruk Nakornchai  
                                 Assoc. Prof. Dr. Nirada Dhanesuan

### Editorial Board

Assoc. Prof. Dr. Chaiwat Maneenut	(Chulalongkorn University, Thailand)
Assist. Prof. Dr. Yaowaluk Ngoenwiwatkul	(Mahidol University, Thailand)
Prof. Dr. Anak Iamaroon	(Chiang Mai University, Thailand)
Assist. Prof. Dr. Lertrit Sarinnaphakorn	(Chulalongkorn University, Thailand)
Prof. Dr. Suttichai Krisanaprakornkit	(Chiang Mai University, Thailand)
Assoc. Prof. Dr. Somsak Mitirattanakul	(Mahidol University, Thailand)
Assist. Prof. Dr. Ichaya Yiemwattana	(Naresuan University, Thailand)
Prof. Boonlert Kukiattrakoon	(Prince of Songkla University, Thailand)
Assist. Prof. Dr. Chootima Ratisoontom	(Chulalongkorn University, Thailand)
Assoc. Prof. Dr. Oranat Matungkasombut	(Chulalongkorn University, Thailand)
Assist. Prof. Dr. Napapa Aimjirakul	(Srinakharinwirot University, Thailand)
Assist. Prof. Dr. Vanthana Sattabanasuk	(Royal College of Dental Surgeons, Thailand)
Assist. Prof. Dr. Sutee Suksudaj	(Thammasat University, Thailand)
Assoc. Prof. Kajorn Kungsadalpipob	(Chulalongkorn University, Thailand)
Assoc. Prof. Dr. Supatchai Boonpratham	(Mahidol University, Thailand)
Dr. Jaruma Sakdee	(Srinakharinwirot University, Thailand)
Assist. Prof. Dr. Aroonwan Lam-ubol	(Srinakharinwirot University, Thailand)
Prof. Dr. Thantrira Pornraveet	(Chulalongkorn University, Thailand)
Assoc. Prof. Pintu-On Chantarawatit	(Chulalongkorn University, Thailand)
Assoc. Prof. Wannakorn Sriarj	(Chulalongkorn University, Thailand)
Assist. Prof. Dr. Pisha Pittayapat	(Chulalongkorn University, Thailand)
Prof. Dr. Antheunis Versluis	(The University of Tennessee Health Science Center, USA)
Assoc. Prof. Dr. Hiroshi Ogawa	(Niigata University, JAPAN)
Assoc. Prof. Dr. Anwar Merchant	(University of South Carolina, USA)
Dr. Brian Foster	(NIAMS/NIH, USA)
Dr. Ahmed Abbas Mohamed	(University of Warwick, UK)

**Editorial Staff**      Pimpanid Laomana  
                                 Anyamanee Kongcheepa

**Manage**      Assoc. Prof. Poranee Berananda  
                                 Journal published trimonthly. Foreign subscription rate US\$ 200 including postage.  
                                 Publisher and artwork: Rungsilp Printing Co., Ltd  
                                 Please send manuscripts to Dr. Ekamon Mahapoka

**Address:** 71 Ladprao 95 Wangtonglang, Bangkok 10310, Thailand    E-mail: [jdateditor@thaidental.or.th](mailto:jdateditor@thaidental.or.th)

## Instruction for Authors

The Journal of the Dental Association of Thailand (*J DENT ASSOC THAI*) supported by the Dental Association of Thailand, is an online open access and peer-reviewed journal. The journal welcomes for submission on the field of Dentistry and related dental science. We publish 4 issues per year in January, April, July and October.

### » Categories of the Articles «

**1. Review Articles:** a comprehensive article with technical knowledge collected from journals and/or textbooks which is profoundly criticized or analyzed, or tutorial with the scientific writing.

**2. Case Reports:** a clinically report of an update or rare case or case series related to dental field which has been carefully analyzed and criticized with scientific observation.

**3. Original Articles:** a research report which has never been published elsewhere and represent new significant contributions, investigations or observations, with appropriate experimental design and statistical analysis in the filed of dentistry.

### » Manuscript Submission «

The Journal of the Dental Association of Thailand welcome submissions from the field of dentistry and related dental science through only online submission. The manuscript must be submitted via <http://www.jdat.org>. Registration by corresponding author is once required for the article's submission. We accept articles written in both English and Thai. However, for Thai article, English abstract is required whereas for English article, there is no need for Thai abstract submission. The main manuscript should be submitted as .doc (word97-2003). All figures, and tables should be submitted as separated files (1 file for each figure or table). For the acceptable file formats and resolution of image will be mentioned in 8. of manuscript preparation section.

### » Scope of Article «

Journal of Dental association of Thailand (JDAT) is a quarterly peer-reviewed scientific dental journal aims to the dissemination and publication of new knowledges and researches including all field of dentistry and related dental sciences

### » Manuscript Preparation «

1. For English article, use font to TH Sarabun New Style size 14 in a standard A4 paper (21.2 x 29.7 cm) with 2.5 cm margin on a four sides. The manuscript should be typewritten.

2. For Thai article, use font of TH Sarabun New Style size 14 in a standard A4 paper (21.2 x 29.7 cm) with 2.5 cm margin on a four sides. The manuscript should be typewritten

with 1.5 line spacing. Thai article must also provide English abstract. All reference must be in English. For the article written in Thai, please visit the Royal Institute of Thailand (<http://www.royin.go.th>) for the assigned Thai medical and technical terms. The original English words must be put in the parenthesis mentioned at the first time.

3. Numbers of page must be placed on the top right corner. The length of article should be 10-12 pages including the maximum of 5 figures, 5 tables and 40 references for original articles. (The numbers of references are not limited for review article).

4. Measurement units such as length, height, weight, capacity etc. should be in metric units. Temperature should be in degree Celsius. Pressure units should be in mmHg. The hematologic measurement and clinical chemistry should follow International System Units or SI.

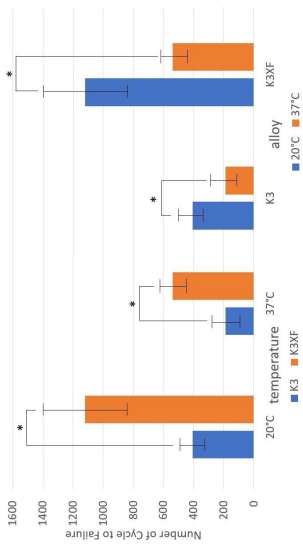
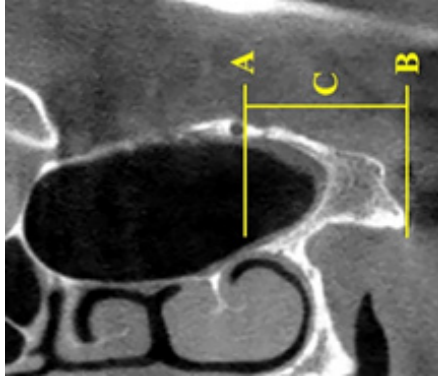

5. Standard abbreviation must be used for abbreviation and symbols. The abbreviation should not be used in the title and abstract. Full words of the abbreviation should be referred at the end of the first abbreviation in the content except the standard measurement units.

6. Position of the teeth may use full proper name such as maxillary right canine of symbols according to FDI two-digit notation and write full name in the parenthesis after the first mention such as tooth 31 (mandibular left central incisor)

7. Table: should be typed on separate sheets and number consecutively with the Arabic numbers. Table should self-explanatory and include a brief descriptive title. Footnotes to tables indicated by lower-case superscript letters are acceptable.

8. Figure : the photographs and figures must be clearly illustrated with legend and must have a high resolution and acceptable file types to meet technical evaluation of JDAT that is adapted from file submissions specifications of Pubmed (<https://www.ncbi.nlm.nih.gov/pmc/pub/filespec-images/#int-disp>). We classify type of figure as 3 types following: line art, halftones and combo (line art and halftone combinations) The details of description, required format, color mode and resolution requirement are given in table below.

Numbers, letters and symbols must be clear and even throughout which used in Arabic form and limited as necessary. During the submission process, all photos and tables must be submitted in the separate files. Once the manuscript is accepted, an author may be requested to resubmit the high quality photos.

Image type	Description	Example	Recommended format	Color mode	Resolution
Line art	An image which is composed of line and text and is not contained of tonal or shading areas.		tif. of eps.	Monochrome 1-bit of RGB	900-1200 dpi
Half tone	A continuous tone photograph which does not compose of text.		tif.	RGB of Grayscale	300 dpi
Combo	Combination of line art and half tone.		tif. of eps.	RGB of Grayscale	500-900 dpi

## » Contact Address «

### Editorial Staff of JDAT

The Dental Association of Thailand

71 Ladprao 95, Wangtonglang, Bangkok 10310, Thailand.

Email: [jdateditor@thaidental.or.th](mailto:jdateditor@thaidental.or.th) Tel: +669-7007-0341

## » Preparation of the Research Articles «

### 1. Title Page

The first page of the article should contain the following information

- Category of the manuscript
- Article title
- Authors' names and affiliated institutions
- Author's details (name, mailing address, E-mail, telephone and FAX number)

### 2. Abstract

The abstract must be typed in only paragraph. Only English abstract is required for English article. Both English and Thai abstract are required for Thai article and put in separate pages. The abstract should contain title, objectives, methods, results and conclusion continuously without heading on each section. Do not refer any documents, illustrations or tables in the abstract. The teeth must be written by its proper name not by symbol. Do not use English words in Thai abstract but translate or transliterate it into Thai words and do not put the original words in the parenthesis. English abstract must not exceed 300 words. Key words (3-5 words) are written at the end of the abstract in alphabetical order with comma (,) in-between.

### 3. Text

The text of the original articles should be organized in section as follows

- **Introduction:** indicates reasons or importances of the research, objectives, scope of the study. Introduction should review new documents in order to show the correlation of the contents in the article and original knowledge. It must also clearly indicate the hypothesis.

- **Materials and Methods:** indicate details of materials and methods used in the study for readers to be able to repeat such as chemical product names, types of experimental animals, details of patients including sources, sex, age etc. It must also indicate name, type, specification, and other information of materials for each method. For a research report performed in human subjects, human material samples, human participants and animal samples, authors should indicate that the study was performed according to the Experiment involving human or animal subjects such as Declaration of Helsinki 2000, available at: <https://www.wma.net/what-we-do/medical-ethics/declaration-of-helsinki/doh-oct2000/>, or has been approved by

the ethic committees of each institute (\*ethic number is required).

- **Results:** Results are presentation of the discovery of experiment or researches. It should be categorized and related to the objectives of the articles. The results can be presented in various forms such as words, tables, graphs of illustrations etc. Avoid repeating the results both untables and in paragraph =. Emphasize only important issues.

- **Discussion:** The topics to be discussed include the objectives of the study, advantages and disadvantages of materials and methods. However, the important points to be especially considered are the experimental results compared directly with the concerned experimental study. It should indicate the new discovery and/or important issues including the conclusion from the study. New suggestion problems and informed in the discussion and indicate the ways to make good use of the results.

- **Conclusion:** indicates the brief results and the conclusion of the analysis.

- **Acknowledge:** indicates the institute or persons helping the authors, especially on capital sources of researches and numbers of research funds (if any).

- **Conflicts of interest :** for the transparency and helping the reviewers assess any potential bias. JDAT requires all authors to declare any competing commercial interests in conjunction with the submitted work.

- **Reference:** include every concerned document that the authors referred in the articles. Names of the journals must be abbreviated according to the journal name lists in "Index Medicus" published annually of from the website <http://www.nlm.nih.gov>

### » Writing the References «

The references of both Thai and English articles must be written only in English. Reference system must be Vancouver reference style using Arabic numbers, making order according to the texts chronologically. Titles of the Journal must be in Bold and Italics. The publication year, issue and pages are listed respectively without volume.

### Sample of references from articles in Journals

#### - Authors

Zhao Y, Zhu J: *In vivo* color measurement of 410 maxillary anterior teeth. *Chin J Dent Res* 1998;1(3):49-51.

#### - Institutional authors

Council in Dental Materials and Devices. New American Dental Association Specification No.27 for direct filling resins. *J Am Dent Assoc* 1977;94(6):1191-4

#### - No author

Cancer in South Africa [editorial]. *S Afr Med J* 1994;84:15

## Sample of references from books and other monographs

### - Authors being writers

Neville BW, Damn DD, Allen CM, Bouquot JE. Oral and maxillofacial pathology. Philadelphia: WB Saunders; 1995. P. 17-20

### - Authors being both writer and editor

Norman IJ, Redfern SJ, editors. Mental health care for the elderly people. New York: Churchill Livingstone; 1996.

### - Books with authors for each separate chapter

### - Books with authors for each separate chapter

## and also have editor

Sanders BJ, Handerson HZ, Avery DR. Pit and fissure sealants; In: McDonald RE, Avery DR, editors. Dentistry for the child and adolescent. 7th ed. St Louis: Mosby; 2000. P. 373-83.

### - Institutional authors

International Organization for Standardization. ISO/TR 11405 Dental materials-Guidance on testing of adhesion to tooth structure. Geneva: ISO; 1994.

## Samples of references from academic conferences

### - Conference proceedings

Kimura J, Shibasaki H, editors. R The Journal of the Dental Association of Thailand (JDAT): (ISSN 2408-1434) online open access and double-blind peer review journal and also supported by the Dental Association of Thailand advances in clinical neurophysiology. Proceeding of the 10th International Congress of EMG and Clinical Neurophysiology; 1995 Oct 15-19; Kyoto, Japan. Amsterdam; Elsevier; 1996.

### - Conference paper

Hotz PR. Dental plaque control and caries. In: Lang PN, Attstrom R, Loe H, editors. Proceedings of the European Work shop on Mechanical Plaque Control; 1998 May 9-12; Berne, Switzerland. Chicago: Quintessence Publishing; 1998. p. 25-49.

### - Documents from scientific or technical reports

Fluoride and human health. WHO Monograph; 1970. Series no.59.

## Samples of reference from thesis

Muandmingsuk A. The adhesion of a composite resin to etched enamel of young and old teeth [dissertation]. Texas: The University of Texas, Dental Branch at Houston; 1974.

## Samples of reference from these articles are only accepted in electronic format

### - Online-only Article (With doi (digital identification object number))

Rasperini G, Acunzo R, Limioli E. Decision making in gingival rec experience. *Clin Adv Periodontics* 2011;1: 41-52. doi:10.1902 cap.2011.1000002.

### - Online only article (without doi)

Aboud S. Quality improvement initiative in nursing homes: the ANA acts in an advisory role. *Am J Nurs* 2002; 102(6)[cited 2002 Aug 12] Available from: <http://nursingworld.org/AJN/2002/june/WaWatch.htmArticle>

## Samples of references from patents/petty patents

### - Patent

Pagedas AC, inventor; Ancel Surgical R&D Inc., assignee. Flexible endoscopic grasping and cutting device and positioning tool assembly. United States patent US 20020103498. 2002 Aug 1.

### - Petty patent

Priprem A, inventor, Khon Kaen University. Sunscreen gel and its manufacturing process. Thailand petty patent TH1003001008. 2010 Sep 20.

## » Preparation of the Review articles and Case reports «

Review articles and case reports should follow the same format with separate pages for abstract, introduction, discussion, conclusion, acknowledgement and references.

## » The Editorial and Peer Review Process «

The submitted manuscript will be reviewed by at least 2 qualified experts in the respective fields. In general, this process takes around 4-8 weeks before the author be noticed whether the submitted article is accepted for publication, rejected, or subject to revision before acceptance.

The author should realize the importance of correct format manuscript, which would affect the duration of the review process and the acceptance of the articles. The Editorial office will not accept a submission if the author has not supplied all parts of the manuscript as outlined in this document.

## » Copyright «

Upon acceptance, copyright of the manuscript must be transferred to the Dental Association of Thailand.

PDF files of the articles are available at <http://www.jdat.org>

**Publication fee for journals:** Free for Black and white printing this article. The price of color printing is extra charged 10,000 bath/article/1,500 copy (vat included).

Note: Color printing of selected article is considered by editorial board. (no extra charge)

» Updated January, 2024 «



## Contents

VOL.75 NO.4 OCTOBER - DECEMBER 2025

### Review Article

- Masticatory Performance After Orthodontic Treatment** 194  
Chookiat Wachiralarpphathoon  
Pongthep Somsriphang

### Original Article

- Anatomical Study of the Mandibular Canal in Thai Patients with Mandibular Prognathism: Implications for BSSRO** 207  
Sappasith Panya  
Thitirat Tungtorsakul  
Natnisha Arkarapattarawong  
Parintorn Sutthiprapa  
Puthita Leewisutthikul  
Keskanya Subbalekha
- Inflammatory Response and Proliferation of Stem Cells Isolated from Human Exfoliated Deciduous Teeth to Lipopolysaccharide from *Porphyromonas Gingivalis*** 216  
Panicha Sroithong  
Waleerat Sukarawan  
Thanaphum Osathanon
- The Effect of Powered Toothbrushes on Surface Roughness and Wear of Direct Restorative Materials** 224  
Sookwasa Hirunmekavanich  
Chaiwat Maneenut
- FTIR Spectroscopic Comparison of Fish Scale Collagen and Acemannan-Modified Porcine Collagen for Oral Mucosal Scaffolds** 238  
Orakarn Kanwiwatthanakun  
Utaisar Chunmanus  
Ratsa Sripirom  
Pasutha Thunyakitoisal
- Implant Stability in the Era of Digital Dentistry: Comparing Traditional and Technology-Enhanced Surgical Methods** 249  
Myo Thiri Win  
Sirida Arunjarosuk  
Atiphan Pimkhaokham  
Boosana Kaboosaya

## Contents

VOL.75 NO.4 OCTOBER - DECEMBER 2025

### Original Article

- Manufacturing Method and Build Orientation Influence Alkali-Heat Treated Titanium (Ti-6Al-4V) Dental Implant Surface Characteristics** 257  
Tuan Hoang Nguyen  
Phetcharat Dhammayannarangsi  
Viritpon Srimaneepong  
Patcharapit Promoppatum  
Chalida Nakalekha Limjeerajarus  
Nuttapol Limjeerajarus
- Biodentine™ and MAC28 Inhibit Lipopolysaccharides-Induced Pulpal Inflammation in Human Dental Pulp Cells** 266  
Witsuta Pongphaladisai  
Sitthikorn Kunawarote  
Guang Liang  
Siriporn C. Chattipakorn  
Savitri Vaseenon
- Effect of Lemongrass Essential Oil on *Candida albicans*-infected Raw 264.7 Macrophages: An *In Vitro* Study** 274  
Myat Thiri  
Matsayapan Pudla  
Suwan Choonharuangdej
- Author index** 280

#### Front cover image:

adapted from Figure 1 Characterization of the cells isolated from dental pulp tissues. (a) Cell morphology of isolated cells from primary teeth exhibited a spindle-like morphology under phase-contrast microscopy (left) (scale bar at 4X = 300  $\mu$ m.) and colony forming unit ability (right). (b) Presence of mesenchymal stem cell markers CD44 and CD90 by flow cytometric analysis, and the absence of the hematopoietic marker CD45. (black line: negative control) (c) The osteogenic differentiation was examined using alkaline phosphatase on day 7, Alizarin Red S and Von Kossa staining on day 14 after osteogenic induction (Scale bar at 4X = 300  $\mu$ m.) (see *Sroithong et al.*, page 219 for detail)

# Masticatory Performance After Orthodontic Treatment

Chookiat Wachiralarpphaithoon<sup>1</sup> and Pongthep Somsriphang<sup>1</sup>

<sup>1</sup>Department of Masticatory Science, Faculty of Dentistry, Mahidol University, Bangkok

## Abstract

Orthodontic treatment aims to enhance dental aesthetics and functionality. Its impact on masticatory performance, which encompasses the efficiency and effectiveness of chewing, remains an important area of study. Factors influencing masticatory performance include dental alignment, occlusal contact, and muscular coordination. This review aims to summarize both the relationship between masticatory performance after orthodontic treatment and the commonly used methods for measuring masticatory performance following orthodontic treatment. A systematic search of electronic databases (PubMed [including MEDLINE] and Scopus) was conducted for studies published from January 2000 up to May 2024, focusing on masticatory performance in patients undergoing orthodontic treatment. Studies were selected based on predefined eligibility criteria, data on study characteristics, orthodontic interventions, masticatory assessment methods, and key findings regarding masticatory changes that were extracted. Out of 797 records identified, 13 studies met the inclusion criteria. These studies evaluated masticatory performance before and after orthodontic treatment using both subjective and objective measurements, with maximum bite force and occlusal contact area being the most used methods. The review found that non-extraction orthodontic treatment generally improved masticatory performance, as evidenced by comminution tests and self-reported ability, although performance still lagged behind natural occlusion post-treatment. Extraction orthodontic treatment presented mixed results, with lower masticatory performance in the early retention phase that gradually increased, ultimately showing no significant differences in occlusal contact area or force between extraction and non-extraction groups over time. Orthognathic surgery enhanced masticatory function, but it still did not reach the levels observed in individuals with natural occlusion, despite improvements in bite force and occlusal contact area over time. Overall, non-extraction treatment showed improvements but remained inferior to controls, while extraction treatment had variable outcomes and orthognathic surgery improved function but fell short of natural occlusion.

**Keywords:** Chewing performance, Extraction, Malocclusion, Masticatory performance, Non-extraction, Orthodontic treatment, Orthognathic surgery

Received date: Jan 27, 2025

Revised date: May 20, 2025

Accepted date: Jul 3, 2025

Doi: 10.14456/jdat.2025.20

## Correspondence to:

Chookiat Wachiralarpphaithoon. Department of Masticatory Science, Faculty of Dentistry, Mahidol University, 6 Yothi road., Ratchathewi, Bangkok, 10400 Thailand Tel: 02-200-7856, 02-200-7857 ext 0 Email: Chookiat.wac@mahidol.ac.th.

## Introduction

Orthodontic treatment primarily focuses on correcting dentofacial abnormalities to improve dental

aesthetics and occlusal function (Proffit *et al.*, 2013). A key area of interest in research is the impact of orthodontic



treatment on masticatory performance—the efficiency and effectiveness of chewing, which plays a crucial role in oral function and overall health.<sup>1</sup>

Masticatory performance refers to the ability to effectively break down and process food during chewing. Optimal chewing function relies on a complex interaction of factors, such as dental occlusion, tooth positioning, jaw movement, and neuromuscular coordination. Malocclusions, or misalignments of the teeth and jaws, can negatively impact masticatory efficiency by disrupting the smooth coordination of these factors, making chewing less effective.<sup>2</sup>

The relationship between orthodontic treatment and masticatory performance has been the subject of extensive research efforts, yielding a diverse array of findings. While some studies suggest that orthodontic interventions can improve masticatory function by correcting malocclusions and optimizing dental occlusion, others indicate that the presence of orthodontic appliances or the initial stages of treatment may temporarily impair chewing efficiency due to factors such as dental discomfort, altered occlusal contacts, and neuromuscular adaptations.<sup>4</sup>

Investigating the impact of orthodontic interventions on masticatory performance is crucial for both clinicians and patients. From a clinical perspective, understanding these effects helps guide treatment decisions, patient counseling, and the implementation of strategies to minimize any potential negative impacts on chewing function during treatment. For patients, being informed about these potential effects can help set realistic treatment goals and encourage necessary dietary or behavioral adjustments throughout the treatment process.<sup>3</sup>

This review aims to investigate the relationship between masticatory performance after orthodontic treatment and determine the most used measure of masticatory performance after orthodontic treatment.

## 1. Masticatory performance

Masticatory performance refers to the efficiency and effectiveness of the chewing process, which is critical for breaking food into smaller, more digestible particles. This ability can be measured using various methods, each designed to quantify different aspects of the masticatory process. One common approach is to assess an individual's

capacity to comminute a standardized test food, such as almonds, or artificial materials like chewing gum or paraffin wax. These methods involve evaluating the particle size distribution after a set number of chewing cycles, thereby providing an objective measure of masticatory performance.<sup>5,6</sup>

In other words, masticatory performance refers to the individual's ability to grind a specimen of test food after a predetermined number of mastication cycles. While masticatory efficiency refers to the number of chewing cycles necessary to attain half the original particle size.<sup>7-9</sup>

## 2. Assessment of masticatory performance

This assessment typically involves measuring the ability to break down food, the number of chewing cycles, and the time taken to achieve a specific degree of food fragmentation. Methods include the use of artificial test foods, such as silicone-based particles or chewing gums, and natural foods like almonds or carrots. Objective measurements may involve particle size analysis through sieving or image processing, while subjective evaluations might include patient questionnaires on chewing ability and comfort. Factors influencing masticatory performance include dental status, occlusal patterns, muscle function, and the use of prosthetic appliances.<sup>10</sup>

Masticatory performance assessment refers to evaluating the outcome of the mastication process using various methodologies and techniques. The consensus paper outlines two primary approaches:

### 2.1 Objective assessment

Comminution tests: These involve chewing brittle food (e.g., nuts, raw carrots) for a predetermined number of cycles, followed by sieving or optical scanning of the chewed particles to analyze their size distribution.

Mixing ability tests: These use non-nutritive materials like two-colored chewing gum or wax, chewed for a fixed number of cycles, and then analyzed for color mixing to assess the kneading efficiency of the oro-facial system.

Other chewing tests: These include using gummy jelly or encapsulating granules with dyes to measure masticatory performance through spectrophotometric analysis.

Swallowing threshold: This assesses the number of chewing cycles until the food is ready to be swallowed

and analyzes the particle size and textural properties of the bolus.

## 2.2 Objective assessment (indirect analysis)

Jaw kinematics: Recording jaw movements during chewing using magnetic, electromagnetic, or optical motion analysis systems.

Jaw muscle activity and bite force: Measuring muscle activity with surface electrodes and bite force with transducers.

Tongue and lip function: Assessing maximum tongue pressure and lip force.

Saliva: Measuring mechanically stimulated salivary flow rate and analyzing its composition.

## 2.3 Subjective assessment:

Self or proxy-assessed masticatory function: using questionnaires to evaluate the perceived quality of masticatory function and difficulties in chewing different types of food.

## 2.4 Advantages and Limitations

Each method has distinct advantages and limitations, which must be considered when selecting the appropriate assessment technique.

Comminution tests:

Advantages: Detailed, reliable, and suitable for a wide range of populations.

Limitations: Requires precise control of conditions and may not be suitable for all demographics.

Mixing ability tests:

Advantages: Quick, simple, and cost-effective.

Limitations: May not detect subtle differences in high-capacity chewers and requires immediate analysis.

Other chewing tests:

Advantages: Easy to apply and measure, suitable for epidemiological studies.

Limitations: Limited by the specificity of test materials and potential type II errors.

Swallowing threshold:

Advantages: Reflects real-life chewing behavior and provides comprehensive bolus characteristics.

Limitations: Highly influenced by food characteristics and individual variability.

Jaw kinematics and muscle activity:

Advantages: Detailed neuromuscular analysis and insights into chewing dynamics.

Limitations: Limited to laboratory settings and requires specialized equipment.

Subjective assessments:

Advantages: Captures patient perceptions and psychological factors.

Limitations: Poor correlation with objective measures and influenced by individual biases.

# Materials and Methods

## 1. Search strategy

A digital electronic search of publications from three electronic databases—PubMed (including MEDLINE) and Scopus, was conducted up to May 2024. No publication date limits were applied, although only articles published in English were included. The search query was implemented using the following combinations of keywords: (Mastication OR Chewing) AND (performance or productivity or efficiency or success or outcomes) AND (orthodontic treatment. The digital search was implemented by manually searching the reference lists from full-text articles and related reviews. Detailed individual search strategies and word combinations were developed following the PICOS criteria. In addition, a hand-search of the references of the included articles was performed.

## 2. Eligibility criteria

The PICO criteria related to research questions are detailed below:

**2.1 Population:** patients with malocclusion and skeletal discrepancy.

**2.2 Intervention:** non-extraction, extraction, orthognathic surgery in the maxilla, mandible, or both.

**2.3 Comparison:** Control (normal occlusion) or before treatment vs. post-orthodontic treatment at any follow-up periods.

**2.4 Outcome:** Masticatory performance (chewing performance, masticatory efficacy, masticatory ability) evaluated using subjective and objective assessment of masticatory performance.

The inclusion criteria comprised randomized controlled trials, prospective controlled studies, and observational

studies with a comparison group, as well as English-language publications focusing on orthodontic treatment.

The exclusion criteria consisted of studies that did not provide sufficient data to calculate the masticatory performance, case reports, literature reviews, and opinion articles.

### 3. Study selection

The electronic search was used to identify relevant studies, which then underwent an initial screening of titles, abstracts, and study designs by two independent reviewers. In cases where abstracts were ambiguous or insufficient, full-text articles were retrieved for detailed assessment. Selected studies were then reevaluated against predefined inclusion and exclusion criteria. Any disagreements between reviewers were resolved through discussion, and a third reviewer was consulted when consensus could not be reached. Data extraction was performed independently by two reviewers using a standardized form. Any discrepancies were addressed through rechecking source material and, when necessary, by contacting the original authors to obtain missing information related to masticatory performance.

### 4. Outcome measures / Measurement of treatment effect

Outcome measures aim to interpret masticatory performance after various types of orthodontic treatment,

evaluated according to the criteria specified in the individual studies. As various assessment methods exist for evaluating masticatory performance, the clinical methods used were listed to create a dataset of efficacy criteria. Objective assessment of masticatory performance in this review is measured by three main parameters: the results from the comminution method, bite force, and occlusal contact area. Subjective assessment of masticatory ability is conducted using a self-perceived questionnaire.

## Result

### 1. Study selection

The final electronic search on PubMed, which includes MEDLINE-indexed articles, and Scopus retrieved 797 studies. After removing 332 duplicates, 465 titles and abstracts were screened. A total of 349 studies were excluded for irrelevance. Of the remaining 66 studies, 27 were retrieved for full text review and 14 studies were excluded during full-text screening due to the absence of a control group, a requirement specified in our inclusion criteria. As a result, 13 studies met all inclusion criteria and were included in the final analysis.<sup>26-38</sup>, as depicted in Figure 1.

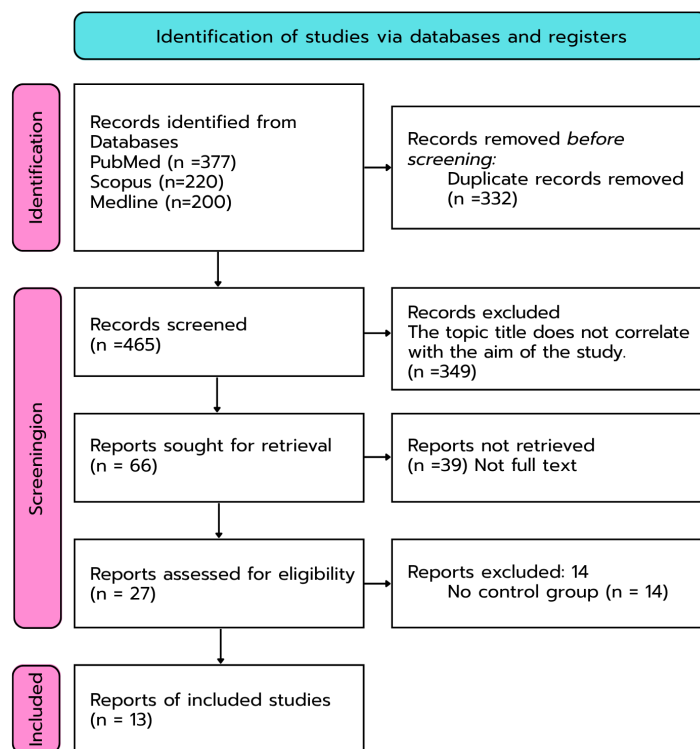


Figure 1 Flowchart diagram of the research search. Exclusions and final number included in the review.



## 2. Study characteristics

This literature review thoroughly collected and examined studies carried out on volunteer groups. These studies were then categorized into three main groups. These groups specifically explored the efficacy of masticatory function after orthodontic treatments. The studies within these categories concentrated on patients who underwent different orthodontic methods, including non-extraction, extraction, and combined surgical

orthodontic procedures. The mean ages of participants in the included studies varied from 21 to 30 years. Additionally, gender information was available in the articles, comprising 629 females and 355 males. In one study, the gender of the volunteer participants was not specified. Furthermore, several articles examined various measures of masticatory performance. Regarding study design, the included studies comprised 13 prospective cohort studies as described in Table 1.<sup>26-38</sup>

**Table 1** Descriptive characteristics of the included studies.

Author, Year	Study type	Number of Control group	Number of Experimental group	Type of Treatment
Gameiro <i>et al.</i> , 2002	prospective cohort study	30 (F15, M15)	17 (M9, F8)	Non-extraction
Henrikson <i>et al.</i> , 2009	prospective cohort study	F58	F65	Non-extraction
Lee <i>et al.</i> , 2023	prospective cohort study	20 (M10, F10)	18 (M9, F9)	Extraction
Yoon <i>et al.</i> , 2017	prospective cohort study	F36	F49	Extraction
Harada <i>et al.</i> , 2000	prospective cohort study	20 (M10, F10)	25 (M10, F15)	Surgery
Kato <i>et al.</i> , 2012	prospective cohort study	20 (M7, F13)	13 (M2, F11)	Surgery
Kobayashi <i>et al.</i> , 2001	prospective cohort study	40 (M24, F16)	27 (M7, F20)	Surgery
Nagai <i>et al.</i> , 2001	prospective cohort study	32 (M16, F16)	43 (M21, F22)	Surgery
Choi <i>et al.</i> , 2014	prospective cohort study	67 (M32, F35)	78 (M=39, F=39)	Surgery
Ohkura <i>et al.</i> , 2001	prospective cohort study	40 (M20, F20)	57 (M26, F31)	Surgery
Ueki <i>et al.</i> , 2014	prospective cohort study	40 (M20, F20)	54 (M26, F28)	Surgery
van den Braber <i>et al.</i> , 2004	prospective cohort study	12 (M4, F8)	11 (M5, F6)	Surgery
van den Braber <i>et al.</i> , 2006	prospective cohort study	12 (M8, F4)	12 (M8, F4)	Surgery

## 3. Assessment of masticatory performance

The assessment of masticatory performance, based on an intensive analysis of 13 research publications, highlights the variety of approaches used to evaluate masticatory performance in patients following orthodontic procedures. This study reveals that research may employ a broad array of approaches, exceeding the limitations of a single methodology, thereby increasing the efficacy and comprehensiveness of the assessment process. Parameters indicating masticatory performance (comminution, bite force, occlusal contact area, and self-perceived questionnaires) were measured pre-treatment and post-treatment in before-and-after studies. The studies provided post-treatment data compared with control patients (normal occlusion).

The findings from the inclusion studies, as summarized in Table 2, reveal that the most frequently utilized parameters for assessing masticatory performance following orthodontic treatment are maximum bite force and occlusal contact area. These metrics were employed in 11 of the 13 selected studies. Comminution (median particle size X50) and masticatory efficiency were the second most used parameters, featuring in three of the 13 studies. Furthermore, the mixing ability test and self-perceived masticatory ability were each reported in one study. These diverse measures are applied across multiple studies, offering a comprehensive evaluation that encompasses both the objective and subjective facets of masticatory performance.

**Table 2** Summary of frequently used measures of masticatory performance of inclusion studies.

Parameter	Method	Studies	sum
Maximum Bite Force or Occlusal Contact Area	Bite on the pressure-sensitive film for a few seconds	Lee <i>et al.</i> (2023), Yoon <i>et al.</i> (2017), Choi <i>et al.</i> (2014), Harada <i>et al.</i> (2000), Kato <i>et al.</i> (2012), Kobayashi <i>et al.</i> (2001), Nagai <i>et al.</i> (2001), Ohkura <i>et al.</i> (2001), Ueki <i>et al.</i> (2014) van den Braber <i>et al.</i> (2004, 2006)	11
Comminution (Median Particle Size X50)	Chewing artificial test food (Optocal) or silicon impression material (Optosil® Bayer) for specific cycles	Gameiro <i>et al.</i> (2002), van den Braber <i>et al.</i> (2004, 2006)	3
Masticatory Efficiency	Chewing silicon impression material (Optosil® Bayer) for specific cycles	Henrikson <i>et al.</i> (2009), Kato <i>et al.</i> (2012), Kobayashi <i>et al.</i> (2001)	3
Mixing Ability Test	Chewing two-color gum on the preferred chewing side for specific cycles	Lee <i>et al.</i> (2023)	1
Self-Perceived Masticatory Ability	Questionnaire visual analog scale	Henrikson <i>et al.</i> (2009)	1

#### 4. Relationship between masticatory performance after orthodontic treatment

This is an overview of this literature review on investigations on masticatory performance following orthodontic treatment. Participants were classified into many groups compared to a control group that did not get such an intervention. The selection process yielded 13 academic articles for review, categorized as follows: two studies investigated participants undergoing non-extraction orthodontic treatment, two studies examined those receiving tooth extraction orthodontic interventions, and nine studies delved into cases involving orthodontic treatment coupled with orthognathic surgical procedures.

##### 4.1 Masticatory performance after non-extraction orthodontic treatment

Two studies examined participants treated orthodontically without tooth extractions and compared them to a control group with natural occlusion that did not receive orthodontic therapy. Objective measurements were used in these studies to assess masticatory performance. In this context, measurements related to masticatory performance were collected by comparing the control and post-treatment groups using a comminution test for

chewing synthetic test food, colorimetric analysis with a spectrophotometer, and the distribution of occlusal load. The subjective evaluation of masticatory performance assessed self-reported masticatory capacity using a Visual Analog Scale questionnaire.

The masticatory performance in the malocclusion patients during the baseline examination was notably reduced compared to the control group. The X50 (median) particle size after 15 strokes of chewing was higher in the malocclusion group, at 5.7 mm, than it was in the control group, at 4.8 mm, suggesting less effective mastication. The improvement in masticatory performance after orthodontic treatment in the malocclusion group was significant. After 15 chewing strokes, the median particle size was reduced to 5.1 mm, closer to the 4.8 mm of the control group. This indicates that orthodontic treatment managed to enhance the patients' chewing performance.<sup>26</sup>

The swallowing performance was as expected. The malocclusion group also presented a higher median particle size at the instance of swallowing (X50-sw) than the control group before treatment (4.5 mm vs. 3.0 mm). This indicates that patients with malocclusion were swallowing larger particles, reflecting poor masticatory

performance. In the post-treatment group, the X50-sw was 3.4 mm. In the malocclusion group, which was not significantly different from the control group the X50-sw was at 3.0 mm. This indicates a considerable increase in the ability of patients to reduce food particle size in the mouth before swallowing, making it comparable to the controls.

The self-perceived masticatory ability in prospective and longitudinal studies evaluate both self-perceived masticatory ability and objectively tested masticatory efficiency. The study evaluated the impact of orthodontic treatment on self-perceived masticatory ability and masticatory efficiency among adolescent girls with Class II malocclusion, comparing them to untreated Class II and normal occlusion groups. The self-perceived masticatory ability significantly increased in the Orthodontic group from a mean score of 74.4 to 86.4 ( $p=0.001$ ), indicating that orthodontic treatment had a positive effect on how these individuals perceived their chewing ability. In contrast, the untreated Class II group and the Normal group showed no significant changes over the two-year period. Initially, the Normal group had significantly higher self-perceived masticatory ability scores than both Class II groups ( $p<0.001$ ), but after two years, there were no significant differences between any groups.<sup>27</sup>

Masticatory efficiency, measured by the Masticatory Efficiency Index (MEI), improved in all groups over the two-year period. The Orthodontic group's MEI increased from 10.3 to 15.2 (95% CI = 1.9-7.1;  $p=0.001$ ), while the Class II group's MEI increased from 12.4 to 16.4 (95% CI = 1.7-6.5;  $p=0.001$ ), and the Normal group's MEI rose from 17.1 to 21.5 (95% CI = 2.1-6.4;  $p<0.001$ ). Despite these improvements, the Normal group consistently had a significantly higher MEI compared to both the Orthodontic and Class II groups at both the start and after two years ( $p<0.001$  for both comparisons). No significant differences in MEI were observed between the Orthodontic and Class II groups at any point, suggesting that orthodontic treatment did not bring the masticatory efficiency of treated individuals up to the level of those with normal occlusion.

The study also examined preferred chewing sides and occlusal characteristics. No significant differences were found between groups regarding preferred chewing sides

both at the start and after two years. However, significant improvements in occlusal characteristics were observed in the Orthodontic group, such as reduced overjet and normalization of sagittal and transverse relationships, demonstrating the effectiveness of orthodontic treatment in correcting occlusal issues.

While orthodontic treatment significantly enhances self-perceived masticatory ability, it does not completely normalize masticatory efficiency compared to individuals with normal occlusion. The increase in masticatory efficiency across all groups likely reflects natural growth and development rather than the effect of orthodontic treatment alone.

#### **4.2 Masticatory performance after orthodontic treatment and tooth extraction**

All groups (non-extraction, two maxillary premolar extraction, and four premolar extraction) exhibited a significant reduction in occlusal contact area and force immediately after treatment. Over the two-year post-treatment period, these metrics gradually increased. The non-extraction and two maxillary premolar extraction groups achieved full recovery to pre-treatment levels, while the four premolar extraction group did not fully regain its initial occlusal contact area.<sup>28</sup>

Statistical analysis revealed that the changes in occlusal contact area and force were significantly correlated with the time elapsed since treatment ( $P < .001$ ). This correlation underscores the gradual improvement in masticatory performance over the two-year period. The non-extraction and two maxillary premolar extraction groups demonstrated a positive correlation between the recovery of occlusal function and improved masticatory performance, as indicated by the full recovery of occlusal contact area and force to pre-treatment levels ( $P > .05$ ). Conversely, the four premolar extraction group, which did not fully recover its occlusal contact area, highlighted a negative correlation, suggesting that more extensive extractions could have a lasting adverse effect on masticatory performance. While orthodontic treatment initially impairs occlusal function, significant recovery is observed over two years, positively correlating with improved masticatory performance in non-extraction and two maxillary premolar extraction cases. The incomplete



recovery in the four premolar extraction groups indicates a potential long-term negative impact on masticatory performance which is supported by the statistical evidence showing a significant correlation between the degree of extraction and the extent of functional recovery.

Immediately after orthodontic treatment, the experimental groups (non-extraction and extraction) demonstrated lower mixing ability (MA), maximum bite force (MBF), and occlusal contact area (OCA) compared to the normal occlusion group. This initial deficiency highlighted the immediate impact of orthodontic treatment on masticatory performance.<sup>29</sup>

Over the one-year retention period, significant improvements were observed in all three parameters for both experimental groups. Mixing ability (MA), measured as the standard deviation of hue (SDHue) in chewed gum, improved significantly over time. By one-month post-treatment (T1), MA levels in both experimental groups were comparable to those in the normal occlusion group. This improvement continued, with MA reaching levels similar to the normal occlusion group by one-year post-treatment (T3). These results indicate a positive recovery trajectory for chewing efficiency post-orthodontic treatment.

Maximum bite force (MBF) and occlusal contact area (OCA) also showed significant increases during the retention period. However, despite these improvements, both MBF and OCA remained lower than those in the normal occlusion group at all measured time points (T1, T2, and T3). Statistical correlations between these parameters provided further insights. There was a significant negative correlation between MA and MBF (correlation coefficient: -0.382,  $P < 0.01$ ) and between MA and OCA (correlation coefficient: -0.350,  $P < 0.01$ ). This implies that as mixing ability improves (i.e., SDHue decreases), both maximum bite force and occlusal contact area tend to increase. Additionally, a strong positive correlation was found between MBF and OCA (correlation coefficient: 0.899,  $P < 0.01$ ), indicating that higher bite force is strongly associated with a larger occlusal contact area.

The MP immediately after orthodontic treatment in the experimental groups was lower than that in the normal occlusion group but increased gradually over time

during the retention period and improved to levels similar to those in the normal occlusion group at 1-month post-treatment (T1). Furthermore, extraction did not affect the recovery of the MP after orthodontic treatment.

#### 4.3. Masticatory performance after orthognathic surgery

Assessment of masticatory performance following orthognathic surgery shows that while surgical orthodontic treatment improves function—particularly bite force and occlusal contact area—these gains often fall short of those seen in individuals with normal occlusion. Nine studies evaluated masticatory performance using parameters such as absorbance from the comminution method, bite force, and occlusal contact area.

Across these studies, outcomes like masticatory efficiency and electromyographic (EMG) activity were measured both before and at various intervals after surgery. Harada *et al.* reported that bite force and occlusal contact area were lowest at two weeks postoperatively, recovered to baseline between eight weeks and three months, and exceeded preoperative levels by six months—yet remained below those of healthy subjects. Kobayashi *et al.* similarly noted improvements in masticatory efficiency, occlusal contacts, and muscle activity, though still significantly lower than in control groups. Nagai *et al.* observed that occlusal contact area and bite force declined further one-month post-surgery but gradually improved over the year. While occlusal pressure peaked at one month and neared control values by 12 months, overall performance remained below that of individuals with normal occlusion.

Ohkura *et al.* supported these findings, reporting significant improvements in bite force and occlusal contact area after surgery that exceeded preoperative levels by six months, though still remaining below control levels even at three years post-surgery.<sup>32</sup> In contrast, van den Braber *et al.* presented mixed results: one study found no significant changes in chewing efficiency, maximum bite force, or EMG activity post-surgery, while another observed notable improvements in chewing performance five years after surgery without a corresponding increase in maximum bite force.<sup>33,34</sup> Kato *et al.* and Ueki *et al.* both documented significant postoperative gains in masticatory

efficiency, occlusal contacts, and maximal occlusal force, particularly among patients who engaged in masticatory exercises, although these parameters remained inferior to those of individuals with normal occlusion.<sup>35,36</sup>

Overall, these studies consistently show post-operative improvements in masticatory function, with many parameters gradually recovering and sometimes surpassing pre-surgery levels—but still falling short of healthy controls. Various assessment methods, including Dental-Prescale, ATP granules, and EMG analysis, provided strong evidence supporting these trends. Collectively, the findings highlight the importance of ongoing postoperative monitoring and suggest that masticatory exercises can further enhance recovery.

Some discrepancies exist regarding the overall effectiveness of surgical interventions. For instance, van den Braber et al. found no significant changes in chewing efficiency, maximum bite force, or EMG activity, contrasting with other studies that reported improvements in these parameters.<sup>33</sup> Additionally, while Kato *et al.* and Ueki *et al.* emphasized the positive impact of masticatory exercises on recovery, this factor was not consistently addressed across all studies. These variations highlight the diversity in recovery outcomes and underscore the need for personalized rehabilitation strategies to optimize masticatory function after orthognathic surgery.<sup>35,36</sup>

Overall, time plays a critical role in masticatory recovery, with significant improvements observed up to two years post-surgery. However, persistent deficits relative to individuals with normal occlusion indicate the necessity for comprehensive postoperative care and potentially adjunctive therapies to maximize functional outcomes. The findings also stress the importance of standardized assessment protocols in future research to enhance comparability and reliability, facilitating a better understanding of long-term effects and improving rehabilitation strategies following orthognathic treatment.

## Discussion

The primary objective of this study is to summarize the relationship between masticatory performance and orthodontic treatment. Participants were divided into two

groups: those who have had dental extractions, those who have not, and orthodontic treatment. The study examines various aspects of masticatory performance over periods ranging from one month to two years after orthodontic stabilization. Additionally, the secondary aim is to identify the most used metric for evaluating masticatory performance after orthodontic treatment.

Masticatory performance can be affected by factors such as tooth alignment and occlusion, muscle strength, and neuromuscular coordination. Orthodontic treatment has the potential to enhance masticatory performance by improving dental alignment and occlusion.

### 1. Assessment of masticatory performance

The findings from the inclusion studies reveal that the most frequently utilized parameters for assessing masticatory performance following orthodontic treatment are maximum bite force and occlusal contact area. These metrics were employed in 11 of the 13 selected studies. Comminution (median particle size X50) and masticatory efficiency were the second most used parameters, featuring in three of the 13 studies. Furthermore, the mixing ability test and self-perceived masticatory ability were each reported in one study. These diverse measures are applied across multiple studies, offering a comprehensive evaluation that encompasses both the objective and subjective facets of masticatory performance.

Bite force and occlusal contact area are critical parameters in assessing masticatory performance during orthodontic treatment because they provide objective measures of the functional efficiency and health of the masticatory system. Research indicates that these metrics are reliable indicators of improvements in muscle activity, occlusal stability, and overall dental function. Bite force and occlusal contact area are commonly used for masticatory assessment in orthodontic treatment due to several reasons.<sup>39-41</sup>

### 2. Relation of masticatory performance after orthodontic treatment

#### 2.1 Masticatory performance after non-extraction orthodontic treatment

Orthodontic treatments without extractions have been shown to enhance masticatory performance, with

studies providing both objective and subjective measures. Gameiro *et al.* found significant improvements in masticatory efficiency post-treatment, evidenced by a reduction in the median particle size of chewed food. These findings are consistent with the overall literature, which supports the positive impact of orthodontic treatments on masticatory function.<sup>26,42,43</sup>

Thor Henrikson *et al.* reported improvements in self-perceived masticatory ability in adolescent girls with Class II malocclusion but noted that masticatory efficiency remained higher in peers with normal occlusion. This suggests that natural growth and development may play a more significant role than orthodontic treatment alone. This view is supported by van den Braber *et al.*, who found that skeletal morphology and muscle strength are critical factors in masticatory efficiency, with no significant improvements observed post-mandibular advancement surgery.<sup>33</sup>

Ashok *et al.* further confirmed increased chewing efficiency after orthodontic treatment in Class II malocclusion cases using fixed functional appliances. They reported improvements in the molar extinction coefficient and occlusal load distribution, emphasizing the benefits of functional jaw orthopedics in promoting proper nutrition and growth in adolescents.<sup>41</sup> Shim *et al.* demonstrated that post-orthodontic dental occlusion significantly impacts masticatory performance, stressing the importance of maintaining proper occlusal relationships. This aligns with findings from studies that show improved masticatory functions and enhanced quality of life post-orthodontic treatment.<sup>45</sup> The reviewed studies provide strong evidence of the functional and psychological benefits of such treatments. However, continued research is necessary to further validate these findings and explore the long-term impacts of non-extraction orthodontic treatments across diverse patient populations.

## **2.2 Masticatory performance after orthodontic treatment and tooth extraction**

The impact of orthodontic treatment involving tooth extraction on masticatory performance has been studied extensively, revealing both consistent and differing findings. Lee *et al.* observed significant improvements in

mixing ability, bite force, and occlusal contact area over a year. However, these measures did not return to normal occlusion levels, indicating only partial recovery of masticatory function post-treatment. Similarly, Yoon *et al.* found that recovery varied with the extent of tooth extractions, with less extensive extractions showing better recovery compared to more extensive ones.<sup>28,29,46</sup>

Zanon *et al.* reported enhancements in masticatory and chewing functions following orthodontic treatment, leading to improved health-related quality of life.<sup>3</sup> However, this recovery is contingent on the extent of the extractions, with fewer extractions associated with better functional outcomes.<sup>46,47</sup>

A notable point of difference arises in the long-term functional outcomes. Yoon *et al.* emphasized the long-term adverse effects of more extensive extractions, which contrasts with Nasir *et al.*, who suggested that proper orthodontic treatment can mitigate these negative impacts. Additionally, Gözler *et al.* emphasized the importance of long-term follow-up for achieving optimal masticatory performance, aligning with the findings of Sabzevari *et al.*, who demonstrated significant enhancements in masticatory performance and quality of life through a meta-analysis.<sup>28,46,48,49</sup>

The occlusal contact area and force recovery correlate significantly with time post-treatment, highlighting the necessity of longitudinal assessments. The precise orthodontic detailing of occlusion contributes to balanced muscle activation and more efficient muscle recruitment, though it does not significantly improve chewing efficiency. This underscores the complexity of factors influencing masticatory performance recovery and the need for individualized treatment planning.<sup>45</sup>

The consensus across these studies suggests that while orthodontic treatment involving premolar extractions initially impairs masticatory performance, significant recovery is achievable, particularly with fewer extractions. The extent of extractions plays a critical role in long-term outcomes, and long-term monitoring and individualized treatment plans are crucial for optimizing functional recovery. Future research should further explore the nuances of different extraction patterns and retention strategies to refine orthodontic treatment protocols.

### 2.3 Masticatory performance after orthognathic surgery.

The study of masticatory performance following orthognathic surgery offers key insights into functional outcomes post-treatment. Findings indicate a significant decline in masticatory performance—measured by the comminution method—at three months post-surgery, primarily due to postoperative discomfort and muscle adaptation. However, a gradual recovery was observed at six months and one year, although performance remained below that of individuals with normal occlusion. This trend is supported by Bunpu *et al.*, who reported improvements in absorbance values and particle size reduction over time, yet consistently lower than in control groups.<sup>39</sup> Bite force assessments similarly revealed marked reductions at three months post-surgery, followed by notable improvements at six months, one year, and two years. Regression analyses confirmed a positive correlation between postoperative duration and bite force recovery. Nonetheless, even two years post-surgery, bite force levels in surgical patients remained below those of individuals with normal occlusion, underscoring the need for extended follow-up and potential adjunctive therapies to support full functional restoration.<sup>50</sup>

Likewise, the occlusal contact area—which reflects the contact surface between upper and lower teeth during occlusion—showed significant early reductions, with progressive recovery over time. The pattern paralleled that of bite force improvements, yet occlusal contact area values remained lower than those of control groups at the two-year mark. This persistent deficit highlights the importance of comprehensive postoperative care and the establishment of standardized assessment protocols to ensure consistency and comparability in future studies.<sup>51</sup>

In conclusion, while orthognathic surgery significantly improves masticatory performance, the outcomes often fall short of normal occlusion benchmarks. Ongoing deficits in absorbance values, bite force, and occlusal contact area underscore the need for long-term monitoring and adjunctive interventions. Future research should aim to refine assessment methodologies and explore therapeutic strategies to optimize functional recovery after surgery.

Despite the rigorous methodology, this review has several limitations. Restricting inclusion to English-

language studies may have introduced language bias. Study heterogeneity in design, outcomes, and populations limited meta-analysis. Some studies had small sample sizes or insufficient reporting, affecting reliability. Publication bias remains a concern, and the exclusion of unpublished or gray literature may have led to an incomplete evidence base. This review provides sufficient evidence that non-extraction orthodontic treatment, extraction orthodontic treatment, and orthognathic surgery all contribute to improvements in patients' masticatory performance.

## Conclusion

The literature review highlights the effectiveness of orthodontic treatments in improving masticatory performance, with varying results depending on the treatment approach. Key points include:

1. Non-Extraction Orthodontic Treatments: These treatments generally lead to significant improvements in masticatory performance, often approaching normal chewing function. The improvements tend to be quicker and more consistent in non-extraction cases.

2. Extraction Orthodontic Treatments: These treatments, which involve tooth extractions, usually result in slower recovery of masticatory performance. The long-term effects depend on the number of extractions performed. Studies suggest that patients undergoing extraction treatments take longer to achieve optimal chewing function compared to those undergoing non-extraction treatments.

3. Orthognathic Surgery: This is effective in correcting severe malocclusions and can lead to significant improvements in masticatory function. However, it requires a prolonged recovery period and meticulous postoperative care to achieve optimal outcomes. Continued follow-up is essential to monitor progress and address any functional deficits during the recovery process.

The review recommends that future research focus on creating standardized assessment protocols and developing supplementary therapies to enhance recovery, which would provide a more comprehensive approach to improve masticatory performance following orthodontic treatment.



## Acknowledgement

I am grateful to the Department of Occlusion and Orofacial Pain at Mahidol University for providing the resources and environment for promoting my articles.

## References

1. Turley PK. Evolution of esthetic considerations in orthodontics. *Am J Orthod Dentofacial Orthop* 2015;148(3):374-9.
2. Magalhães IB, Pereira LJ, Marques LS, Gameiro GH. The influence of malocclusion on masticatory performance. A systematic review. *Angle Orthod* 2010;80(5):981-7.
3. Zanon G, Contardo L, Reda B. The Impact of Orthodontic Treatment on Masticatory Performance: A Literature Review. *Cureus* 2022;14(10):e30453.
4. Zhan Y, Yang M, Bai S, Zhang S, Huang Y, Gong F, et al. Effects of orthodontic treatment on masticatory muscles activity: a meta-analysis. *Ann Hum Biol* 2023;50(1):465-71.
5. Van Der Bilt A, Mojet J, Tekamp FA, Abbink JH. Comparing masticatory performance and mixing ability. *J Oral Rehabil* 2010;37(2):79-84.
6. The Glossary of Prosthodontic Terms 2023: Tenth Edition. *J Prosthet Dent* 2023;130(4):e1-e3.
7. Bates JF, Stafford GD, Harrison A. Masticatory function - a review of the literature. III. Masticatory performance and efficiency. *J Oral Rehabil* 1976;3(1):57-67.
8. van der Bilt A, Olthoff LW, van der Glas HW, van der Weelen K, Bosman F. A mathematical description of the comminution of food during mastication in man. *Arch Oral Biol* 1987;32(8):579-86.
9. van der Glas HW, Liu T, Zhang Y, Wang X, Chen J. Optimizing a determination of chewing efficiency using a solid test food. *J Texture Stud* 2020;51(1):169-84.
10. Gonçalves T, Schimmel M, van der Bilt A, Chen J, van der Glas HW, Kohyama K, et al. Consensus on the terminologies and methodologies for masticatory assessment. *J Oral Rehabil* 2021;48(6):745-61.
11. Owens S, Buschang PH, Throckmorton GS, Palmer L, English J. Masticatory performance and areas of occlusal contact and near contact in subjects with normal occlusion and malocclusion. *Am J Orthod Dentofacial Orthop* 2002;121(6):602-9.
12. Consolação Soares ME, Ramos-Jorge ML, de Alencar BM, Marques LS, Pereira LJ, Ramos-Jorge J. Factors associated with masticatory performance among preschool children. *Clin Oral Investig* 2017;21(1):159-66.
13. English JD, Buschang PH, Throckmorton GS. Does malocclusion affect masticatory performance? *Angle Orthod* 2002;72(1):21-7.
14. Fontijn-Tekamp FA, Slagter AP, Van Der Bilt A, Van THMA, Witter DJ, Kalk W, et al. Biting and chewing in overdentures, full dentures, and natural dentitions. *J Dent Res* 2000;79(7):1519-24.
15. Hatch JP, Shinkai RSA, Sakai S, Rugh JD, Paunovich ED. Determinants of masticatory performance in dentate adults. *Arch Oral Bio* 2001;46(7):641-8.
16. Schimmel M, Christou P, Miyazaki H, Halazonetis D, Herrmann FR, Müller F. A novel colourimetric technique to assess chewing function using two-coloured specimens: Validation and application. *J Dent* 2015;43(8):955-64.
17. Buschang PH. Masticatory Ability and Performance: The Effects of Mutilated and Maloccluded Dentitions. *Semi Orthod* 2006;12(2):92-101.
18. Van Der Bilt A. Assessment of mastication with implications for oral rehabilitation: a review. *J Oral Rehabil* 2011;38(10):754-80.
19. Gavião MB, Raymundo VG, Sobrinho LC. Masticatory efficiency in children with primary dentition. *Pediatr Dent J* 2001;23(6):499-505.
20. Toro A, Buschang PH, Throckmorton G, Roldán S. Masticatory performance in children and adolescents with Class I and II malocclusions. *Eur J Orthod* 2006;28(2):112-9.
21. Nalamliang N, Thongudomporn U. Effects of class II intermaxillary elastics on masticatory muscle activity balance, occlusal contact area and masticatory performance: A multicenter randomised controlled trial. *J Oral Rehabil* 2023;50(2):131-9.
22. Zarrinkelk HM, Throckmorton GS, Ellis E, Sinn DP. A longitudinal study of changes in masticatory performance of patients undergoing orthognathic surgery. *Oral Maxillofac Surg* 1995;53(7):777-82.
23. Bae J, Son WS, Kim SS, Park SB, Kim YI. Comparison of masticatory efficiency according to Angle's classification of malocclusion. *Korean J Orthod* 2017;47(3):151-7.
24. Souto-Souza D, Soares MEC, Primo-Miranda EF, Pereira LJ, Ramos-Jorge ML, Ramos-Jorge J. The influence of malocclusion, sucking habits and dental caries in the masticatory function of preschool children. *Braz Oral Res* 2020;34:e059.
25. Barbosa Tde S, Tureli MC, Nobre-dos-Santos M, Puppini-Rontani RM, Gavião MB. The relationship between oral conditions, masticatory performance and oral health-related quality of life in children. *Arch Oral Biol* 2013;58(9):1070-7.
26. Gameiro GH, Magalhães IB, Szymanski MM, Andrade AS. Is the main goal of mastication achieved after orthodontic treatment? A prospective longitudinal study. *Dental Press J Orthod* 2017;22(3):72-8.
27. Henrikson T, Ekberg E, Nilner M. Can orthodontic treatment improve mastication? A controlled, prospective and longitudinal study. *Swed Dent J* 2009;33(2):59-65.
28. Yoon W, Hwang S, Chung C, Kim KH. Changes in occlusal function after extraction of premolars: 2-year follow-up. *Angle Orthod* 2017;87(5):703-8.
29. Lee SH, Fang ML, Choi YJ, Yu HS, Kim JH, Hu KS, et al. Changes in masticatory performance during the retention period following 4-premolar extraction and non-extraction orthodontic treatment. *Clin Oral Investig* 2023;27(6):2609-19.

30. Harada K, Watanabe M, Ohkura K, Enomoto S. Measure of bite force and occlusal contact area before and after bilateral sagittal split ramus osteotomy of the mandible using a new pressure-sensitive device: a preliminary report. *J Oral Maxillofac Surg* 2000;58(4):370-3; discussion 3-4.
31. Kobayashi T, Honma K, Shingaki S, Nakajima T. Changes in masticatory function after orthognathic treatment in patients with mandibular prognathism. *Br J Oral Maxillofac Surg* 2001;39(4):260-5.
32. Ohkura K, Harada K, Morishima S, Enomoto S. Changes in bite force and occlusal contact area after orthognathic surgery for correction of mandibular prognathism. *Oral Surg Oral Med Oral Pathol Oral Radiol Endod* 2001;91(2):141-5.
33. van den Braber W, van der Glas H, van der Bilt A, Bosman F. Masticatory function in retrognathic patients, before and after mandibular advancement surgery. *J Oral Maxillofac Surg* 2004;62(5):549-54.
34. van den Braber W, van der Bilt A, van der Glas H, Rosenberg T, Koole R. The influence of mandibular advancement surgery on oral function in retrognathic patients: a 5-year follow-up study. *J Oral Maxillofac Surg* 2006;64(8):1237-40.
35. Kato K, Kobayashi T, Kato Y, Takata Y, Yoshizawa M, Saito C. Changes in masticatory functions after surgical orthognathic treatment in patients with jaw deformities: Efficacy of masticatory exercise using chewing gum. *J Oral Maxillofac Surg Med Pathol* 2012;24(3):147-51.
36. Ueki K, Moroi A, Sotobori M, Ishihara Y, Marukawa K, Iguchi R, *et al.* Evaluation of recovery in lip closing pressure and occlusal force and contact area after orthognathic surgery. *J Cranio Maxill Sur* 2014;42(7):1148-53.
37. Choi YJ, Lim H, Chung CJ, Park KH, Kim KH. Two-year follow-up of changes in bite force and occlusal contact area after intraoral vertical ramus osteotomy with and without Le Fort I osteotomy. *Int J Oral Maxillofac Surg* 2014;43(6):742-7.
38. Nagai I, Tanaka N, Noguchi M, Suda Y, Sonoda T, Kohama G. Changes in occlusal state of patients with mandibular prognathism after orthognathic surgery: a pilot study. *Br J Oral Maxillofac Surg* 2001;39(6):429-33.
39. Bunpu P, Changsiripun C. Assessment of masticatory performance in patients undergoing orthognathic surgery: A systematic review and meta-analysis. *J Oral Rehabil* 2023;50(7):596-616
40. Therkildsen NM, Sonnesen L. Bite Force, Occlusal Contact and Pain in Orthodontic Patients during Fixed-Appliance Treatment. *J Dent* 2022;10(2):14.
41. Abutayyem H, M Annamma L, Desai VB, Alam MK. Evaluation of occlusal bite force distribution by T-Scan in orthodontic patients with different occlusal characteristics: a cross sectional-observational study. *BMC Oral Health* 2023;23(1):888.
42. Magalhães IB, Pereira LJ, Andrade AS, Gouvea DB, Gameiro GH. The influence of fixed orthodontic appliances on masticatory and swallowing threshold performances. *J Oral Rehabil* 2014;41(12):897-903.
43. Makino E, Nomura M, Motegi E, Iijima Y, Ishii T, Koizumi Y, *et al.* Effect of orthodontic treatment on occlusal condition and masticatory function. *Bull Tokyo Dent Coll* 2014;55(4):185-97.
44. Ashok S, Batra P, Sharma K, Raghavan S, Talwar A, Srivastava A, *et al.* An assessment of masticatory efficiency and occlusal load distribution in adolescent patients undergoing orthodontic treatment with functional jaw orthopedics: A prospective cohort study. *J Stomatol Oral and Maxillofac Surg* 2023;124(6, Supplement 2):101570.
45. Shim J, Ho KCJ, Shim BC, Metaxas A, Somogyi-Ganss E, Di Sipio R, *et al.* Impact of post-orthodontic dental occlusion on masticatory performance and chewing efficiency. *Eur J Orthod* 2020;42(6):587-95.
46. Nasir M, Erwanyah E, Susilowati. The effect of orthodontic treatment with and without tooth extraction on stomatognathic function: Pengaruh perawatan ortodonti dengan dan tanpa pencabutan gigi terhadap fungsi stomatognatik. *M D J* 2023;12:153-8.
47. Sultana MH, Yamada K, Hanada K. Changes in occlusal force and occlusal contact area after active orthodontic treatment: a pilot study using pressure-sensitive sheets. *J Oral Rehabil* 2002;29(5):484-91.
48. Gözler S, Sadry S. Examination of chewing performance with extraction and non-extraction fixed orthodontic treatment – A prospective clinical 1-year study. *APOS Trends Orthod* 2022;1-9.
49. Sabzevari B, Fatemi A, Soleimani M, Sajedi SM, Babazadehkhoushrodi R. Masticatory performance and oral health related to quality of life before and after orthodontic treatment: a systematic review and meta-analysis. *Eur J Transl Myol* 2024;34(1):12101.
50. Iwase M, Ohashi M, Tachibana H, Toyoshima T, Nagumo M. Bite force, occlusal contact area and masticatory efficiency before and after orthognathic surgical correction of mandibular prognathism. *Int J Oral Maxillofac Surg* 2006;35(12):1102-7.
51. Nakata Y, Ueda HM, Kato M, Tabe H, Shikata-Wakisaka N, Matsumoto E, *et al.* Changes in stomatognathic function induced by orthognathic surgery in patients with mandibular prognathism. *J Oral Maxillofac Surg* 2007;65(3):444-51.

# Anatomical Study of the Mandibular Canal in Thai Patients with Mandibular Prognathism: Implications for BSSRO

Sappasith Panya<sup>1,2</sup>, Thitirat Tungtorsakul<sup>3</sup>, Natnisha Arkarapattarawong<sup>3</sup>, Parintorn Sutthiprapa<sup>3</sup>, Puthita Leewisutthikul<sup>3</sup>, Keskanya Subbalekha<sup>1,2</sup>

<sup>1</sup>Department of Oral and Maxillofacial Surgery, Faculty of Dentistry, Chulalongkorn University, Bangkok, Thailand

<sup>2</sup>Oral and Maxillofacial Surgery and Digital Implant Surgery Research Unit, Faculty of Dentistry, Chulalongkorn University, Bangkok, Thailand

<sup>3</sup>Dental student, Faculty of Dentistry, Chulalongkorn University, Bangkok, Thailand

## Abstract

This retrospective study analyzed the mandibular canal (MC) anatomy in relation to bilateral sagittal split ramus osteotomy (BSSRO) in mandibular prognathism patients, comparing measurements obtained from cone beam computed tomography (CBCT) and ortho-panoramic (OP) images. Twenty-seven pre-operative radiographs (12 males, 15 females; mean age 26.3 years) revealed significant differences in MC distances to the anterior border of the ramus and sigmoid notch between CBCT ( $13.80 \pm 2.20$  and  $15.89 \pm 2.00$  mm) and OP ( $10.27 \pm 1.27$  and  $14.93 \pm 2.25$  mm) at  $p < 0.001$  and  $p = 0.007$ , respectively. However, measurements of MC distances to the alveolar crest and inferior border of the mandible were consistent. Side differences were observed in MC to ramus distances as well as in buccal/lingual bone thickness. There were no significant differences between males and females. However, the buccal bone at the second molar area was thicker than the first molar area. The findings emphasize the superiority of CBCT over OP in the ramus region, which is critical for avoiding inferior alveolar neurovascular injury during BSSRO. Based on this, performing vertical osteotomies in the second molar region may lead to safer surgical outcomes.

**Keywords:** Bilateral sagittal split ramus osteotomy, Cone beam computed tomography, Mandibular canal, Mandibular prognathism, Ortho-panoramic radiograph

**Received date:** Jan 23, 2025

**Revised date:** Apr 20, 2025

**Accepted date:** Jun 4, 2025

**Doi:** 10.14456/jdat.2025.21

## Correspondence to:

Keskanya Subbalekha, Department of Oral and Maxillofacial Surgery, Faculty of Dentistry, Chulalongkorn University, 34 Henri-Dunant Road, Patumwan, Bangkok, Thailand 10330. Tel and fax no. 02-2188581 Email: skeskanya@gmail.com

## Introduction

Mandibular prognathism, as defined by John Hunter<sup>1</sup> in 'The Natural History of the Human Teeth' (1778), refers to the protrusion of the lower jaw resulting in anterior positioning of the lower teeth relative to the upper teeth, leading to facial disfigurement and malocclusion. Additional defining characteristics include Class III malocclusion, incomplete lip closure, midline deviation, and reduced

labiomental fold.<sup>1</sup> Class III malocclusion is notably more prevalent among Asians than Caucasians. Etiological factors contributing to mandibular prognathism encompass hereditary predisposition, congenital conditions (e.g. cleft lip and palate), endocrine disorders (e.g., acromegaly, gigantism, pituitary adenomas), upper airway obstruction (e.g., enlarged tonsils), habitual mandibular protrusion

posture, birth trauma (e.g., instrumental deliveries), tongue position, and tonsillar hypertrophy.<sup>2</sup> Treatment strategies vary by age group: facial growth modification using dentofacial orthopedic appliances is employed for growing patients, while orthognathic surgery combined with orthodontic treatment is indicated for adults. Treatment goals include correcting jaw relationship, reducing negative incisal overlap, achieving intermaxillary skeletal stability, and optimizing dental occlusion to enhance both functional and aesthetic outcomes.<sup>2</sup>

Bilateral Sagittal Split Osteotomy (BSSRO) is a widely utilized surgical technique for correcting mandibular deformities, particularly retrognathism (retracted mandible) and prognathism (protruding mandible). This procedure enables the repositioning of the mandible to improve both functional occlusion and aesthetic outcomes.<sup>3</sup> The osteotomy begins with a horizontal incision on the medial aspect of the ramus, just above and behind the mandibular foramen (MF), extending to the anterior border of the ramus. The sagittal cut is then carried anteriorly along the external oblique ridge to the body of the mandible, near the first or second molar. A downward vertical cut toward the inferior border of the mandible is made.<sup>4</sup> After completing the osteotomy, the ramus is split into medial and lateral segments (Fig. 1).<sup>5</sup> Once both rami are separated, the medial segment can be repositioned either forward or backward to achieve the desired occlusion and aesthetic alignment. The nerve bundle typically remains in the medial segment.

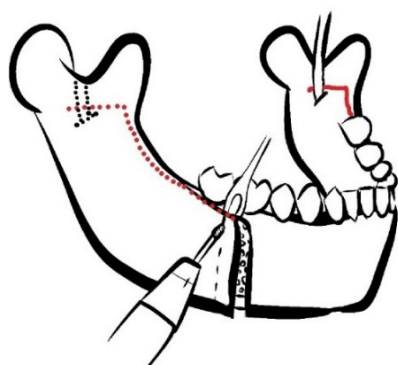


**Figure 1** The BSSRO osteotomy line. A horizontal cut is made on the lingual cortex just superior to the mandibular foramen, followed by a sagittal cut extending along the anterior border of the ramus. A vertical cut is performed anteriorly on the buccal side, ensuring proper segmentation for surgical manipulation.

Complications associated with BSSRO include bleeding from the inferior alveolar artery, injury to the inferior alveolar nerve (IAN), unfavorable fractures, infection, limited mouth opening, condylar resorption leading to skeletal relapse, loss of masticatory force, discomfort from screws, screw loosening, postoperative swelling, malocclusion, and worsening temporomandibular joint disease (TMD).<sup>6-8</sup> Although the complications are documented, they may not necessarily occur in every case or during the actual procedure. Among these, injury to the IAN is of particular concern due to the potential for neurosensory dysfunction, which can range from numbness in the lower lip and chin to more severe issues such as drooling and speech difficulties. Postoperative sensory function data indicates that 28% of sites maintained normal function after two months, with further improvements observed at follow-up, suggesting a reparative potential of nerve injury. However, many patients experience prolonged sensory deficits, which can impact decisions regarding surgical approaches and the need for rehabilitation.<sup>9</sup>

The IAN, a key branch of the mandibular nerve in the trigeminal complex, enters the MF on the medial surface of the mandibular ramus, marking the start of the mandibular canal (MC). Within the MC, it provides innervation to the lower teeth via its terminal branches. The mental nerve exits the canal at the mental foramen, usually located between the first and second premolars, and innervates the chin and lower lip. The incisive nerve continues anteriorly, supplying sensory innervation to the mandibular incisors and canines. Direct visualization of the IAN on conventional radiographs is not possible; however, the MC is often visible, allowing clinicians to infer the IAN's location. To minimize the risk of IAN injury, careful identification of the MC position is essential.

The position of the MC is influenced by two main factors: the thickness of the surrounding bone (buccal, lingual, inferior, and superior borders) and the diameter of the canal.<sup>10</sup> The greatest distance between the MC and the buccal border occurs at the lower first and second molars, while the shortest distance is found at the third molar.<sup>11</sup> The mean distance from the MC to the buccal cortex is 3.5 mm (ranging from 1.8 to 6.5 mm) around the



lower first and second molars, and 2.5 mm (ranging from 0.4 to 5.9 mm) distal to the lower third molar.<sup>12</sup> The mean distance to the lingual cortex is 0.6 mm (ranging from 0.0 to 3.2 mm) around the lower first and second molars, and 0.6 mm (ranging from 0.0 to 3.0 mm) distal to the third molar. The mean MC's diameter is 2.1 mm (ranging from 1.2 to 3.0 mm).<sup>13</sup> Additionally, the IAN may be near the buccal cortex in cases of thick rami.<sup>12</sup> Yamamoto *et al.*<sup>14</sup> found that 25% of MC were in contact with the external cortical bone. Correlations between age, race, and the position of the MC have been noted, with older and white patients showing a thinner bone between the buccal cortex and the MC.<sup>16</sup> Moreover, the MC in Class III molar relationship is located closer to the inferior border of the mandible compared to other Classes.<sup>17</sup> However, no reports exist regarding these anatomical relationship in Thai patients with mandibular prognathism.

Cone Beam Computed Tomography (CBCT) provides three-dimensional images that can be viewed in any plane, offering more detailed visualization of the mandibular canal (MC) compared to conventional two-dimensional orthopantomograms (OP).<sup>18</sup> da Fontoura<sup>19</sup> reported that distortion in the ramus from OP images is 0.9%. CBCT, developed specifically for high-quality maxillofacial hard tissue imaging, offers minimal distortion, shorter scanning times, and lower radiation doses compared to traditional computed tomography (CT).<sup>20</sup> The high contrast in CBCT images is particularly useful for evaluating bone structures, making it a more advantageous tool for craniofacial bone evaluation, especially before surgery.<sup>21</sup> CBCT has been shown to accurately determine the three-dimensional position of the MC.<sup>23</sup> It can measure the gap width between the MC and the external cortical bone (marrow space), which is critical for surgical planning in BSSRO. When the marrow space width is 0.8 mm or less, there is a higher likelihood of neurosensory complications.<sup>14</sup> However, there has been no study comparing the MC position between OP and CBCT images.

At the Faculty of Dentistry, Chulalongkorn University, the i-Dixel 2.0 3D Imaging Software (J Morita) is used to produce high-quality CBCT images with low radiation doses, utilizing a high-sensitivity, high-resolution

flat panel detector for multi-purpose diagnostic scanning in the maxillofacial region.<sup>24</sup>

This study aimed to investigate the MC anatomy in mandibular prognathism patients undergoing BSSRO and to compare the measurements obtained from OP and CBCT images.

## Materials and methods

This retrospective study was conducted on a cohort of Thai patients diagnosed with mandibular prognathism who underwent BSSRO at the Dental Hospital, Faculty of Dentistry, Chulalongkorn University. The selected patients had both pre-operative OP and CBCT images of the mandible. All CBCT images were performed using 3D Accuitomo170® (Morita, Osaka, Japan) with a resolution of 0.25 mm, 90 kVp, 5mA, standard mode, field of view (FOV) 10x10 cm<sup>2</sup>, and CB MercuRay® (Hitachi Medico Technology Corporation, Chiba-ken, Japan) with a resolution of 0.2 mm, 90 kVp, 5mA standard mode, FOV 150 mm.

### Data collection

#### Data from CBCT images

CBCT data were exported as digital and communication in medicine (DICOM) format and imported into a computer DELL OptiPlex745 using INFINITT PACS® software (Seoul, Korea) for image analysis. All measurements were performed by a single examiner, with an intra-Class correlation coefficient (ICC) greater than 0.75, indicating good reliability.

First, prior to the measurement of the location of the MC, the three planes were oriented. Cross-sectional images were generated perpendicular to the arch form of the mandible. In the axial view, the sagittal plane was adjusted parallel to the left or right side of the buccal cortex of the mandibular first and second molar region. The coronal plane was oriented to bisect the crown at the furcation area of the first molars and second molars in the sagittal view. Second, to locate the tip of the lingula, the sagittal plane was generated parallel to the buccal cortex of the mandible, and the coronal plane was generated to lingula area in the axial view. The sagittal plane in the coronal view was adjusted along to medial surface of the left or right ramus.

Five measurements were done from cross-sectional view of mandibular first molar and of second molar including: (A) outer diameter of MC, (B) distance of outer surface of buccal cortex to the buccal surface of MC, (C) distance of outer surface of lingual cortex to the lingual surface of MC, (D) distance of superior border of alveolar bone to superior surface of MC, (E) distance of outer surface of inferior cortex to inferior surface of MC (Fig. 2).<sup>4</sup> Moreover, the distances between the lingula tip and the ascending ramus's anterior border and to the sigmoid notch were measured from the sagittal view (Fig. 3).

#### Data from two-dimensional OP radiograph

The distances from the MF, the most anterior and superior border of the canal, to the anterior border of ascending ramus and to the sigmoid notch were recorded. The distances from MC to the superior border of alveolar bone and to the inferior border of mandible at the first and second molars were measured (Fig. 4).

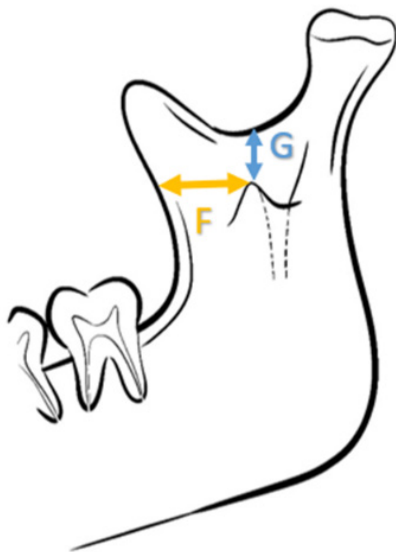


**Figure 3** The distances relating to the lingula measured in the sagittal plane, F: distance of the tip of lingula to the anterior border of ascending ramus, G: distance of the tip of lingula to sigmoid notch.

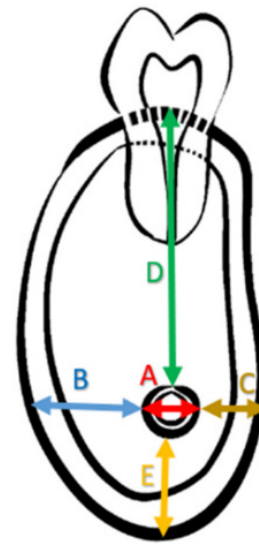


**Figure 2** The distances measured from a cross-sectional view at the mandibular first molar and second molar, A: outer diameter of the mandibular canal (MC), B: distance of the outer surface of buccal cortex to the buccal surface of MC, C: distance of the outer surface of lingual cortex to the lingual surface of MC, D: distance of superior border of alveolar bone to superior surface of MC, E: distance of outer surface of inferior cortex to inferior surface of MC.

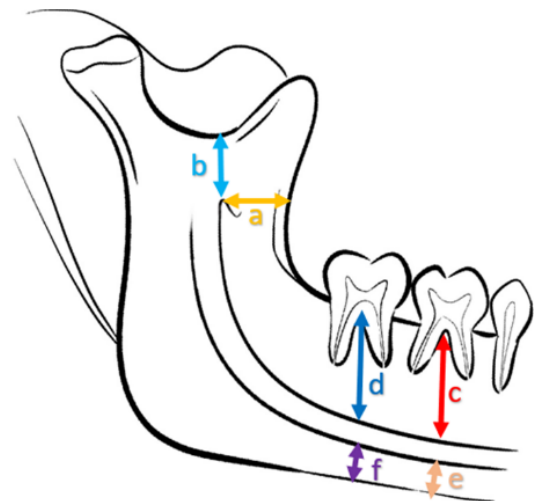


**Figure 4** Measurements performed in orthopantomogram image, a: distance from anterior border of mandibular foramen (MF) to anterior border of ascending ramus, b: distance from MF to sigmoid notch, c: distance from MC to superior border of alveolar bone at the first molar, d: distance from MC to superior border of alveolar bone at the second molar, e: distance from MC to inferior border of mandible at the first molar, f: distance from MC to inferior border of mandible at the second molar.



**Figure 5** Examples of measurement of images by image software, A: CBCT from a cross-sectional view, B: CBCT from a sagittal view, C: Measurements performed in orthopantomogram image.

## Data analysis

All statistical analyses were performed using SPSS software version 24 (IBM Corp., Chicago, IL, USA). As the data followed a normal distribution, an independent Student's *t*-test was applied. Paired Sample *t*-test was used to analyze differences between the left and right sides and between OP and CBCT radiographs. Pearson's correlation was used to analyze the corresponding distance between CBCT and OP images. The *p*-value less than .05 was considered a significant difference.

## Results

The study subjects consisted of CBCT and OP images from 27 patients (12 males and 15 females), whose ages ranged from 20 to 40 (average 26.3 years).

### Comparison of distances measured from CBCT and OP images

The measurements between CBCT and OP radiographs revealed statistically significant difference in distances of MF to the anterior border and to the sigmoid

notch ( $p < 0.001$  and  $p = 0.007$ , respectively) (Table 1).

### Comparison of the measured distances between the first and second molars

The distance of the outer surface of the buccal cortex to the buccal surface of MC (buccal thickness) of the mandibular second molar (left =  $7.37 \pm 1.72$  mm, right =  $7.31 \pm 1.60$  mm) was greater than that of the mandibular first molar (left =  $5.98 \pm 1.30$  mm, right =  $5.63 \pm 1.20$  mm). (Table 2 and Table 3).

### Comparison of the measured distances between sides

The distances of the lingula to the anterior border of ramus and from the buccal cortex to the MC at the mandibular first molar differed significantly between the left and right sides ( $p = 0.028$  and  $p = 0.025$ , respectively), while other distances showed no significant differences ( $p > 0.05$ ) (Table 2 and Table 3).

### Comparison of the measured distances between sexes

There were no significant differences in all measurements between males and females ( $p > 0.05$ ) (Table 3).

**Table 1** Comparison of Average Distances ( $\pm$  SD) Between CBCT and Panoramic Radiography (OP)

Measurement	CBCT (mm)	OP (mm)	<i>p</i> -value ( <i>t</i> -test)
Mandibular foramen to anterior border	$13.80 \pm 2.20$	$10.27 \pm 1.27$	$< 0.001^*$
Mandibular foramen to sigmoid notch	$15.89 \pm 2.00$	$14.93 \pm 2.25$	$0.007^*$
Superior cortex at the first molar	$16.40 \pm 2.26$	$16.47 \pm 2.38$	0.767
Superior cortex at the second molar	$12.38 \pm 2.25$	$12.56 \pm 2.01$	0.500
Inferior cortex at the first molar	$7.69 \pm 2.07$	$7.47 \pm 1.67$	0.323
Inferior cortex at the second molar	$7.94 \pm 2.02$	$7.75 \pm 1.88$	0.070

**Table 2** Comparison of Average Distances ( $\pm$  SD) Between Left and Right Sides Measured by CBCT

	Tooth	Left (mm)	Right (mm)	p-value (t-test)
Diameter	6	2.96 $\pm$ 0.52	2.94 $\pm$ 0.55	0.879
	7	3.17 $\pm$ 0.53	3.27 $\pm$ 0.49	0.382
Buccal cortex distance	6	5.98 $\pm$ 1.30	5.63 $\pm$ 1.20	0.025*
	7	7.37 $\pm$ 1.72	7.31 $\pm$ 1.60	0.103
Lingual cortex distance	6	2.28 $\pm$ 0.98	2.57 $\pm$ 0.99	< 0.001*
	7	2.44 $\pm$ 1.19	2.52 $\pm$ 0.99	0.713
Superior cortex distance	6	16.59 $\pm$ 2.42	16.24 $\pm$ 2.72	0.464
	7	12.16 $\pm$ 2.76	12.66 $\pm$ 2.34	0.290
Inferior cortex distance	6	7.36 $\pm$ 1.84	7.96 $\pm$ 2.57	0.073
	7	7.87 $\pm$ 2.17	7.94 $\pm$ 1.99	0.711
Mandibular foramen to anterior border		13.24 $\pm$ 2.24	14.33 $\pm$ 2.76	0.028*
Mandibular foramen to sigmoid notch		15.88 $\pm$ 2.50	15.83 $\pm$ 2.23	0.928

**Table 3** Comparison of Average Distances ( $\pm$  SD) Between Males and Females Measured by CBCT

	Tooth	Left (mm)	Right (mm)	p-value (t-test)
Diameter	6	2.92 $\pm$ 0.56	2.97 $\pm$ 0.34	0.800
	7	3.20 $\pm$ 0.49	3.23 $\pm$ 0.35	0.853
Buccal cortex distance	6	6.06 $\pm$ 0.94	5.60 $\pm$ 1.35	0.325
	7	7.85 $\pm$ 1.68	6.69 $\pm$ 1.33	0.056
Lingual cortex distance	6	2.12 $\pm$ 0.70	2.67 $\pm$ 0.97	0.108
	7	2.27 $\pm$ 1.04	2.65 $\pm$ 0.88	0.317
Superior cortex distance	6	16.16 $\pm$ 2.20	16.62 $\pm$ 2.36	0.609
	7	11.82 $\pm$ 2.09	12.88 $\pm$ 2.34	0.235
Inferior cortex distance	6	8.24 $\pm$ 1.79	7.19 $\pm$ 2.22	0.196
	7	8.57 $\pm$ 1.83	7.37 $\pm$ 2.06	0.125
Mandibular foramen to anterior border		14.17 $\pm$ 2.04	13.47 $\pm$ 2.34	0.422
Mandibular foramen to sigmoid notch		16.60 $\pm$ 1.57	15.26 $\pm$ 2.16	0.083

## Discussion

The MF is the opening on the internal surface of the mandibular ramus through which the MC passes. The lingula of the mandible is a bone projection on the medial aspect of the ramus and lies close to the MF. Therefore, the lingula is an important anatomical landmark for locating the IAN before it enters the mandible. The position of lingula and MF varies from person to person. From the Taiwanese study, the distances from the sigmoid notch to MF measured by CBCT were 22.7 mm in males and 20.59 mm in females.<sup>18</sup> The distances measured by CBCT in Korean patients were 21.59 mm in skeletal Class I, 20.49 mm in skeletal Class II, and 18.77 mm in skeletal Class III.<sup>25</sup>

The distances from anterior border of ramus to MF in Taiwanese patients measured by CBCT were 18.00 mm and 19.30 mm in women and men, respectively.<sup>18</sup> In Korean patients, CBCT measurements showed distances of 19.41 mm in skeletal Class I, 19.01 mm in the skeletal Class II, and 19.85 mm in the skeletal Class III.<sup>25</sup> From our study, the distances from the sigmoid notch to MF and from the anterior border of the ramus to MF were shorter compared to those of other studies. Some possible explanations for this discrepancy may be 1) the varied craniofacial morphology across ethnicities and populations, 2) the use of different imaging technologies and software platforms, or 3) the



measurement method (e.g., manual vs software-assisted measurements).

From another perspective, the thickness of the buccal cortical bone (the distance from the buccal surface of the mandible to the MC) is a critical factor in ensuring the safety of the vertical osteotomy cut in the BSSRO procedure. Consistent with the findings of Nagadia *et al.*,<sup>4</sup> the greatest distance from the buccal cortex to the MC was observed in the second molar region, indicating that the buccal bone is thicker there than in the first molar region. Therefore, performing osteotomy at the second molar region is considered safer. This information is particularly valuable in skeletal Class III patients, for whom BSSRO is typically performed as a setback procedure. In such cases, it is unnecessary to extend the vertical cut anteriorly to the first molar region, as is often required in BSSRO advancement for skeletal Class II patients to achieve sufficient bone contact. When comparing buccal bone thickness between the left and right sides of the mandible, a statistically significant difference was found at the first molar region. Further studies with more robust designs are needed to clarify the underlying cause of this asymmetry.

Although Hoseini Zarch *et al.*,<sup>27</sup> reported that linear measurements on OP are generally more reliable in the posterior region than in the anterior region, our findings demonstrated significant discrepancies in measurements at the ramus region between CBCT and OP radiographs. This may be attributed to the susceptibility of panoramic radiographs to distortion, which can result from patient positioning errors and the inherent limitations of the two-dimensional imaging technique.<sup>28,29</sup>

CBCT imaging is particularly valuable when assessing complex anatomical structures in the mandible due to its ability to provide three-dimensional view. This imaging modality offers numerous advantages over traditional two-dimensional imaging methods, such as OP, in several key areas: (1) Enhanced Visualization: CBCT allows the detailed visualization of critical anatomical landmarks, including the lingula, borders of the mandible, and the MC. This degree of clarity aids in precise surgical planning. (2) High Contrast Resolution: The high contrast resolution provided by CBCT enables practitioners to distinguish

between closely situated structures, such as root tips, which is particularly crucial when close to vital nerves and blood vessels. A systematic review by Haas *et al.*<sup>30</sup> explains a remarkably high frequency of variation of MC detected by CT or CBCT compared with OP. (3) Pre-operative Planning: Prior to major surgical procedures, such as osteotomies, utilizing CBCT enables surgeons to assess the spatial relationship between the MC and other vital structures. This pre-operative evaluation is essential for reducing the risk of injury to these structures, thus mitigating complications during and after surgery. (4) 3D Reconstruction: CBCT imaging can produce 3D reconstruction of the mandible, providing a comprehensive view that allows for more accurate analysis of the path of the IAN and the location of the MC compared to traditional imaging methods. In summary, incorporating CBCT into the pre-operative workflow improves surgical outcomes by enhancing the surgeon's ability to visualize and plan for anatomical complexities, ultimately leading to a reduction in the risk of complications associated with nerve and vascular injuries. A Systematic review by Araujo *et al.*<sup>26</sup> showed a significant influence of CBCT versus OP to avoid injury to vital structures during third molar surgical procedure. This technology represents a significant advancement in the field of dental surgery, aligning with modern practices aimed at enhancing patient safety and care.

Limitations of our study include a relatively small sample size and the lack of data on normal jaw relationship in the Thai population for comparison. The effect of missing first or second molars on the MC morphology cannot be underestimated, as bone resorption and bone remodeling usually follow dental extraction, which can affect the position of the MC. Further studies may evaluate the post-operative complications after follow-up and may explore other mandibular Classifications such as retrognathism.

## Conclusion

The differences between preoperative measurements from CBCT and OP highlight the importance of using the appropriate imaging modality. CBCT provides three-dimensional views and more accurate spatial relationships, which are crucial for assessing the position of the inferior

alveolar canal, especially in the mandibular ramus. This can help to reduce the risk of complications during osteotomies or other surgical procedures. Performing a vertical osteotomy at the second molar area, where the buccal bone is thicker and the inferior alveolar canal is more favorably positioned, may reduce the risk of nerve injury and improve healing. Overall, utilizing CBCT for preoperative evaluation in cases requiring surgical intervention in the mandible is recommended. It allows for a more thorough understanding of anatomical variations and potential risks, leading to a more refined approach to surgical planning and execution. This careful evaluation ultimately aims to enhance patient safety and surgical outcomes.

## Acknowledgement

We thank Assistant Prof. Dr. Soranun Chandransu for her advice on statistical analysis.

**Funding:** This study was supported by the Dental Research Fund, Dental Research Project 3200502#22/2016, Faculty of Dentistry, Chulalongkorn University

## References

1. Park CG, Yoo JW, Park IC. Surgical treatment of mandibular prognathism in collaboration with orthodontic treatment in Korea. *Aesthetic Plast Surg* 1994;18(4):407-12.
2. Chang HP, Tseng YC, Chang HF. Treatment of mandibular prognathism. *J Formos Med Assoc* 2006;105(10):781-90.
3. Nesari S, Kahnberg KE, Rasmusson L. Neurosensory function of the inferior alveolar nerve after bilateral sagittal ramus osteotomy: a retrospective study of 68 patients. *Int J Oral Maxillofac Surg* 2005;34(5):495-8.
4. Nagadia R, Tay AB, Chan LL, Chan ES. The spatial location of the mandibular canal in Chinese: a CT study. *Int J Oral Maxillofac Surg* 2011;40(12):1401-5.
5. Miloro M, Ghali GE, Larsen PE, Waite PD. Peterson's principles of oral and maxillofacial surgery. 2nd ed. Hamilton, Ont. ; London: BC Decker; 2004.
6. Panula K, Finne K, Oikarinen K. Incidence of complications and problems related to orthognathic surgery: a review of 655 patients. *J Oral Maxillofac Surg* 2001;59(10):1128-36; discussion 37.
7. Bays RA, Bouloux GF. Complications of orthognathic surgery. *Oral Maxillofac Surg Clin North Am* 2003;15(2):229-42.
8. Eshghpour M, Shaban B, Shahakbari R, Shamsabadi RM, Nejat AH. Complications of Bilateral Sagittal Split Osteotomy in Patients with Mandibular Prognathism. *JDMT*. 2014;3. Doi: 10.22038/jdmt.2013.2050
9. Phillips C, Essick G, Preisser JS, Turvey TA, Tucker M, Lin D. Sensory retraining after orthognathic surgery: effect on patients' perception of altered sensation. *J Oral Maxillofac Surg* 2007;65(6):1162-73.
10. Lee JH, Son YJ, Hwang JH, Baek SH, Jeon JH. Influence of anatomic position and intraoperative exposure of the inferior alveolar nerve on neurosensory disturbance after sagittal split ramus osteotomy: a three-dimensional computed tomography study. *Oral Surg Oral Med Oral Pathol Oral Radiol* 2016;122(3):300-5.
11. Rajchel J, Ellis E 3rd, Fonseca RJ. The anatomical location of the mandibular canal: its relationship to the sagittal ramus osteotomy. *Int J Adult Orthodon Orthognath Surg* 1986;1(1):37-47.
12. Ylikontiola L, Moberg K, Huuonen S, Soikkonen K, Oikarinen K. Comparison of three radiographic methods used to locate the mandibular canal in the buccolingual direction before bilateral sagittal split osteotomy. *Oral Surg Oral Med Oral Pathol Oral Radiol Endod* 2002;93(6):736-42.
13. Sekerci AE, Sahman H. Cone beam computed tomographic analyses of the position and course of the mandibular canal: relevance to the sagittal split ramus osteotomy. *Biomed Res Int* 2014;2014:945671.
14. Yamamoto R, Nakamura A, Ohno K, Michi KI. Relationship of the mandibular canal to the lateral cortex of the mandibular ramus as a factor in the development of neurosensory disturbance after bilateral sagittal split osteotomy. *J Oral Maxillofac Surg* 2002;60(5):490-5.
15. Chrcanovic BR, de Carvalho Machado V, Gjelvold B. A morphometric analysis of the mandibular canal by cone beam computed tomography and its relevance to the sagittal split ramus osteotomy. *Oral Maxillofac Surg* 2016;20(2):183-90.
16. Levine MH, Goddard AL, Dodson TB. Inferior alveolar nerve canal position: a clinical and radiographic study. *J Oral Maxillofac Surg* 2007;65(3):470-4.
17. Falkine RZ, Rossi AC, Freire AR, Figueroba SR, Groppo FC, Caria PHF, et al. Relations Between the Mandibular Canal and I, II and III Angle Classes in Panoramic Radiographs. *Int J Morphol* 2014;32(2):449-54.
18. Yu IH, Wong YK. Evaluation of mandibular anatomy related to sagittal split ramus osteotomy using 3-dimensional computed tomography scan images. *Int J Oral Maxillofac Surg* 2008;37(6):521-8.
19. da Fontoura RA, Vasconcellos HA, Campos AE. Morphologic basis for the intraoral vertical ramus osteotomy: anatomic and radiographic localization of the mandibular foramen. *J Oral Maxillofac Surg* 2002;60(6):660-5; discussion 5-6.
20. Ludlow JB, Davies-Ludlow LE, Brooks SL, Howerton WB. Dosimetry of 3 CBCT devices for oral and maxillofacial radiology: CB Mercuray, NewTom 3G and i-CAT. *Dentomaxillofac Radiol* 2006;35(4):219-26.
21. Scarfe WC, Farman AG, Sukovic P. Clinical applications of cone-beam computed tomography in dental practice. *J Can Dent Assoc* 2006;72(1):75-80.
22. Nair UP, Yazdi MH, Nayar GM, Parry H, Katkar RA, Nair MK. Configuration of the inferior alveolar canal as detected by cone beam computed tomography. *J Conserv Dent* 2013;16(6):518-21.

23. Kwon KH. Evaluation of the course of the inferior alveolar canal in the mandibular ramus using cone beam computed tomography. *J Korean Assoc Oral Maxillofac Surg* 2012;38(4):231-9.
24. J. MORITA USA I. i-Dixel 2.0 3D Imaging Software. 2017.
25. Park HS, Lee JH. A Comparative Study on the Location of the Mandibular Foramen in CBCT of Normal Occlusion and Skeletal Class II and III Malocclusion. *Maxillofac Plast Reconstr Surg* 2015;37(1):25.
26. Araujo GTT, Mamani MP, Silva AFMD, Rubira CMF, Honório HM, Rubira-Bullen IRF. Influence of cone beam computed tomography versus panoramic radiography on the surgical technique of third molar removal: a systematic review. *Int J Oral Maxillofac Surg* 2019;48(10):1340-7.
27. Hoseini Zarch SH, Bagherpour A, Javadian Langaroodi A, Ahmadian Yazdi A, Safaei A. Evaluation of the accuracy of panoramic radiography in linear measurements of the jaws. *Iran J Radiol* 2011;8(2):97-102.
28. Suparno N, Faizah A, Nafisah A. Assessment of Panoramic Radiograph Errors: An Evaluation of Patient Preparation and Positioning Quality at Soelastri Dental and Oral Hospital. *Open Dent J* 2023;17: e187421062309120.
29. Dhillon M, Raju SM, Verma S, Tomar D, Mohan RS, Lakhnarpal M, *et al*. Positioning errors and quality assessment in panoramic radiography. *Imaging Sci Dent* 2012;42(4):207-12.
30. Haas LF, Dutra K, Porporatti AL, Mezzomo LA, Canto GDL, Flores-Mir C, *et al*. Anatomical variations of mandibular canal detected by panoramic radiography and CT: a systematic review and meta-analysis. *Dentomaxillofac Radiol* 2016;45(2):20150310.

# Inflammatory Response and Proliferation of Stem Cells Isolated from Human Exfoliated Deciduous Teeth to Lipopolysaccharide from *Porphyromonas Gingivalis*

Panicha Sroithong<sup>1</sup>, Waleerat Sukarawan<sup>1</sup>, Thanaphum Osathanon<sup>2</sup>

<sup>1</sup>Department of Pediatric Dentistry, Faculty of Dentistry, Chulalongkorn University, Bangkok, Thailand

<sup>2</sup>Department of Anatomy, Faculty of Dentistry, Chulalongkorn University, Bangkok, Thailand

## Abstract

The effects of various concentrations of 0.01, 0.1, and 1.0 µg/mL of lipopolysaccharide (LPS) from *Porphyromonas gingivalis* (*P. gingivalis*) on inflammatory response and proliferation of stem cells isolated from human exfoliated deciduous teeth (SHEDs) were compared. The MTT test was utilized to assess cell growth. Our research indicated that *P. gingivalis* LPS administration did not influence the proliferation of SHEDs. The expression levels of *IL1B*, *IL6*, and *IFNG* escalated in a dose-dependent way. Statistical significance was noted in the expression of *IL1B* at a concentration of 0.1 µg/mL of *P. gingivalis* LPS ( $p < 0.05$ ) and in the expression of *IL6* at a concentration of 1.0 µg/mL of *P. gingivalis* LPS ( $p < 0.05$ ). Moreover, treatment with *P. gingivalis* LPS at doses of 0.01 and 0.1 µg/mL resulted in enhanced TNF gene expression. Notably, at the maximum concentration (1.0 µg/mL), the gene expression level substantially diminished. Statistical significance was observed just in the expression of TNF at a concentration of 0.1 ( $p < 0.05$ ). In conclusion, within the limitation of this study, findings indicate that 0.1 µg/mL *P. gingivalis* LPS is the optimal concentration for subsequent experiments involving SHEDs.

**Keywords:** Cell proliferation, *P. gingivalis* lipopolysaccharide (*P. gingivalis* LPS), Pro-inflammatory cytokines, SHEDs

Received date: Apr 3, 2025

Revised date: Jun 17, 2025

Accepted date: Jun 25, 2025

Doi: 10.14456/jdat.2025.22

## Correspondence to:

Waleerat Sukarawan, Department of Pediatric Dentistry, Faculty of Dentistry, Chulalongkorn University, 34 Henri-Dunant Road, Wangmai, Patumwan, Bangkok 10330, Thailand. Tel: 02-218-8906 E-mail: wsukarawan@hotmail.com

## Introduction

Pulpitis is among the most common dental infections. Teeth affected by pulpitis frequently lead to various physiological and pathological changes, such as localized inflammation, edema, and congestion of the pulp tissue.<sup>1</sup> Moreover, pulpal infection that extends beyond the periodontium in deciduous teeth may adversely affect the development of permanent tooth germs. *Porphyromonas gingivalis* (*P. gingivalis*) is a gram-negative anaerobic bacillus that is frequently encountered as a pathogen in dental pulp infections and has been recognized as the causative

agent in the first stages of pulp and periodontal disease.<sup>2,3</sup> A critical virulence factor of *P. gingivalis* is lipopolysaccharide (LPS), a major component of the outer membrane of gram-negative bacteria and serves as a strong endotoxin exhibiting a wide range of biological action.<sup>4</sup> The host response to LPS is primarily mediated through its recognition by Toll-like receptor 4 (TLR4), which, upon activation, initiates intracellular signaling cascades such as the NF- $\kappa$ B and MAPK pathways via Myeloid differentiation primary response 88 (MyD88) dependent signaling.<sup>5,6</sup> NF- $\kappa$ B plays a critical role



in the migration and adhesion of various cell types.<sup>7,8</sup> Moreover, IFNG regulates the odonto/osteogenic differentiation of dental pulp stem cells (DPSCs) through both NF- $\kappa$ B and MAPK signaling pathways.<sup>9</sup> MAPK has also been associated with the proliferation of endothelial progenitor cell-like cells generated from the periodontal ligament (PDL) via MEK/ERK and JNK-mediated signaling pathways.<sup>10</sup> *Porphyromonas gingivalis* lipopolysaccharides (*P. gingivalis* LPS) initiates the inflammatory process by inducing the expression of pro-inflammatory cytokines and chemokines such as interleukin 1 beta (*IL1B*), *IL6*, *IL8*, *TNF* in periodontal ligament stem cells (PDLSCs)<sup>11</sup> and human monocytic cell.<sup>12</sup> Consequently, DNA methylation or the expression of microRNAs alters gene expression.<sup>6</sup> Considering this, there is growing interest in understanding how *P. gingivalis* LPS affects various stem cell populations relevant to dental tissue repair and regeneration, particularly stem cells from human exfoliated deciduous teeth (SHEDs).

SHEDs are a type of mesenchymal stem cells (MSCs) capable of multipotential differentiation, including osteoblastic/odontogenic, adipogenic, neurogenic, and angiogenic differentiation after induction.<sup>13</sup> SHEDs are isolated from dental pulp tissues that remain in naturally shedding deciduous teeth, making them easily accessible without requiring invasive procedures for cell collection. SHEDs offer distinct advantages over other MSC sources, including non-invasive collection, high proliferation, and potent regenerative capacity, supporting their relevance for inflammation-related studies in dental tissues. Several studies have examined the effect of the inflammatory microenvironment on the proliferative potential, multilineage differentiation, migration, and inflammatory cytokine secretion of oral MSCs. Notably, SHEDs have been shown to express Toll-like receptors TLR2 and TLR4, enabling them to respond to LPS.<sup>14</sup> Of particular interest is the response of SHEDs to *P. gingivalis* LPS, although current findings remain inconsistent due to variations in MSC sources, inflammatory stimuli types and concentrations, and experimental designs.<sup>15</sup> Previous studies have reported that *P. gingivalis* LPS can promote cell proliferation in PDLSCs<sup>11</sup> and fibroblasts,<sup>16</sup> whereas other reports suggest

that *P. gingivalis* LPS inhibit proliferation in dental follicle progenitor cells (DFPCs).<sup>17</sup> A similar inhibitory effect was observed in PDLSCs, where *P. gingivalis* LPS suppressed cell proliferation via TLR4 activation, increased reactive oxygen species (ROS) production, induced apoptosis, and altered the cell cycle through upregulation of cyclins D1, A, and B1.<sup>18</sup> Furthermore, *P. gingivalis* LPS has been shown to stimulate bone marrow mesenchymal stem cell (BMMSC) proliferation at low concentrations while inhibiting it at higher doses.<sup>19</sup> These conflicting results may stem from differences in LPS concentration, exposure duration, or donor variability, suggesting that the cellular response to *P. gingivalis* LPS may be dose- and context-dependent.

Despite this growing body of evidence, no studies have specifically investigated the effects of *P. gingivalis* LPS on SHEDs, representing a critical gap in understanding their roles in tooth tissue regeneration. Therefore, the purpose of this study is to examine how *P. gingivalis* LPS affects SHEDs, including the expression of pro-inflammatory cytokine genes and cell proliferation. The results of this study will facilitate the establishment of SHEDs for dental tissue regeneration and may contribute to the development of a new valuable pulp treatment protocol in the future.

## Materials and Methods

### Cell Isolation and culture of SHEDs

SHEDs were obtained from healthy pediatric patients aged 7-10 years, from deciduous teeth with no carious lesions or pathologic lesions. The teeth were extracted following the treatment plan such as prolonged retention teeth and stored in a culture medium. Ethical approval was submitted by the Ethics Committee, Faculty of Dentistry, Chulalongkorn University (approval no. 018/2023). The study protocol and informed consent were provided to the child's parent. To clarify, extracted teeth were washed three times with sterile phosphate buffer saline (PBS). The pulp tissues were carefully removed from the teeth and cut into small pieces with a surgical blade and placed on a 35-mm tissue culture plate (Corning, New York, NY, USA) containing Dulbecco's Modified Eagle Medium (DMEM, Gibco, USA) supplemented with 10% fetal bovine serum

(HyClone, USA (Gibco, USA), 2mM L-glutamine (Gibco, USA), 100 Units/ml Penicillin (Gibco, USA), 100 µg/mL Streptomycin (Gibco, USA), and 5 µg/mL Amphotericin B (Gibco, USA). The cell explants were incubated at 37°C in a humidified atmosphere of 5 %CO<sub>2</sub> in the air. The medium was changed every two days. When cell confluence was achieved, cells were detached with 0.25 % trypsin-EDTA (Gibco, USA) and subcultured at a 1:3 ratio into 60-mm tissue culture plates for the first passage. Cells from passages 3-6 were used for subsequent experiments.

**Characterization of SHEDs**

To characterize the cells, cultured cells were tested for properties as multipotent mesenchymal stem cells by plastic adhesion, shape, and morphology, as well as for their multipotential differential differentiation ability, using *in vitro* mineralization. Flow cytometry was used to determine the expression of cell surface antigens in SHEDs cells. Single cell suspensions were obtained by detaching cells with 0.25 % trypsin-EDTA solution. Cells were centrifuged and the supernatant culture medium was discarded. Then, cells were rinsed with PBS and stained with primary antibodies conjugated to fluorescent dye, including FITC-conjugated anti-human CD44 (BD Bioscience Pharmingen, USA), FITC-conjugated anti-human CD90 (BD Bioscience Pharmingen, USA), and PerCP-conjugated anti-human CD45 (BD Bioscience Pharmingen, USA). Stained cells were analyzed using a FACS<sup>Calibur</sup> flow cytometer using the CellQuest software (BD Biosciences, USA).

**LPS media preparation and treatment of SHEDs with various LPS concentrations**

*P. gingivalis* LPS powder purified by phenol extraction (Sigma-Aldrich, USA) was dissolved in endotoxin-free water and homogenized to prepare the *P. gingivalis* LPS stock solution of 1 mg/mL. From this, a series of concentrations namely 0.01, 0.1, and 1.0 µg/mL were prepared via serial solution.

**Pro-inflammatory cytokine gene expression**

SHEDs were seeded at a density of 100,000 cells/well in 12-well plates in culture medium and incubated for 24 hours to allow cell attachment. The medium was changed to serum-free medium with various *P. gingivalis* LPS concentrations for 24 hours. The expression levels

of pro-inflammatory cytokines were determined by quantitative RT-PCR (qRT-PCR). The extraction of cellular RNA was performed using Trizol Reagent, following the guidelines provided by the manufacturer and converted into complementary DNA (cDNA) by using reverse transcriptase iScript cDNA Synthesis Kits (Bio-Rad, USA). After that, qPCR was performed on MiniOpticon real-time PCR system (Bio-Rad, USA) using FastStart Essential DNA Green Master kit (Roche Diagnostic, USA). Glyceraldehyde 3-phosphate dehydrogenase (GAPDH) gene was used for normalization of each sample as the housekeeping gene. The primer sequences for qRT-PCR are listed in Table 1.

**Table 1** Primer sequences of pro-inflammatory cytokine genes used in this study

Gene	Primer sequence
<i>GAPDH</i>	Forward: 5' CAC TGC CAA CGT GTC AGT GGT G' Reverse: 5' GTA GCC CAG GAT GCC CTT GAG 3'
<i>IL1B</i>	Forward: 5' GCA GAA GTA CCT GAG CTC GC 3' Reverse: 5' CTT GCT GTA GTG GTG GTC GG 3'
<i>IL6</i>	Forward: 5' CCT GAA CCT TCC AAA GAT GGC 3' Reverse: 5' CTG ACC AGA AGA AGG AAT GCC 3'
<i>IFNG</i>	Forward: 5' CCA ACT AGG CAG CCA ACC TAA 3' Reverse: 5' AGC ACT GGC TCA GAT TGC AG 3'
<i>TNF</i>	Forward: 5' CAC AGT GAA GTG CTG GCA AC 3' Reverse: 5' ACA TTG GGT CCC CCA GGA TA 3'

**Cell proliferation assay**

SHEDs were seeded at a density of 25,000 cells/well in 24-well plates in culture medium. After 24 hours, the culture medium was replenished with fresh medium containing the respective concentrations of *P. gingivalis* LPS, and this process was repeated three times for each concentration. On days 1, 3, and 7, changes in cell growth viability were analyzed using the 3-(4,5-dimethylthiazol-2-yl)-2,5-diphenyltetrazolium bromide (MTT) assay. The existing medium in every well were removed and replaced with 300 µL MTT solution (USB Corporation, USA) for 15 minutes at 37°C in a humidified atmosphere of 5 % CO<sub>2</sub> to allow formazan crystal formation. Next, the formazan was dissolved using eluting agents that contained dimethylsulfoxide and glycine buffer. The solutions were determined for optical density (OD) by a microplate reader

(ELx800; BIO-TEK®) at 570 nm. using the vehicle-treated group as the baseline for comparison.

### Statistical analysis

The experiments were duplicated using cells obtained from at least four different donors (n=4). Data were reported in the form of mean  $\pm$  standard deviation (SD). The statistical analysis of the results was performed using the Kruskal-Wallis test and Dunn's multiple comparison test. The statistical analyses were created using GraphPad Prism 10.2.3 (GraphPad Software, CA, USA). A *p*-value of less than 0.05 was considered statistically significant.

## Results

### Isolation and characterization of SHEDs

Cells isolated from primary teeth were characterized by spindle-shaped, fibroblast-like morphology and formed distinguishable colonies (Fig. 1a). Flow cytometry analysis demonstrated the presence of mesenchymal stem cell markers CD44 (99.36) and CD90 (99.87), while the hematopoietic cell marker CD45 was absent (2.69) (Fig. 1b). Upon osteogenic induction, these cells exhibited increased mineral deposition compared to undifferentiated control cells, indicating their osteoblastic potential (Fig. 1c).

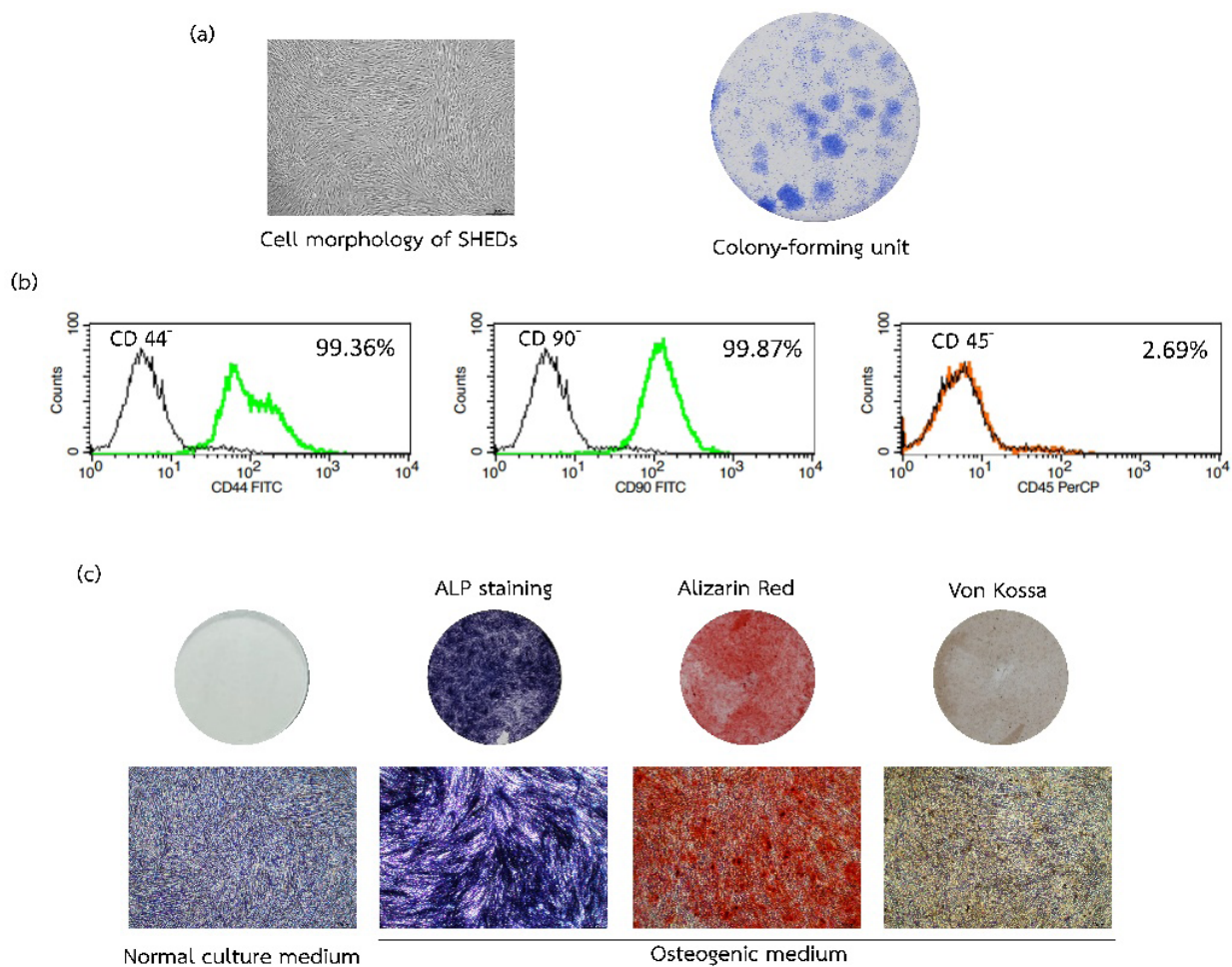


**Figure 1** Characterization of the cells isolated from dental pulp tissues. (a) Cell morphology of isolated cells from primary teeth exhibited a spindle-like morphology under phase-contrast microscopy (left) (scale bar at 4X = 300  $\mu$ m.) and colony forming unit ability (right). (b) Presence of mesenchymal stem cell markers CD44 and CD90 by flow cytometric analysis, and the absence of the hematopoietic marker CD45. (black line: negative control) (c) The osteogenic differentiation was examined using alkaline phosphatase on day 7, Alizarin Red S and Von Kossa staining on day 14 after osteogenic induction (Scale bar at 4X = 300  $\mu$ m.)

***P. gingivalis* LPS Upregulates Pro-inflammatory Cytokine Gene Expression**

Upon *P. gingivalis* LPS treatment, qRT-PCR revealed an upregulation in the expression of *IL1B*, *IL6* and *IFNG* in a dose-dependent manner. Statistical significance was observed in the expression of *IL1B* when cells were treated with 0.1 µg/mL of *P. gingivalis* LPS ( $p<0.05$ ) (Fig. 2a) and the expression of *IL6* at concentration of 1.0 µg/mL of

*P. gingivalis* LPS ( $p<0.05$ ) (Fig. 2b). Furthermore, exposure to *P. gingivalis* LPS also induced increased gene expression levels of *TNF* when treated with concentrations of 0.1 µg/mL (Fig. 2c). Interestingly, at the highest concentration (1.0 µg/mL), the gene expression level gradually decreased (Fig. 2c). However, statistical significance was only observed in the expression of *TNF* at concentrations of 0.1 ( $p<0.05$ ) (Fig. 2c).

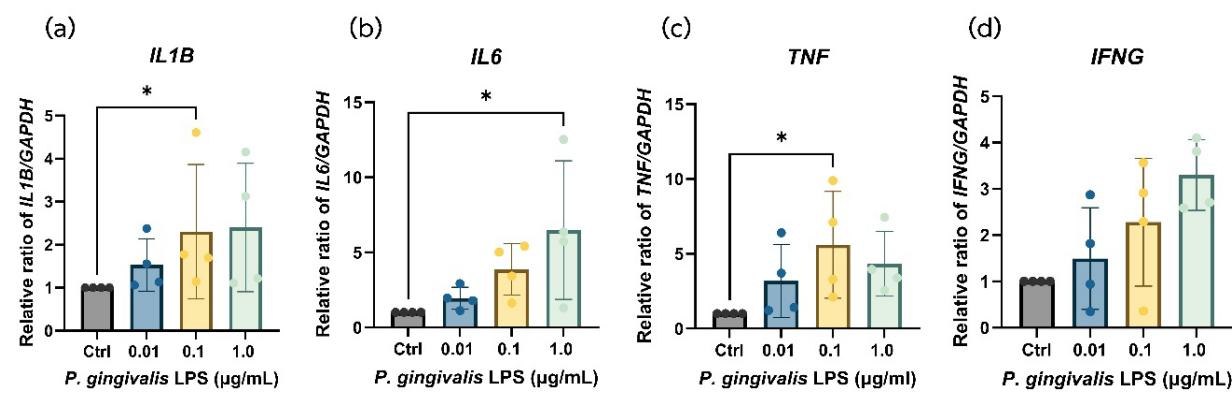


**Figure 2** The effect of *P. gingivalis* LPS on the expression of pro-inflammatory cytokines of SHEDs. The relative gene expression of (a) *IL1B*, (b) *IL6*, (c) *TNF*, and (d) *IFNG* in SHEDs after treatment with *P. gingivalis* LPS at concentrations of 0.01, 0.1, and 1.0 µg/mL were compared to SHEDs without *P. gingivalis* LPS treatment. Data are shown as mean  $\pm$  SD. Statistical analysis was performed using the Kruskal-Wallis test with Dunn’s multiple comparison ( $n=4$ ); \* $p < 0.05$

**Effects of *P. gingivalis* LPS on the proliferation of SHEDs**

Results revealed no statistically significant difference in cell proliferation ability between the control group and

the experimental groups treated with *P. gingivalis* LPS at concentrations of 0.01, 0.1, and 1.0 µg/mL ( $p>0.05$ ) (Fig. 3).

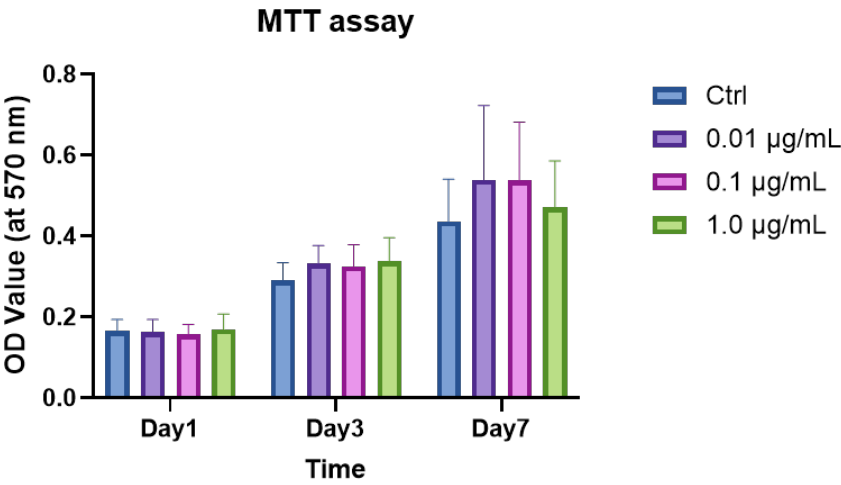


**Figure 3** The effect of *P. gingivalis* LPS on the proliferation of SHEDs. Increasing *P. gingivalis* LPS concentration did not result in statistically different cell proliferative ability between the control group and the experimental groups ( $p>0.05$ ). Data are shown as mean  $\pm$  SD. Statistical analysis was conducted using the Kruskal-Wallis test with Dunn’s multiple comparison ( $n=4$ )



## Discussion

This study is the first to explore the effects of *P. gingivalis* LPS on SHEDs, particularly at low concentrations. Our findings offer valuable insight into how clinically relevant LPS stimuli may influence SHEDs behavior in the context of dental inflammation and regeneration.

Dental caries is a chronic infectious condition driven by oral bacterial invasion into enamel and dentin. As the infection progresses, bacterial toxins such as LPS induces inflammation, triggering a host immune response and initiating tissue repair through the formation of tertiary dentin mediated by dental stem cells.<sup>20-22</sup> Among the various LPS sources studied, *P. gingivalis* LPS stands out due to its relevance in mimicking the pathophysiological environment of the carious pulp.<sup>23</sup> While *Escherichia coli* (*E. coli*) LPS has been shown to be a potent stimulator of immune responses in dental stem cells, its clinical relevance remains debated.<sup>24-27</sup> In contrast, although *P. gingivalis* LPS is less potent, it more accurately reflects the natural inflammatory processes occurring in carious lesions and may therefore serve as a superior model for studying pulpal inflammation.<sup>24,28</sup>

Our preliminary results confirmed that *P. gingivalis* LPS at concentration lower than 0.01 µg/mL had minimal impact on SHEDs proliferation, while higher concentration (10 µg/mL) had deleterious effects. Based on these observations, we focused on a dose range of 0.01–1.0 µg/mL for subsequent experiments. *P. gingivalis* LPS exposure led to a dose-dependent increase in pro-inflammatory cytokine gene expression, specifically *IL1B*, *IL6*, and IFNG. Statistically significant upregulation of *IL1B* and *IL6* was observed at 0.1 µg/mL and 1.0 µg/mL, respectively ( $p < 0.05$ ) (Fig. 2a-b), consistent with previous findings in PDLSCs treated with 1 µg/mL *P. gingivalis* LPS.<sup>11</sup> TNF expression also increased at 0.1 µg/mL *P. gingivalis* LPS, similar to trends reported in DPSCs and stem cell from the apical papilla (SCAPs) exposed to *P. gingivalis* LPS.<sup>29,30</sup> Interestingly, TNF levels declined at 1.0 µg/mL but remained elevated compared to control levels, indicating a possible threshold effect or feedback regulation. Notably, while these cytokines are known for their pro-inflammatory roles, they also contribute to regenerative signaling cascades, particularly

those involved in odontoblastic differentiation and reparative dentinogenesis. This dual role highlights the complexity of interpreting inflammatory cytokine profiles, as they may simultaneously mediate damage and repair.<sup>31,32</sup>

In terms of cell proliferation, *P. gingivalis* LPS at concentration below 1.0 µg/mL produced a mild increase in SHEDs proliferation by day 7; however, this effect did not reach statistical significance (Fig. 3). The concentration of 0.1 µg/mL *P. gingivalis* LPS was found to preserve SHEDs viability, suggesting it may represent a biologically relevant dose for mimicking mild inflammatory conditions *in vitro*. These results are partially aligned with earlier studies demonstrating enhanced PDLSCs proliferation at 10 µg/mL *P. gingivalis* LPS<sup>11</sup> and increased BMMSC proliferation at 0.1 µg/mL, whereas higher concentrations were inhibitory.<sup>19</sup> A similar biphasic response was also noted in DPSCs treated with *E. coli* LPS.<sup>33</sup> However, other cell types such as SCAPs, DFPCs, and BMMSCs have shown no significant proliferative response to *P. gingivalis* LPS<sup>34,35</sup>, reinforcing the notion that LPS effects are highly context-dependent. These variations may also reflect inherent differences between permanent and deciduous tooth-derived stem cells, as SHEDs possess higher proliferative capacity and neurotrophic potential compared to other dental stem cell types. Thus, SHEDs offer a unique and underutilized *in vitro* model for examining host–pathogen interactions specific to primary dentition, which is especially relevant in pediatric oral health research. A limitation of this study is that it focused solely on cell proliferation; the potential effects of *P. gingivalis* LPS on SHEDs differentiation were not evaluated. As LPS may influence differentiation without affecting viability, this warrants further investigation in future studies.

The discrepancies observed among different studies likely stem from several factors, including heterogeneity in donor cell sources (genetic background, age, gender), the stage of cellular differentiation, and inter-individual variability that may affect stem cell bioactivity.<sup>24</sup> Methodological variables such as culture duration, frequency of medium changes, and experimental timelines also influence outcomes. Importantly, differences in the molecular structure



of LPS especially the lipid A moiety and variations in receptor binding affinity further complicate interpretations. For instance, The activation of *E. coli* LPS in dental pulp cells is initiated through pattern recognition receptors (PRRs), such as TLR4 and TLR2, located on the cell membrane.<sup>24</sup> These receptors detect pathogen-associated molecular patterns (PAMPs) like LPS and trigger downstream inflammatory signaling pathways. These include the MyD88-dependent pathway, NF- $\kappa$ B signaling, MAPK activation via TIR domain-containing adaptors, and the PI3K-Akt pathway, all of which contribute to the production of pro-inflammatory cytokines.<sup>32</sup> However, the interaction of *P. gingivalis* LPS with TLR2 and TLR4 remains controversial. While *E. coli* LPS increases TLR4 expression without affecting TLR2 in DPSCs, *P. gingivalis* LPS does not appear to alter the expression of either receptor in these cells.<sup>24</sup> Therefore, examining the effects of *P. gingivalis* LPS on TLR2 and TLR4 expression in SHEDs may help determine whether *P. gingivalis* LPS activates similar signaling pathways, providing further insight into immune response mechanisms in dental pulp-derived stem cells. Whether *P. gingivalis* LPS activates SHEDs via TLR2, TLR4, or alternative signaling pathways remains unresolved and warrants further investigation. It is also important to acknowledge the potential variability introduced by differences in LPS purification methods across suppliers and batches. These inconsistencies may influence cellular responses and highlight the need for standardization in future studies.

Despite the absence of statistically significant proliferation changes, our study suggests that low-dose *P. gingivalis* LPS may subtly promote SHEDs proliferation and inflammatory cytokine production in a dose-dependent manner. This finding may have implications for modeling chronic pulpal inflammation and studying early tissue responses in regenerative endodontic research. Further investigations are needed to delineate the molecular pathways involved and to evaluate the long-term regenerative capacity of SHEDs under sustained *P. gingivalis* LPS stimulation.

## Conclusions

This study demonstrates that Porphyromonas gingivalis LPS induces a dose-dependent inflammatory

response in SHEDs, characterized by upregulation of *IL1B*, *IL6*, *IFNG*, and *TNF*. While low concentrations of *P. gingivalis* LPS did not significantly enhance SHEDs proliferation, a subtle promotive trend was observed, suggesting a potential role in early-stage tissue responses. These results support the use of *P. gingivalis* LPS as a clinically relevant stimulus to model chronic pulpal inflammation and highlight SHEDs as a promising *in vitro* system for investigating host–pathogen interactions and inflammation-mediated regenerative processes in the primary dentition.

## Acknowledgements

This project was supported by Faculty Research Grant (DRF 67\_026), the Faculty of Dentistry, Chulalongkorn University. The authors would like to thank the staff of the Research Unit of Mineralized Tissue, Faculty of Dentistry, Chulalongkorn University, for their valuable technical support and assistance throughout this study.

## References

1. Khorasani MMY, Hassanshahi G, Brodzikowska A, Khorramdelazad H. Role(s) of cytokines in pulpitis: Latest evidence and therapeutic approaches. *Cytokine* 2020;126:154896.
2. Zhang W, Xu T, Li X, Zhang Y, Zou XY, Chen F, *et al.* Single-cell atlas of dental pulp stem cells exposed to the oral bacteria Porphyromonas gingivalis and Enterococcus faecalis. *Front Cell Dev Biol* 2023; 11:1166934.
3. Chen WA, Dou Y, Fletcher HM, Boskovic DS. Local and Systemic Effects of Porphyromonas gingivalis Infection. *Microorganisms* 2023;11(2)470.
4. Wang X, Quinn PJ. Lipopolysaccharide: Biosynthetic pathway and structure modification. *Prog Lipid Res* 2010;49(2):97-107.
5. Tan Y, Kagan JC. A cross-disciplinary perspective on the innate immune responses to bacterial lipopolysaccharide. *Mol Cell* 2014; 54(2):212-23.
6. Brodzikowska A, Ciechanowska M, Kopka M, Stachura A, Włodarski PK. Role of Lipopolysaccharide, Derived from Various Bacterial Species, in Pulpitis-A Systematic Review. *Biomolecules* 2022;12(1)138.
7. Anand AR, Bradley R, Ganju RK. LPS-induced MCP-1 expression in human microvascular endothelial cells is mediated by the tyrosine kinase, Pyk2 via the p38 MAPK/NF-kappaB-dependent pathway. *Mol Immunol* 2009;46(5):962-8.
8. Zhao Y, Kong X, Li X, Yan S, Yuan C, Hu W, *et al.* Metadherin mediates lipopolysaccharide-induced migration and invasion of breast cancer cells. *PLoS One* 2011;6(12):e29363.

9. He X, Jiang W, Luo Z, Qu T, Wang Z, Liu N, et al. IFN- $\gamma$  regulates human dental pulp stem cells behavior via NF- $\kappa$ B and MAPK signaling. *Sci Rep* 2017;7:40681.
10. Kimura H, Okubo N, Chosa N, Kyakumoto S, Kamo M, Miura H, et al. EGF positively regulates the proliferation and migration, and negatively regulates the myofibroblast differentiation of periodontal ligament-derived endothelial progenitor cells through MEK/ERK- and JNK-dependent signals. *Cell Physiol Biochem* 2013;32(4):899-914.
11. Kato H, Taguchi Y, Tominaga K, Umeda M, Tanaka A. Porphyromonas gingivalis LPS inhibits osteoblastic differentiation and promotes pro-inflammatory cytokine production in human periodontal ligament stem cells. *Arch Oral Biol* 2014;59(2):167-75.
12. Diya Z, Lili C, Shenglai L, Zhiyuan G, Jie Y. Lipopolysaccharide (LPS) of Porphyromonas gingivalis induces IL-1 $\beta$ , TNF- $\alpha$  and IL-6 production by THP-1 cells in a way different from that of Escherichia coli LPS. *Innate Immun* 2008;14(2):99-107.
13. Sukarawan W, Osathanon T. Stem Cells from Human Exfoliated Deciduous Teeth: Biology and Therapeutic Potential. 2017.
14. Zhai Y, Wang Y, Rao N, Li J, Li X, Fang T, et al. Activation and Biological Properties of Human  $\beta$  Defensin 4 in Stem Cells Derived From Human Exfoliated Deciduous Teeth. *Front Physiol* 2019;10:1304.
15. Zhou LL, Liu W, Wu YM, Sun WL, Dörfer CE, Fawzy El-Sayed KM. Oral Mesenchymal Stem/Progenitor Cells: The Immunomodulatory Masters. *Stem Cells Int* 2020;2020:1327405.
16. Takemura A, Matsuda N, Kimura S, Fujiwara T, Nakagawa I, Hamada S. Porphyromonas gingivalis lipopolysaccharide modulates the responsiveness of human periodontal ligament fibroblasts to platelet-derived growth factor. *J Periodontol Res* 1998;33(7):400-7.
17. Morsczech CO, Dress J, Gosau M. Lipopolysaccharide from Escherichia coli but not from Porphyromonas gingivalis induce pro-inflammatory cytokines and alkaline phosphatase in dental follicle cells. *Arch Oral Biol* 2012;57(12):1595-601.
18. Yu B, Li Q, Zhou M. LPS-induced upregulation of the TLR4 signaling pathway inhibits osteogenic differentiation of human periodontal ligament stem cells under inflammatory conditions. *Int J Mol Med* 2019;43(6):2341-51.
19. Tang J, Wu T, Xiong J, Su Y, Zhang C, Wang S, et al. Porphyromonas gingivalis lipopolysaccharides regulate functions of bone marrow mesenchymal stem cells. *Cell Prolif* 2015;48(2):239-48.
20. Mysak J, Podzimek S, Sommerova P, Lyuya-Mi Y, Bartova J, Janatova T, et al. Porphyromonas gingivalis: major periodontopathic pathogen overview. *J Immunol Res* 2014;2014:476068.
21. Bostanci N, Belibasakis GN. Porphyromonas gingivalis: an invasive and evasive opportunistic oral pathogen. *FEMS Microbiol Lett* 2012;333(1):1-9.
22. Siqueira JF, Jr., Rôças IN, Silva MG. Prevalence and clonal analysis of Porphyromonas gingivalis in primary endodontic infections. *J Endod* 2008;34(11):1332-6.
23. Zargar N, Ashraf H, Marashi SMA, Sabeti M, Aziz A. Identification of microorganisms in irreversible pulpitis and primary endodontic infections with respect to clinical and radiographic findings. *Clin Oral Investig* 2020;24(6):2099-108.
24. Lan C, Chen S, Jiang S, Lei H, Cai Z, Huang X. Different expression patterns of inflammatory cytokines induced by lipopolysaccharides from Escherichia coli or Porphyromonas gingivalis in human dental pulp stem cells. *BMC Oral Health* 2022;22(1):121.
25. Nebel D, Arvidsson J, Lillqvist J, Holm A, Nilsson BO. Differential effects of LPS from Escherichia coli and Porphyromonas gingivalis on IL-6 production in human periodontal ligament cells. *Acta Odontol Scand* 2013;71(3-4):892-8.
26. Jones KJ, Ekhlasi S, Montufar-Solis D, Klein JR, Schaefer JS. Differential cytokine patterns in mouse macrophages and gingival fibroblasts after stimulation with porphyromonas gingivalis or Escherichia coli lipopolysaccharide. *J Periodontol* 2010;81(12):1850-7.
27. Martin M, Katz J, Vogel SN, Michalek SM. Differential induction of endotoxin tolerance by lipopolysaccharides derived from Porphyromonas gingivalis and Escherichia coli. *J Immunol* 2001;167(9):5278-85.
28. Rothermund K, Calabrese TC, Syed-Picard FN. Differential Effects of Escherichia coli- Versus Porphyromonas gingivalis-derived Lipopolysaccharides on Dental Pulp Stem Cell Differentiation in Scaffold-free Engineered Tissues. *J Endod* 2022;48(11):1378-86.e2.
29. Wang J, Dai J, Liu B, Gu S, Cheng L, Liang J. Porphyromonas gingivalis lipopolysaccharide activates canonical Wnt/ $\beta$ -catenin and p38 MAPK signalling in stem cells from the apical papilla. *Inflammation* 2013;36(6):1393-402.
30. Firouzi N, Yavari HR, Rahimi S, Roshangar L, Chitsazha R, Amini M. Concentrated Growth Factors Combined with Lipopolysaccharide Stimulate the *In Vitro* Regenerative and Osteogenic Activities of Human Dental Pulp Stem Cells by Balancing Inflammation. *Int J Dent* 2022;2022:2316666.
31. Sattari M, Masoudnia M, Mashayekhi K, Hashemi SM, Khannazer N, Sattari S, et al. Evaluating the effect of LPS from periodontal pathogenic bacteria on the expression of senescence-related genes in human dental pulp stem cells. *J Cell Mol Med* 2022;26(22):5647-56.
32. Rodas-Junco BA, Hernández-Solis SE, Serralta-Interian AA, Rueda-Gordillo F. Dental Stem Cells and Lipopolysaccharides: A Concise Review. *Int J Mol Sci* 2024;25(8):4338.
33. He W, Wang Z, Luo Z, Yu Q, Jiang Y, Zhang Y, et al. LPS promote the odontoblastic differentiation of human dental pulp stem cells via MAPK signaling pathway. *J Cell Physiol* 2015;230(3):554-61.
34. Lertchirakarn V, Aguilar P. Effects of Lipopolysaccharide on the Proliferation and Osteogenic Differentiation of Stem Cells from the Apical Papilla. *J Endod* 2017;43(11):1835-40.
35. Chatzivasileiou K, Lux CA, Steinhoff G, Lang H. Dental follicle progenitor cells responses to Porphyromonas gingivalis LPS. *J Cell Mol Med* 2013;17(6):766-73.

# The Effect of Powered Toothbrushes on Surface Roughness and Wear of Direct Restorative Materials

Sookwasa Hirunmekavanich<sup>1</sup> and Chaiwat Maneenut<sup>1</sup>

<sup>1</sup>Department of Operative Dentistry, Faculty of Dentistry, Chulalongkorn University, Bangkok, Thailand

## Abstract

The study aims to evaluate surface roughness and wear or volume loss of three direct restorative materials after brushing with oscillating and sonic-vibrating powered toothbrushes. Twenty specimens of each material: conventional nanofilled resin composite (FiltekZ350XT), flowable resin composite (Filtek Supreme flowable restorative) and resin-modified glass ionomer cement (Fuji II LC), were prepared and divided into two groups according to the type of powered toothbrush used. Brushing was conducted using a toothbrushing simulator that applied a consistent force of 1 newton (N) for one hour, simulating one year of brushing. Surface roughness and wear or volume loss tests were performed on each specimen before and after brushing to assess the impact of the different toothbrush types and materials. The surface roughness (Sa), the differences of roughness change ( $\Delta Sa$ ) and volume loss were analysed using the paired *t*-test and two-way ANOVA with LSD post hoc tests. The results showed no statistically significant difference of roughness, roughness change and wear after one year of simulated tooth brushing by the powered toothbrush in all groups. Two-way ANOVA analysis showed that type of powered toothbrush and material do not significantly influence the surface roughness alteration of all three direct restorative materials. However, the type of materials significantly influenced the volume loss. A greater surface roughness value changes were observed in sonic-vibrating powered toothbrush groups. Resin-modified glass ionomer cement brushed by a sonic-vibrating powered toothbrush (GS) showed the most surface roughness change. The highest volume loss was detected in resin-modified glass ionomer cement brushed by the oscillating powered toothbrush (GO) group. There is a statistically significant difference in wear between resin-modified glass ionomer cement groups and resin composite groups in both powered toothbrush types. In conclusion, in this *in vitro* study, brushing with powered toothbrushes does not affect the surface roughness and wear of direct restorative materials.

**Keywords:** Powered toothbrush, Resin composite, Resin-modified glass ionomer, Surface roughness, Wear

**Received date:** Feb 28, 2025

**Revised date:** Jul 1, 2025

**Accepted date:** Jul 10, 2025

**Doi:** 10.14456/jdat.2025.23

## Correspondence to:

Chaiwat Maneenut, Department of Operative Dentistry, Faculty of Dentistry, Chulalongkorn University, Bangkok, Thailand  
Tel. 081-6979682 E-mail: chaiwat.m@chula.ac.th

## Introduction

Tooth brushing is the act or method of cleaning the teeth with a toothbrush together with toothpaste. It is the simplest and the most effective way to eliminate dental plaque. Incorrect tooth brushing (toothbrush, toothpaste and technique), resulting in inadequate plaque removal,

could lead to many problems including dental caries, periodontal problems and malodor breath.<sup>1</sup> In addition, excessive brushing force could cause tooth wear and non-carious cervical lesions (NCCLs).<sup>2</sup> These oral health problems can occur in all groups of age and eventually affect their quality of life.

The powered toothbrush was developed to be more user-friendly, eliminate incorrect brushing techniques and provide consistent ability to eliminate dental plaque.<sup>3</sup> Previous studies found that the safeness of using powered toothbrushes was not significantly different from the conventional manual toothbrush.<sup>3,4</sup> Thus, many people start to pay more attention to the powered toothbrush since it can deliver a simpler method of daily oral care. Moreover, the powered toothbrush is beneficial to people who are geriatric or handicapped who have weakened muscle movement especially fine muscle movement which is important for tooth brushing.<sup>5</sup> So, as a dental professional, it can be assumed that a powered toothbrush is more suitable for some special patients compared to the conventional manual toothbrush and it can eliminate technique sensitivity, control brushing force and help motivate good oral care for everyone.

Powered toothbrushes vary in head size, head shape, speed of movement and the whole brush design. Nowadays marketed powered toothbrushes have three types of action which are rotating or oscillating, sonic vibrating and ionic-powered. The rotating or oscillating toothbrush usually comes with a round head design. The head spins with speed when moving the brush along the teeth and gum line causing the dislodgement of food particles. While the sonic vibrating toothbrush comes with a vibrating head that emits ultrasonic waves that are claimed to cause vibration, resulting in fluid movement and air vibration.<sup>6</sup> Sonic vibration combined with the vibrating bristle will loosen the plaque and food particles. The ionic-powered toothbrush temporarily alters the tooth ion charge from negative to positive by the circuit under the head and handle. This polarity helps push away food particles, which are also positive charges.<sup>7</sup> However, there is no mechanical action from the brush itself unlike as in an oscillating or sonic-vibrating powered toothbrush.

Improper tooth brushing is not only one of the various factors causing oral health problems but also plays a part in damaging dental restoration over time, especially direct restoration.<sup>8</sup> Several previous studies<sup>9,10</sup> showed the effects of tooth brushing to resin composite which were increased surface roughness, decreased surface

gloss and increased wear. These effects can lead to increased plaque accumulation which ultimately results in restoration failure.<sup>9,11,12</sup> However, literature reviews revealed only the effect of manual toothbrushes or compared the effect between manual and powered toothbrushes. There are still limited studies that compared the effect among the powered toothbrushes.

From the knowledge gap and the raising popularity of powered toothbrush and its benefits, this present study aims to investigate and compare the surface roughness and wear of the direct restorative materials which are a conventional nanofilled resin composite, a flowable resin composite and a resin-modified glass ionomer, after brushing using the oscillating and sonic-vibrating powered toothbrushes. The null hypothesis of this study is that the powered toothbrush does not affect the surface roughness and wear of direct restorative material. Clinically, understanding these specific effects can help dental professionals to provide evidence-based recommendations on the most appropriate oral hygiene instruments for patients with direct restorations, potentially influencing restorative material selection, maintenance protocols, and patient education to enhance the survival and esthetic integrity of restorations.

## Materials and Methods

### Sample size calculation

Sample size was calculated using G\*power 3.1.9.4 (Kiel University, Germany) utilizing Power  $\beta = 80\%$  and  $\alpha = 5\%$ , cited from the study of Sayed *et al.*, 2022.<sup>9</sup> The total sample size from the calculation was at least 46.2 (8 specimens per group), including 10% compensation. However, to avoid discrepancy, the specimens in this study were increased to ten specimens per group. A total of 60 specimens were investigated, which were categorized into two divisions based on toothbrush type and further segmented into three types of direct restorative materials.

### Specimen fabrication

Sixty cylindrical specimens (20 for each material) with dimensions of 10 mm in diameter and 2 mm in thickness were prepared using polyethylene molds (Fig. 1.). The materials used in this study are shown in Table 1.

**Table 1** The direct restorative materials and toothpaste used in this study

Material	Type	Composition	Filler content	Manufacturer	Lot number
<b>Filtek™ Z350 XT</b> <b>Universal Restorative</b>  (Shade A3)	Nanofilled resin composite	Bis-GMA, UDMA, TEGDMA and Bis-EMA, PEGDMA photoinitiator	78.5% by weight (63.3% by volume) non-agglomerated/non-aggregated 20 nm silica filler, non-agglomerated/non-aggregated 4 to 11 nm zirconia filler and aggregated zirconia/silica cluster filler (comprised of 20 nm silica and 4 to 11 nm zirconia particles)	3M, ESPE, USA	10136730
<b>Filtek™ Supreme Flowable Restorative</b>  (Shade A3)	Flowable resin composite	Bis-GMA, TEGDMA, Bis-EMA, dimethacrylate polymer photoinitiator	65% by weight (55% by volume) 75 nm diameter non-agglomerated/non-aggregated silica nanofiller, 5-10 nm non-agglomerated/non-aggregated zirconia nanofiller, loosely bound agglomerated zirconia/silica nanocluster, consisting of agglomerates of 5-20nm primary zirconia/silica particles. The cluster particle size range is 0.6 to 1.4 microns.	3M, ESPE, USA	10019057
<b>Fuji II LC® Capsule</b>  (Shade A3)	Resin modified glass ionomer	Liquid: Acrylic maleic acid copolymer, HEMA, UDMA, camphoroquinone Powder: fluoro-alumino-silicate glass		GC, Japan	2302206
<b>Colgate® Cavity Protection Toothpaste</b>	toothpastes	Dicalcium phosphate dihydrate, Water, Sorbitol, Sodium lauryl sulfate, Hydrated silica, Arginine, Sodium monofluorophosphate, Flavor, Cellulose gum, Phosphoric acid, Tetrasodium pyrophosphate, Sodium saccharin, CI 77891, tetrasodium pyrophosphate		Colgate-Palmolive, USA	TH112B



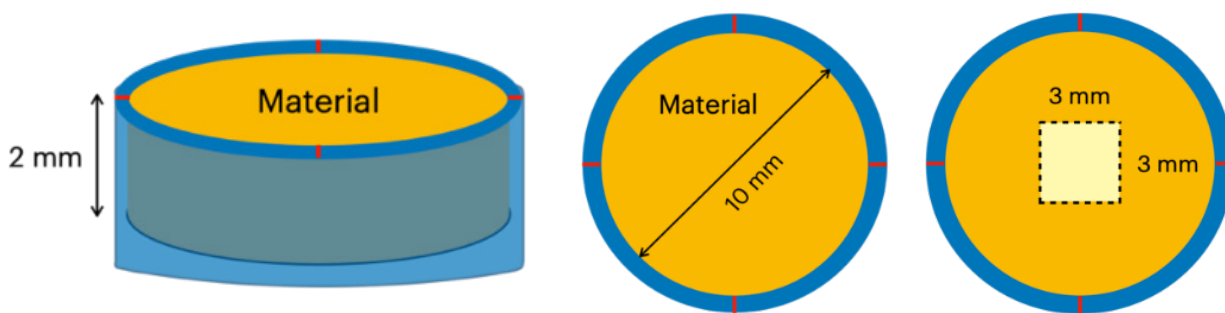


**Figure 1** Specimen fabrication and area of brushing (3x3 mm) at the middle

Conventional resin composite, Filtek™ Z350 XT Universal Restorative shade A3 (3M™, ESPE, USA), was placed in the mold with a plastic instrument. The sample was covered with a celluloid strip and a glass slide, followed by putting a metal weight of 1 kg on the top for 20 seconds to ensure the flat surface of the specimen. The metal weight was removed, the curing tip was placed perpendicularly to the surface of the material and it was light cured through a glass slide with LED light curing unit (Demi™ Plus, Kerr, USA) using approximately 1000 mW<sup>2</sup> for 40 seconds. The light intensity was confirmed with a radiometer (100 Optilux Radiometer®, Sds Kerr, USA). In order to imitate the clinical polishing technique, the top surface of the specimen was polished with Softlex discs (Sof-Lex™ XT Contouring and Polishing Discs, 3M™, ESPE), using coarse, medium, fine and superfine discs respectively, with a micro-motor handpiece at 10,000 rpm for ten strokes in the same linear direction for each disc. After polishing with each disc type, the specimen was rinsed off for ten seconds and air-dried for ten seconds with a triple syringe (Mobile Unit, Super Mobile 85, T.D.P. Thailand). The polishing disc was discarded after every four specimens were polished to ensure the efficiency of the disc.

Flowable resin composite specimens, Filtek™ Supreme Flowable Restorative shade A3 (3M™, ESPE, USA), were prepared by injecting material from tube into the mold, followed by the same procedures as previously described.

Resin-modified glass ionomer specimens, Fuji II LC® Capsule shade A3 (GC, Japan), were prepared by

mixing in an amalgamator (Ultramat 2, SDI, Australia) for ten seconds as per the suggestion of the manufacturer and injected into the mold, followed by the same procedures as previously described.

All specimens were stored in distilled water at a temperature of 37°C in an incubator for 24 hours before submitted to surface roughness analysis (Sa) at a square area of 3 x 3 mm at the middle of the polished surface (Fig. 1). The surface roughness values of all specimens in each material type were verified not to be significantly different to ensure the homogeneity of the baseline value before performing the brushing test.

### Brushing test

Each material specimen was randomly divided into two groups for the powered brushings (n=10). The first group was brushing performed with an oscillating-rotating powered toothbrush (Oral-B pro-2000 powered toothbrush, Procter and Gamble, USA). The bristle type was medium, end-rounded nylon bristle (Braun Oral-B EB17-2 Precision Clean Replacement, Procter and Gamble, USA). The toothbrush head spun using sensitive mode with 33,000 rounds per minute. The second group was brushing performed with a sonic-vibrating power toothbrush (Sonicare 1100 series, Philips, Netherlands) with medium, end-rounded nylon bristle (Sonicare C2 Optimal Plaque Defense HX9022/28, Philips, Netherlands). The sonic-vibrating powered toothbrush ran with 31,000 rounds per minute.



**Figure 2** a). Oral-B pro 2000 powered toothbrush with medium bristle<sup>13</sup> and b). Philips Sonicare 1100 series powered toothbrush with a medium bristle<sup>14</sup>

The powered toothbrush was attached to the modified tooth brushing simulator (Fig. 3). The simulator consisted of two parts which were the adjustable toothbrush holder and the plastic container that had the silicone specimen holder in the middle. The toothbrush holder consisted of three adjustable screws and the toothbrush grip. The first adjustable screw was used to adjust the toothbrush position in the vertical dimension. The other two were used to finely adjust the toothbrush horizontal plain.

In order to keep the margin of the specimen surface to be the unaffected area from the brushing procedure, a waterproof sticker tape was applied on the surface, leaving an area of 3x3 mm square shape at the middle to have direct contact with the brush bristles as shown in Figure 1. The specimen was inserted into the silicone holder followed by the addition of 100 ml of toothpaste solution to completely submerge its surface. The toothpaste solution was prepared by mixing 33.3 g of measured toothpaste (Colgate® Cavity Protection Toothpaste, Colgate-Palmolive, USA) with 100 ml distilled water, following a 1:3 ratio as

ISO11609:2017. The container was placed on the digital scale and the weight was set as zero (0). The powered toothbrush was attached to the toothbrush holder grip. The height and the horizontal plain were adjusted assuring that the bristle was pressed against the specimen surface and the pressure was set at 1 newton (N) (approximately 100 gram), simulating the force applied when brushing the teeth.<sup>15</sup>

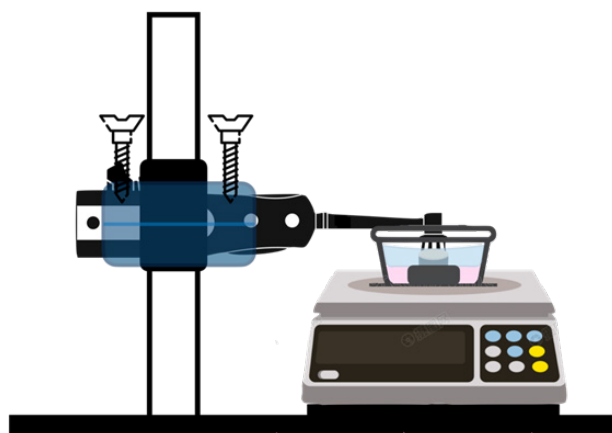


**Figure 3** The modified tooth brushing simulator, consisting of two parts which are the toothbrush holder part (left) and the specimen holder part (right)

Since the powered toothbrush did not require horizontal movement of the head like the manual toothbrush, brushing time was used instead of cycles of movement in this experimental method. Since the American Dental Association recommends two minutes (120 seconds) tooth brushing time, twice a day<sup>16</sup>, and according to a previous study<sup>17</sup> which the maximum duration of toothbrush contact with each tooth surface is five seconds per two-minute interval of brushing (equating to ten seconds per day), in this study, each specimen was brushed for 60 minutes which represent one year of tooth brushing. The toothbrush head was changed after six specimens of brushing, which referred to changing of toothbrush every three months as per the recommendation of the American Dental Association.<sup>1,16</sup>

After the brushing test, the specimen was washed for 60 seconds with water from a triple syringe (Mobile Unit, Super Mobile 85, T.D.P. Thailand) followed by immersion in the ultrasonic bath (Ultrasonic cleanser: 5210 (Heidolph, Germany) for two minutes to remove the smear layer, and air dried for 60 seconds with a triple syringe (triple syringe, Mobile Unit Super Mobile 85, T.D.P. Thailand). The specimens were stored in distilled water at 37°C followed by the surface roughness and wear after brushing evaluations.

### Surface roughness analysis

The surface roughness of all the specimens were measured before brushing simulation by contact profilometer (TalyScan 150, Taylor Hobson Limited, England). The measured area was 3 x 3 mm (Fig. 1) which was saved as the reference area for after the brushing measurement. The profilometer setup was using a cut-off at 0.8 mm, a speed of 1000 µm/s, spacing 0.5 µm in the x-axis and 10 µm in y-axis. The surface roughness was analyzed to Sa value by TalyMap software (Taylor Hobson Limited, UK) which analyzed both surface profile and surface parameters. To standardize the baseline surface roughness value, all the data were collected and statistically analysed for data distribution in each material. The same procedure was done to the specimen after the brushing test. The surface roughness value after the brushing test was collected at the same reference area. The difference in surface roughness between before and after brushing or roughness change ( $\Delta Sa$ ) within the same material and the same toothbrush type were calculated.

### Wear analysis

After the brushing test, the wear of each specimen was measured by measuring the volume loss of the material using the contact profilometer (TalyScan 150, Taylor Hobson Limited, England) and analyzed with The TalyMap software (Taylor Hobson Limited, UK). After removing the sticker tape, the measurement area was 5 x 5 mm area which included the brushing area and the surrounding unaffected area (Fig. 4). The profilometer setup was a speed of 1000 µm/s, spacing 0.5 µm in the x-axis and 20 µm in the y-axis. The volume loss (mm<sup>3</sup>) of the material was calculated by subtracting the whole volume of brushing area out of the surrounding unaffected area. This value was the wear of the material after brushing.

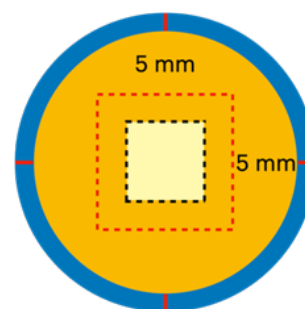


**Figure 4** The measurement area for wear, the red dotted area (5 x 5 mm). The black dotted area was the brushing area

### Statistical analysis

The data was statistically analyzed by SPSS statistics version 22.0 programs. The confidence interval in this study was determined at 95%, ( $p=0.05$ ). The homogeneity test was evaluated using Levene's test. The Shapiro-Wilk test was used to analyze data distribution. The paired *t*-test was applied for analyzing the surface roughness (Sa) value of the same material before and after the test in the same toothbrush group. The Two-way ANOVA was used to analyze the interaction between two factors, types of powered toothbrush and material. Also, the Two-way ANOVA was used for analyzing means of difference in roughness or roughness change ( $\Delta Sa$ ) and wear among materials in the same toothbrush type group followed by post-hoc LSD analysis. To compare between two types of powered toothbrushes in the same material, a two-sample *t*-test was used.

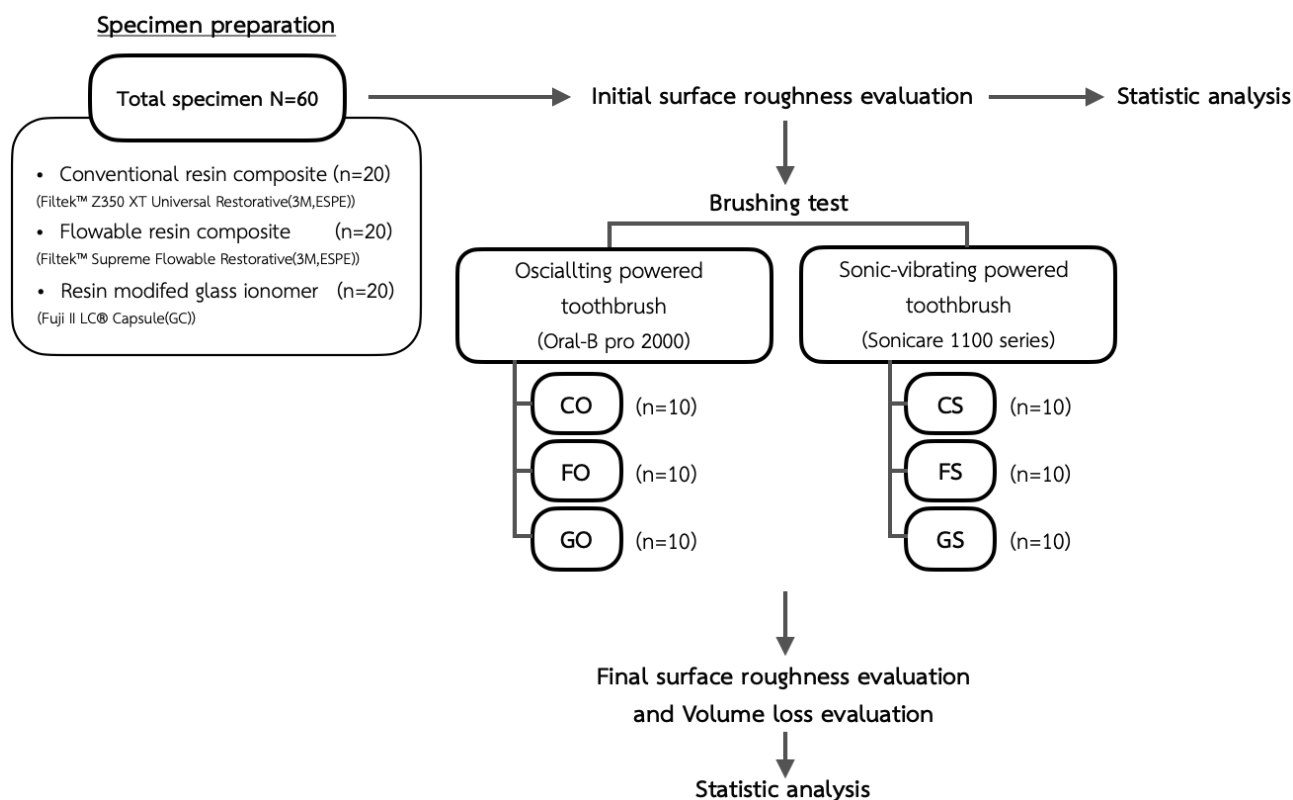


Figure 5 Study design diagram illustrates group deviations, abbreviation and sample size in each group

## Results

### Surface roughness

The surface roughness value (Sa) at baseline, before the brushing test, showed no statistically significant difference between the two powered toothbrush groups of each material (Table 2). After the brushing test, the paired *t*-test demonstrated no statistically significant differences of the surface roughness values in all groups (Table 2).

The mean of the difference in surface roughness between before and after brushing value or roughness change ( $\Delta Sa$ ) of all groups is demonstrated in Table 2. The GS group showed the most surface roughness change followed by the FS, GO, CS, FO and CO groups respectively. All groups, except the GO group, presented a smoother surface after the brushing test, as the means of  $\Delta Sa$  values

were negative values. Oscillating-powered toothbrush groups presented rougher surfaces than sonic-vibrating powered toothbrush groups for all materials. Yet, greater surface roughness value changes were observed in sonic-vibrating powered toothbrush groups compared to oscillating power toothbrush groups.

However, there was no statistical difference when comparing  $\Delta Sa$  values between two different toothbrush types for the same material. Also, there was no statistically significant difference comparing  $\Delta Sa$  values of the same toothbrush type among the three materials (Table 2). The two-way ANOVA indicated that powered toothbrush type and material did not influence  $\Delta Sa$  values ( $p=0.100$ ,  $p=0.859$ ), and these two factors had no interaction with each other ( $p=0.550$ ).

Table 2 Surface roughness (Sa) values and difference ( $\Delta Sa$ ) of before and after brushing test

Groups	Sa before ( $\mu m$ )	Sa after ( $\mu m$ )	Difference ( $\Delta Sa$ )
<b>Conventional resin composite</b>			
CO	$1.361 \pm 0.526^{aA}$	$1.355 \pm 0.608^{dA}$	$-0.006 \pm 0.472^{*A}$
CS	$1.188 \pm 0.298^{aB}$	$1.133 \pm 0.365^{dB}$	$-0.055 \pm 0.297^{*A}$

**Table 2** Surface roughness (Sa) values and difference ( $\Delta Sa$ ) of before and after brushing test (cont.)

Groups	Sa before ( $\mu m$ )	Sa after ( $\mu m$ )	Difference ( $\Delta Sa$ )
<b>Flowable resin composite</b>			
FO	$1.569 \pm 0.534^{bc}$	$1.557 \pm 0.495^{ec}$	$-0.012 \pm 0.336^{*B}$
FS	$1.556 \pm 0.444^{bd}$	$1.344 \pm 0.585^{ed}$	$-0.212 \pm 0.552^{*B}$
<b>Resin-modified glass ionomer</b>			
GO	$2.004 \pm 0.722^{ce}$	$2.149 \pm 0.818^{fe}$	$0.145 \pm 0.504^{*C}$
GS	$2.129 \pm 0.668^{cf}$	$1.888 \pm 0.681^{fe}$	$-0.241 \pm 0.696^{*C}$

The same letters refer to no statistically significant difference ( $p>0.05$ ). The lowercase letters show the column comparison within each material. The uppercase letters show the row comparison of before and after the brushing test in each group.

In  $\Delta Sa$  column, the uppercase letters show the column comparison within each material. The symbols show the column comparison in each toothbrush type among all materials. The same symbol refers to no statistically significant difference ( $p>0.05$ ). The negative value represented a smoother surface after the brushing test.

### Wear (Volume loss)

The two-way ANOVA indicated that the materials significantly influenced volume loss ( $p<0.05$ ). On the other hand, the type of powered toothbrush did not affect the volume loss ( $p=0.414$ ) and both factors showed no interaction with each other ( $p=0.511$ ).

The average volume loss of each group is presented in Table 3. The highest volume loss was detected in resin-modified glass ionomer, the GO group ( $0.011265 \text{ mm}^3 \pm 0.005709$ ) followed by the GS group ( $0.009418 \text{ mm}^3 \pm 0.004194$ ). On the contrary, the lowest volume loss was detected in conventional resin composite, the CO group ( $0.000012 \text{ mm}^3 \pm 0.000006$ ). Comparing between toothbrush types, greater volume loss was observed in oscillating powered toothbrush type of resin-modified

glass ionomer groups and flowable resin composite groups. However, in conventional resin composite groups, the CS group presented a greater volume loss than the CO group.

In the same powered toothbrush type, conventional resin composite and flowable resin composite showed statistically significantly less compared to resin-modified glass ionomer ( $p<0.05$ ). There was no statistically significant difference in volume loss between conventional resin composite and flowable resin composite. These results were similar in both oscillating-powered toothbrush groups ( $p=0.983$ ) and sonic-vibrating powered toothbrush groups ( $p=0.989$ ). In all three material types, there were no statistically significant differences in volume loss between powered toothbrush groups (Table 3)

**Table 3** Mean  $\pm$  standard deviation of wear (Volume loss) ( $\text{mm}^3$ )

Volumes loss ( $\text{mm}^3$ )	Conventional resin composite	Flowable resin composite	Resin-modified glass ionomer
Oscillating powered toothbrush	$0.000012 \pm 0.000006^{aA}$	$0.000039 \pm 0.000020^{bA}$	$0.011265 \pm 0.005709^{cC}$
Sonic vibrating powered toothbrush	$0.000017 \pm 0.000009^{aB}$	$0.000035 \pm 0.000019^{bB}$	$0.009418 \pm 0.004194^{cD}$

Lowercase letters show the comparison between powered toothbrush types. Uppercase letters show the comparison among materials. Different letters refer to a statistically significant difference ( $p<0.05$ )

## Discussions

Toothbrushing can cause various effects on direct restorative materials, especially on the surface of restoration where the toothbrush directly contacts. This could apply to the clinical situation in restoring class V, class IV and

class III cavities. Those restored cavities are affected by toothbrushing more than the occlusal load.<sup>18</sup> Due to the great esthetic properties and dentine-like physical properties of resin composite, nowadays it has become



a popular material of choice for dentists in restorative work.<sup>19</sup> Accordingly, in this present study, high polishing ability, suitability for restoring in anterior teeth, and lower abrasive wear than hybrid composite<sup>19</sup>, a nanofilled resin composite (Filtek™ Z350 XT Universal Restorative, 3M, ESPE) was selected. Additionally, with a lower flexural strength and stiffness than the conventional resin composite, the flowable resin composite was used in a small abfraction class V cavity.<sup>20</sup> Following this reason, flowable resin composite (Filtek™ Supreme Flowable Restorative, 3M, ESPE) were also chosen. And since powered toothbrushes are suggested for patients who are handicapped and geriatric and tend to have high caries risk levels.<sup>21</sup> Fluoride-releasing direct restorative material as resin-modified glass ionomer (Fuji II LC®, GC) was added in this study.

As the result of this study which there is no statistically significant differences in surface roughness and wear in all groups after one year simulated brushing test with both types of powered toothbrushes, the null hypothesis that the powered toothbrush does not affect surface roughness and wear of direct restorative material was accepted. Moreover, there is no statistically significant difference when comparing surface roughness change ( $\Delta Sa$ ) value and wear between two powered toothbrush types. And there is no statistically significant difference in  $\Delta Sa$  value among three different direct restorative materials in the same powered toothbrush group. However, a statistically significant difference exists between the wear of resin-modified glass ionomer and the resin composites.

This statistically significant difference in volume loss may due to material composition and physical properties which resin-modified glass ionomer is inferior to resin composite.<sup>22</sup> According to lower fracture toughness, lower surface hardness<sup>23</sup> and more solubility<sup>22</sup>, resin-modified glass ionomer groups demonstrated significantly greater wear and surface roughness value change than resin composite groups after the brushing test as shown in this current study. Additionally, Kormandal and co-workers, in 2021, found that the surface roughness of resin-modified glass ionomer (Fuji II LC gold label, GC) was significantly different from baseline at three months of the simulated tooth brushing test with an oscillating powered toothbrush.<sup>24</sup>

Moreover, it is found that the resin-modified glass ionomer structure is porous.<sup>25</sup> This air trapping inside the material structure occurs during the mixing process. In this study, a machine mixing method was chosen to avoid mixing errors and minimize the porosity.<sup>25,26</sup> Accordingly, this porous structure of the material can also affect the amount of wear and surface roughness of the material due to the exposure of pores after surface loss, resulting in higher volume loss for the GO and GS groups compared to others. However, this porous structure and high-water sorption of material promote fluoride-releasing ability of resin-modified glass ionomer.<sup>27</sup> Furthermore, in a clinical situation, resin-modified glass ionomer is capable of recharging and releasing fluoride over time which causes the ion exchange of FAS glass that provides strength for the material, resulting in decreasing of surface hardness.<sup>23</sup> This could lead to further surface degradation of the material over time.

On the contrary, the conventional resin composite group (Filtek™ Z350 XT Universal Restorative, 3M, ESPE) presented the least surface roughness alteration and volume loss after brushing test. Resin composite consists of two main parts: organic resin matrix and inorganic filler particles. The filler particle plays an important role in the physical and mechanical properties of the material, including wear resistance.<sup>28</sup> The smaller the filler, the more filler loading could be added to the resin composite. The surface roughness of resin composite can be a result of degradation of the resin matrix and the dislodgement of the filler particle.<sup>29</sup> Increasing the surface roughness of restorative material can eventually lead to the wear of material over time. In this study, Filtek™ Z350 XT Universal Restorative has nano filler size particles, 4-20 nm, with a filler load of 78.5% by weight (66.3% by volume). The small filler size of nanofilled resin composite provides good polishability, performing a smooth surface after the polishing procedure. Heintze and co-workers<sup>29</sup> found that the nanofilled resin composite appears to have the lowest surface roughness increased after brushing test among types of resin composites, including hybrid resin composites. The distribution of the filler also influenced the wear.<sup>30</sup> Densely packed filler leads to less chance of matrix exposure and accelerates the wear. In addition,

the SEM shows that the nanofilled resin composite shows uniform abrasion due to the same filler particle size and distribution<sup>30</sup> and less surface morphology alteration<sup>10</sup> after the toothbrushing test.

To improve the adaptability of conventional resin composite, flowable resin composite was invented with less filler load, 37% - 53% by volume, or adding other modifying agents.<sup>31</sup> Providing flowable resin composite to be less viscosity, to flow and adapt itself into the margin or the irregularity of the tooth structure. This material also be used in small abfraction class V cavity since the flowable resin composite has a lower flexural strength and stiffness than the conventional resin composite, providing more success rate.<sup>20,32</sup> The drawback of the flowable resin composite is the weaker mechanical properties and higher polymerization shrinkage due to the lower percentage of filler load.<sup>33</sup>

For wear resistance, Fernanda and co-workers<sup>34</sup> compared the mass loss of five flowable resin composites and two resin composites after the simulated tooth brushing test. They found no significant mass loss among resin composites. However, all five flowable resin composites showed higher mass loss percentages compared to microfilled resin composite. Corresponding to the previous study results, in this present study, Filtek™ Supreme Flowable Restorative, 3M, ESPE consisted of a filler loading of 65% by weight (55% by volume), which is a lower filler load than the conventional resin composite (Filtek™ Z350 XT Universal Restorative, 3M, ESPE). This results in more difference in roughness or roughness change ( $\Delta Sa$ ) value and more volume loss than conventional resin composite groups in both powered toothbrush types. However, there was no statistically significant difference between conventional resin composite and flowable resin composite. It can be assumed that with the reduced filler content, degradation of the matrix after the dislodgement of filler could be increased, resulting in a lower wear resistance of this material.

Besides the materials factors, using different powered toothbrushes also play an important role in surface roughness alteration and wear of materials. The oscillating powered toothbrush used in this present study was an Oral-B pro 2000 powered toothbrush (Procter and

Gamble, USA) with oscillating-rotating, 45,000 rounds per min (normal mode) and 33,000 rounds per min (sensitive mode). While the sonic-vibrating powered toothbrush (Sonicare 1100 series powered toothbrush, Phillips, Netherland) vibrates with 31,000 rounds/min. An oscillating power toothbrush was selected in sensitive mode to eliminate the amount of cycle factor.

Two-way ANOVA results of the current study showed that toothbrush type did not statistically significantly influence surface roughness alteration and wear of tested materials. However, greater surface roughness value changes ( $\Delta Sa$ ), were observed in sonic-vibrating powered toothbrush groups compared to oscillating power toothbrush groups. The same result was presented in volume loss of the conventional resin composite groups which the CS group presented greater wear than the CO group. Nevertheless, there is no statistical difference of two toothbrush types in both  $\Delta Sa$  value and wear. These results correspond to the results of Ahmed and co-workers, in 2022<sup>9</sup>, that the sonic vibrating powered toothbrush demonstrated a stronger action than the oscillating powered toothbrush in both surface roughness and wear of materials with no statistical difference. These could be explained by the cleaning action of a sonic-vibrating powered toothbrush that used hydrodynamic fluid forces<sup>6,35</sup> other than only actual brittle reaching<sup>6</sup> that benefit in plaque and biofilm removal. Besides, the toothbrush claimed to emit ultrasonic waves which can create cavitation theoretically<sup>35,36</sup> where gas bubbles grow and collapse in an alternating pressure field, resulting in highly destructive shear forces.<sup>35</sup> It was suspected that the wave can promote destruction of the filler-matrix interface in materials, leading to filler dislodgment. However, the effects of cavitation depend on ultrasonic frequency and intensity. Even though, the sonic vibrating powered toothbrush only emits 260 Hz, which is not an actual ultrasonic wave.<sup>35</sup> This sonic wave has also been proven to create fluid and air movement around the bristle, creating turbulent and associated shear force, and effectively removing stain and bacteria adhesion.<sup>37,38</sup>

Furthermore, the previous study found that oscillating power toothbrush also create low sound wave

as sonic-vibrating powered toothbrush does.<sup>39</sup> By only 63 Hz rotating causes dislodgment of plaque in the range of 1 - 2 mm from the bristle tip similar to the result from 260 Hz of sonic vibrating powered toothbrush, which suggest that dynamic fluid activity is not solely restricted to a sonic vibrating powered toothbrush. In this current study, the oscillating powered toothbrush spined 33,000 rounds/minute which is converted to 550 Hz. Combined with the rotating action of the toothbrush head, the oscillating powered toothbrush could lead to greater wear of materials and rougher surface after toothbrushing especially the lower surface hardness material as resin-modified glass ionomer and flowable resin composite. This reason explained the results of the current study in which the GO group demonstrated a rougher surface after brushing and the FO and GO groups showed the greater volume loss compared to the FS and GS groups, respectively. To eliminate the confounding factors, the current study chose the sensitive mode, which was recommended for periodontal problem patients. The normal mode has a greater cycle of rotation (45,000 rounds/min), which could lead to a different result in wear and roughness alteration, this could be further studied. However, this current study only focused on the difference in action of the powered toothbrushes.

Abrasive agents in toothpaste are added to aid the mechanical cleaning efficacy of toothbrushing. Toothbrushing with only saliva does not create wear on the enamel surface, while brushing with toothpaste does.<sup>40</sup> The Relative Dentin Abrasivity (RDA) is a standardized scale for measuring the quantity of abrasiveness of toothpaste. The standard reference abrasive RDA value is around 100. However, the ADA recommends toothpaste with an RDA below 250, which produces no wear to enamel and limited wear to dentin with proper brushing technique.<sup>41</sup> In the current study, low-abrasive toothpaste (Colgate® Cavity Protection) was selected to eliminate the confounding factors. The RDA value is 65.

The hardness of the filler particle and the abrasive agent in toothpaste also impacted the wear.<sup>30</sup> If the filler particle has more hardness than the abrasive particle, there is a lower chance of wear. In the present study, the

main abrasive agents are hydrated silica and dicalcium phosphate dihydrate ( $\text{CaHPO}_4 \cdot \text{H}_2\text{O}$ ), which are medium hard and soft relative hardness<sup>42</sup>, respectively. The Moh's hardness of hydrated silica is 5 and dicalcium phosphate dihydrate ( $\text{CaHPO}_4 \cdot \text{H}_2\text{O}$ ) is 2.5.<sup>43</sup> While the filler particles in nanofilled resin composite (Filtek™ Z350 XT Universal Restorative, 3M, ESPE) and flowable resin composite (Filtek™ Supreme Flowable Restorative, 3M, ESPE) are silica filler and zirconia filler which has Moh's hardness 7 and 8, respectively. Since the filler particles have a higher hardness than toothpaste abrasive agents resulting in less wear from abrasive agents' factor. However, the correlation between the abrasiveness of the toothpaste particle and surface roughness is still controversial.

Boyd and co-worker, in 1997<sup>44</sup> demonstrated the force applied to brushing with a powered toothbrush is only 1/3 of the force applied to brushing with a manual toothbrush. The previous study<sup>45</sup> found that the habitual toothbrushing force using a manual toothbrush was in the range of 1-4 N, depending on multiple factors including measuring technique, gender, age, toothbrushes and dental characteristic of the study group. The most effective brushing force for plaque removal using a manual toothbrush is around 300 mg (3N).<sup>46</sup> In addition, Van der Weijden and co-worker, in 2004<sup>15</sup> found that an oscillating powered toothbrush, a low brushing force ( $\pm 1.5\text{N}$ ) showed more plaque removal efficacy than a high brushing force ( $\pm 3.5\text{N}$ ). In this study, a brushing force at 1 N was chosen, following the literature review. However, the results of this study showed no statistically significant differences when comparing the roughness values before and after the brushing test in all groups. Most groups presented a smoother surface after the brushing test. On the contrary, previous studies<sup>9,12,18</sup> showed a rougher surface of resin composite after brushing, which used greater brushing force with different study designs.

In the present study, although specimens were polished before being submitted to the brushing test, a surface irregularity was still present, as shown in the value at baseline. A low brushing force of 1 N might not cause much dislodgment of filler particles but rather polish the irregularity of the exposed resin matrix, resulting in a smoother

surface of materials. Especially in the resin composite, which consists of the more durable bond of silane coupling agent between glass filler and resin matrix compared to the loosely ionic bond of polyacid molecule in resin-modified glass ionomer.<sup>47</sup> As most groups in the current study, except for the GO group, presented a smoother surface after brushing.

The homogeneity of specimens in the same material group was statistically analysed before undergoing the brushing test. As the baseline values for the material group were effectively controlled, allowing the baseline Sa value of the specimen to function as an internal control for variations in the Sa value after brushing. Nevertheless, this study aimed to compare the difference in the alteration of the Sa value ( $\Delta Sa$ ) among materials. However, different materials have a variety of properties, so the mean Sa values could not be compared directly with one another. For wear measurement, the specimen was partially covered with the adhesive tape, which would be the unaffected area from brushing. This area of the specimen was used as a control or reference area for measuring volume lost (wear).

The limitation of this study was the duration of brushing. The cycle of brushing was one hour straight, which represented one year of brushing. Nevertheless, in the clinical situation tooth brushing occurs twice a day with about eight hours in between, causing more storage time intervals, which could lead to further degradation of material. Further study with intervals brushing time might refer to closer clinical situations. In addition, this current study is still an *in vitro* study.

As the results in the current study demonstrated that brushing with a powered toothbrush with 1 N force does not affect the surface roughness and wear of direct restorative materials - nanofilled resin composite, flowable resin composite and resin-modified glass ionomer, after brushing for one year. Implied in clinical situations, dentists can safely recommend using the powered toothbrush in both types with the proper brushing technique and appropriate brushing force for people who need it such as the elderly and people with handicaps, instead of a manual toothbrush. However, dentists should be aware of greater wear of resin-modified glass ionomer restoration than resin composite restoration over time.

## Conclusion

In this *in vitro* study, brushing with powered toothbrushes showed no significant influence or effect on surface roughness and wear of direct restorative materials.

## Declaration and Acknowledgement

There was no financial interest between the authors and the companies whose materials were used in the experiment. The authors would like to acknowledge the Dental Material Science Research Center and the Oral Biology Research Center, Faculty of Dentistry, Chulalongkorn University for their assistance.

## References

1. Van der Weijden G, van Loveren C. Mechanical plaque removal in step-1 of care. *Periodontol* 2000 2023.
2. Goodacre CJ, Eugene Roberts W, Munoz CA. Noncarious cervical lesions: Morphology and progression, prevalence, etiology, pathophysiology, and clinical guidelines for restoration. *J Prosthodont* 2023;32(2):e1-e18.
3. Yeh CH, Chia-Hsuan Lin CH, Tien-Li M, Tzu-Yu P, Tien VTT, Wei-Ning L, *et al.* Comparison Between Powered and Manual Toothbrushes Effectiveness for Maintaining an Optimal Oral Health Status. *Clin Cosmet Investig Dent* 2024;16:381-96.
4. Väyrynen E, Damgaard C, Almståhl A. Electric powered toothbrush vs manual—which is more efficient? *Nor Tannlegeforen Tid* 2025; 135(2):108-11.
5. Punyanirun N, Sanguanpong R. The Difference in Functions of the Upper Extremity Between Elderly and Young Adult. *Top Geriatr Rehabil* 2023;39(3):179-84.
6. CD WY. Ability of the Sonicare electric toothbrush to generate dynamic fluid activity that removes bacteria. *J Clin Dent* 1994;5:89-93.
7. Ikawa T, Mizutani K, Sudo T, Kano C, Ikeda Y, Akizuki T, *et al.* Clinical comparison of an electric-powered ionic toothbrush and a manual toothbrush in plaque reduction: A randomized clinical trial. *Int J Dent Hyg* 2021;19(1):93-8.
8. Ferracane JL. Resin composite--state of the art. *Dent Mater* 2011;27(1):29-38.
9. Sayed A, Gamal W. The effect of oscillating and sonic electric toothbrushes on the wear resistance of aesthetic restorative dental materials. *Egypt Dent J* 2022;68(3):2635-42.
10. Thanadolpijit N, Maneenut C, Soonthornsawad P, Luangruangrong P. Effect of Tooth Brushing on Surface Roughness and Gloss of Nano Composites. *J Dent Assoc Thai* 2022;72(2):300-10.
11. Al Khuraif AAA. An *in vitro* evaluation of wear and surface roughness of particulate filler composite resin after tooth brushing. *Acta Odontol Scand* 2014;72(8):977-83.

12. Demirel A, Bağış N. The Effects of Manual and Powered Brushing with a Tooth Brush on Surface Roughness Alteration of Different Resin and Glass Ionomer-based Restorative Materials: An *In Vitro* Study. *Meandros Med Dental J* 2021;22(2):164.
13. Gamble P. Precision Clean Brushhead 2025 [Available from: <https://www.service.oralb.com/th/en/products/4721/parts/100004/>].
14. Philips. 1100 Series Sonic electric toothbrush HX3641/41 Thailand: Philips; [Available from: [https://www.philips.co.th/c-p/HX3641\\_41/1100-series-sonic-electric-toothbrush](https://www.philips.co.th/c-p/HX3641_41/1100-series-sonic-electric-toothbrush)].
15. Van der Weijden G, Timmerman M, Versteeg P, Piscoer M, Van der Velden U. High and low brushing force in relation to efficacy and gingival abrasion. *J Clin Periodontol* 2004;31(8):620-4.
16. Department of Scientific Information ESTR, ADA Science & Research Institute, LLC. Toothbrushes October 7, 2022 [Available from: <https://www.ada.org/resources/research/science-and-research-institute/oral-health-topics/toothbrushes>].
17. Nogués L, Martínez-Gomis J, Molina C, Peraire M, Salsench J, Sevilla P, *et al.* Dental casting alloys behaviour during power toothbrushing with toothpastes with various abrasivities. Part I: wear behavior. *J Mater Sci Mater Med* 2008;19(9):3041-8.
18. Heintze SD, Forjanic M, Ohmiti K, Rousson V. Surface deterioration of dental materials after simulated toothbrushing in relation to brushing time and load. *Dent Mater J* 2010;26(4):306-19.
19. Alzraikat H, Burrow MF, Maghaireh G, Taha N. Nanofilled resin composite properties and clinical performance: a review. *Oper Dent* 2018;43(4):E173-E90.
20. Zhou X, Huang X, Li M, Peng X, Wang S, Zhou X, *et al.* Development and status of resin composite as dental restorative materials. *J Appl Polym Sci* 2019;136(44):48180.
21. Chand BR, Kulkarni S, Swamy NK, Bafna Y. Dentition status, treatment needs and risk predictors for dental caries among institutionalised disabled individuals in central India. *J Clin Diagn Res* 2014;8(9):ZC56.
22. Francois P, Fouquet V, Attal JP, Dursun E. Commercially Available Fluoride-Releasing Restorative Materials: A Review and a Proposal for Classification. *Materials* [Internet]. 2020; 13(10).
23. Kasraei S, Haghi S, Farzad A, Malek M, Nejadkarimi S. Comparative of flexural strength, hardness, and fluoride release of two bioactive restorative materials with RMGI and composite resin. *Braz J Oral Sci* 2022;21:e225263.
24. Komandla DR, Acharya SR, Pentapati KC. Comparative Evaluation of Surface Roughness of Resin-Modified Glass Ionomer and Glass Hybrid Restorative Materials Simulated by Tooth Brushing: An *in-Vitro* Study. *Pesqui Bras Odontopediatria Clin Integr* 2021; 21:e0259.
25. Al-Taei L, Deb S, Banerjee A. An *in vitro* assessment of the physical properties of manually- mixed and encapsulated glass-ionomer cements. *BDJ Open* 2020;6(1):12.
26. Al-Kadhim A, Abdullah H. Effect of Porosity on Compressive Strength of Resin Modified Glass Ionomer Luting Cements. *IJUM* 2018;17(2):33-40.
27. May E, Donly KJ. Fluoride release and re-release from a bioactive restorative material. *Am J Dent* 2017;30(6):305-8.
28. Elfakhri F, Alkahtani R, Li C, Khaliq J. Influence of filler characteristics on the performance of dental composites: A comprehensive review. *Ceramics International* 2022;48(19):27280-94.
29. Heintze SD, Forjanic M. Surface roughness of different dental materials before and after simulated toothbrushing *in vitro*. *Oper Dent* 2005;30(5):617-26.
30. Suzuki T, Kyoizumi H, Finger WJ, Kanehira M, Endo T, Utterodt A, *et al.* Resistance of nanofill and nanohybrid resin composites to toothbrush abrasion with calcium carbonate slurry. *Dent Mater J* 2009;28(6):708-16.
31. Baroudi K, Rodrigues JC. Flowable Resin Composites: A Systematic Review and Clinical Considerations. *J Clin Diagn Res* 2015; 9(6):Ze18-24.
32. Estafan D, Schulman A, Calamia J. Clinical effectiveness of a Class V flowable composite resin system. *Compend Contin Educ Dent* 1999;20(1):11-5; quiz 6.
33. Tsujimoto A, Irie M, Teixeira ECN, Jurado CA, Maruo Y, Nishigawa G, *et al.* Relationships between Flexural and Bonding Properties, Marginal Adaptation, and Polymerization Shrinkage in Flowable Composite Restorations for Dental Application. *Polymers* 2021; 13(16):2613.
34. Garcia FC, Wang L, D'Alpino PH, Souza JB, Araújo PA, Mondelli RF. Evaluation of the roughness and mass loss of the flowable composites after simulated toothbrushing abrasion. *Braz Oral Res* 2004;18(2):156-61.
35. Warren P, Cugini M, Chater B, Strate J. A review of the clinical efficacy of the Oral-B oscillating/rotating power toothbrush and the Philips Sonicare toothbrush in normal subject populations. *Int Dent J* 2004;54(6):429-37.
36. Walmsley A. The electric toothbrush: a review. *Br Dent J* 1997; 182(6):209-18.
37. Ng C, Tsoi JKH, Lo EC, Matinlinna JP. Safety and design aspects of powered toothbrush—A narrative review. *Dent J (Basel)* 2020;8(1):15.
38. Khambay B, Walmsley A. An *in vitro* evaluation of electric toothbrushes. *Quintessence Int* 1995;26(12):841-8.
39. Guerrero D, Smith C, Cugini M. Effect of a powered toothbrush on *in vitro* bacterial plaque. *J Dent Res* 1999;78(Special Issue):414.
40. Baig M, Cook R, Pratten J, Wood R. Evolution of wear on enamel caused by tooth brushing with abrasive toothpaste slurries. *Wear* 2021;476:203580.
41. Association AD. Toothpaste 2021 [Available from: <https://www.ada.org/resources/research/science-and-research-institute/oral-health-topics/toothpastes>].
42. Eppele M, Meyer F, Enax J. A Critical Review of Modern Concepts for Teeth Whitening. *Dent J (Basel)* 2019;7(3):79.



43. Subido AJA, Atienza AA. A Qualitative and Quantitative Study on the Abrasivity of five Philippine-brand Toothpastes. *Acta Med Philipp* 2022;56(5):100-5.
44. Boyd R, McLey L, Zahradnik R. Clinical and laboratory evaluation of powered electric toothbrushes: in vivo determination of average force for use of manual and powered toothbrushes. *J Clin Dent* 1997;8(3 Spec No):72-5.
45. Ganss C, Schlueter N, Preiss S, Klimek J. Tooth brushing habits in uninstructed adults—frequency, technique, duration and force. *Clin Oral Investig* 2009;13:203-8.
46. Van der Weijden G, Timmerman M, Danser M, Van der Velden U. Relationship between the plaque removal efficacy of a manual toothbrush and brushing force. *J Clin Periodontol* 1998;25(5):413-6.
47. Komalsingsakul A, Srisatjaluk RL, Senawongse P. Effect of brushing on surface roughness, fluoride release, and biofilm formation with different tooth-colored materials. *J Dent Sci* 2022;17(1):389-98.

## Original Article

## FTIR Spectroscopic Comparison of Fish Scale Collagen and Acemannan-Modified Porcine Collagen for Oral Mucosal Scaffolds

Orakarn Kanwiwatthanakun<sup>1</sup>, Utaisar Chunmanus<sup>2</sup>, Ratsa Sripirom<sup>3</sup>, Pasutha Thunyakitoisal<sup>3</sup><sup>1</sup>Children's Oral Health Department, Institute of Dentistry, Suranaree University of Technology, Nakhonratchasima, Thailand<sup>2</sup>Laboratory Scientist 2, Food and Agriculture Research Section (FRS), Synchrotron Research and Applications Division (SRD), Synchrotron Light Research Institute (Public Organization), Thailand<sup>3</sup>Institute of Dentistry, Suranaree University of Technology, Nakhonratchasima, Thailand

## Abstract

Oral mucosal defects, especially in elderly patients with cancer, trauma, or post-surgical resections, require biomaterials that are biocompatible, promote tissue regeneration, and restore function. Collagen-based scaffolds are extensively researched due to their biocompatibility and structural similarities to natural tissue. However, characterizing the molecular integrity of these scaffolds is essential for ensuring their efficacy. This pilot study employed Fourier transform infrared spectroscopy (FTIR) as a fundamental analytical tool to investigate and compare two collagen-based scaffolds system as two distinct modification strategies: (1) fish scale-derived collagen crosslinked with 1-ethyl-3-(3-dimethylaminopropyl) carbodiimide (EDC) and (2) porcine skin-derived collagen coated with acemannan (AceCol). FTIR was used to investigate structural features, specifically the maintenance of collagen's triple-helix structure (Amide I-III bands) and the integration of bioactive polysaccharide groups. The spectra was analyzed for key vibrational peaks, such as hydroxyl (O-H), amide, and polysaccharide-specific regions. The results indicate that the EDC-crosslinked fish scale collagen scaffold exhibited intact Amide I-III bands, confirming the stability of the triple-helix structure. The acemannan-coated scaffold displayed additional peaks in the range of 1000–1100 cm<sup>-1</sup> and enhanced hydroxyl band intensity (3300–3400 cm<sup>-1</sup>), which indicates successful polysaccharide integration. In conclusion, this pilot study demonstrated that FTIR spectroscopy can differentiate structural signatures between two scaffold modification strategies. EDC crosslinking retained the triple-helix stability of fish scale-derived collagen, while acemannan coating introduced polysaccharide-related features in porcine collagen. These findings provide preliminary evidence supporting the complementary roles of crosslinking for stability and coating for bioactivity, warranting further validation for future applications in oral mucosal regeneration.

**Keywords:** Acemannan, Fish-scale collagen, FTIR, Oral tissue engineering

Received date: Jul7, 2025

Revised date: Sep 3, 2025

Accepted date: Sep 9, 2025

Doi: 10.14456/jdat.2025.24

## Correspondence to:

Orakarn Kanwiwatthanakun, Children's Oral Health Department, Institute of Dentistry, Suranaree University of Technology, Nakhonratchasima, Thailand. Tel 0-4422-3592 Email: s\_orakarn@sut.ac.th

## Introduction

Elderly patients, particularly those suffering from cancer, trauma, or following surgical resection, frequently

have oral mucosal defects.<sup>1</sup> These defects can significantly affect many functions, such as speech, mastication, aesthetics,

and overall quality of life.<sup>2</sup> Therefore, the development of effective and biocompatible scaffolds is essential to support tissue regeneration and restore oral function.<sup>3</sup> Current treatments, like autologous grafts, have limitations due to donor site morbidity, low tissue availability, and unpredictable healing outcomes.<sup>4</sup> This situation has driven the development of tissue-engineered biomaterials that can mimic the structural and biological properties of native oral mucosa.<sup>5</sup> Among the various candidates, collagen-based scaffolds have gained considerable attention due to their favorable properties for soft tissue regeneration.<sup>6</sup> These properties include biocompatibility, biodegradability, low immunogenicity, and structural similarity to the native extracellular matrix.<sup>7</sup>

Comprising about thirty percent of all the proteins in the body, collagen is the main structural protein found in mammals, which is an essential component that provides mechanical strength to connective tissue, including skin, bone, and cartilage.<sup>8</sup> The fundamental structural unit of collagen consists of three polypeptide chains: two identical  $\alpha 1$  chains and one slightly variant  $\alpha 2$  chain, which are intertwined in a unique triple-helical shape. This structure consists of a repeating sequence of amino acids called glycine-X-Y (Gly-X-Y), with X and Y often being proline and hydroxyproline. The stability of the triple helix is mostly maintained by hydrogen bonding between adjacent carbonyl (CO) and amine (NH) groups.<sup>9</sup> Additionally, the unique physical properties of collagen, including high water absorption, gel-forming ability, and surface activity at lipid-free interfaces, make it a versatile material for biomedical applications such as scaffolds, wound-healing material devices, and drug delivery systems.<sup>7-8</sup>

Traditionally, mammalian by-products, such as bovine and porcine tissues, have been the primary source of collagen for medical and industrial applications. However, increasing concerns about zoonotic infectious disease transmission, allergenicity, ethical considerations, and religious restrictions have inspired much research into safer and more sustainable alternative sources.<sup>10</sup> Recently, researchers have focused on thousands of tons of by-products, including fish bones, skin, and scales, which are typically food waste from human consumption, as alternative

sources of collagen.<sup>11</sup> Among these, fish scales are gaining more interest due to their natural qualities that resemble type I collagen, which is composed of two  $\alpha 1$  chains and one  $\alpha 2$  chain<sup>12</sup> and is found in over 90% of the human body<sup>13</sup> within nearly all extracellular matrix and connective tissues.<sup>8</sup> In addition, collagen from fish scales demonstrates proper water absorption and retention properties, which makes it appropriate for the creation of biomedical scaffolds.<sup>14</sup> However, compared to mammalian collagen (39–40°C), collagen derived from fish scales typically has a lower denaturation temperature (Td), around 35–36°C, which limits its use in biomedical applications.<sup>13,15</sup> The lower levels of proline and hydroxyproline in marine collagen, which are essential for hydrogen bonding to stabilize the triple-helix structure, are the main cause of this decreased thermal stability.<sup>7,16</sup> Consequently, collagen derived from fish denatures at temperatures close to physiological values, which presents a major challenge for *in vivo* applications.<sup>12</sup> To overcome this limitation, researchers have employed several physical and chemical crosslinking methods to enhance the structural integrity of fish collagen.<sup>17</sup> Among different crosslinking methods, chemical crosslinking is considered the most suitable for type I collagen-based scaffolds, as it enhances scaffold stability without causing structural changes. Notably, 1-ethyl-3-(3-dimethylaminopropyl) carbodiimide (EDC) stands out as a zero-length crosslinker that enhances mechanical strength and thermal stability without leaving toxic residues or significantly altering the native structure.<sup>18</sup>

Recent studies have also explored the functionalization of collagen scaffolds with bioactive molecules.<sup>19</sup> Acemannan is a significant natural polysaccharide derived from the inner gel of *Aloe vera*. It is a highly acetylated polysaccharide consisting of  $\beta$ -(1,4)-linked mannose units.<sup>20</sup> In previous studies, acemannan demonstrates excellent biocompatibility and biodegradability, along with immunomodulatory, antiviral, antitumor, and antioxidant properties, making it highly suitable for biomedical applications.<sup>21-23</sup> Additionally, it stimulates wound healing, matrix formation, and cell proliferation.<sup>24</sup> Spectroscopic techniques can investigate interactions between its acetylated polysaccharide structure

and the polypeptide chains of collagen.<sup>24</sup> However, to the best of our knowledge, no study has directly compared fish scale-derived collagen crosslinked with EDC and porcine skin-derived collagen functionalized with acemannan using the same analytical framework. This lack of comparative evidence represents a critical knowledge gap, particularly in understanding how scaffold origin (marine vs. mammalian) and modification (crosslinking vs. coating) affect their structural and functional characteristics.

Fourier transform infrared (FTIR) spectroscopy is a vibrational spectroscopic technique employed to investigate molecular-level alterations and identify chemical functional groups, types of chemical bonds, and molecular configurations.<sup>25</sup> Researchers have extensively utilized the FTIR spectroscopy to analyze protein structures and molecular interactions.<sup>26</sup> In the context of collagen, the Amide I band (1600–1700  $\text{cm}^{-1}$ ) primarily results from the stretching vibrations of C=O bonds in the peptide backbone. This band is recognized as a fundamental indicator of the triple-helical conformation and secondary structure of collagen (protein secondary structure elucidation using the FTIR spectroscopy). Additionally, the Amide II band (1470–1570  $\text{cm}^{-1}$ ), which encompasses N–H bending and C–N stretching vibrations, as well as the Amide III band (1250–1350  $\text{cm}^{-1}$ ), which includes C–N stretching and N–H deformation, provides critical information regarding the presence of proteins and polypeptides, along with the stability of the triple-helix structure.<sup>27</sup> Recent technological developments have permitted FTIR data to be acquired with a spatial resolution of approximately 10 microns from small tissue sections, enabling precise structural characterization at the microscale, which is useful in tissue engineering and scaffold evaluation.<sup>28</sup> The FTIR spectroscopy will serve as an essential analytical tool for comparing the chemical structures and molecular arrangements of collagen-based scaffolds derived from different sources, including pure fish scale-derived collagen and porcine skin-derived collagen coated with acemannan.

Accordingly, this work was conducted as a pilot study to assess the feasibility of FTIR spectroscopy in characterizing and distinguishing two scaffold systems as two distinct modification strategies: (1) fish scale-derived

collagen crosslinked with EDC and (2) porcine skin-derived collagen coated with acemannan. The central research question was whether FTIR could reliably differentiate the molecular and structural features arising from crosslinking and bioactive coating. It was hypothesized that the scaffolds would exhibit distinct molecular and structural signatures detectable by FTIR, reflecting differences in crosslinking and bioactive functionalization. The findings are intended to provide preliminary evidence and foundational knowledge that will guide the future optimization of tissue-engineered oral mucosa scaffolds for the treatment and restoration of oral mucosal integrity in elderly patients.

## Materials and Methods

### *Preparation of fish scale-derived collagen scaffold crosslinked with EDC*

Circular collagen scaffolds (16 mm in diameter and 1 mm in thickness) were fabricated using 1.1% (w/v) type I atelocollagen extracted from tilapia fish scales (Collawind Co., Ltd., Niigata, Japan) crosslinked with 1.0% (w/v) 1-ethyl-3-(3-dimethylaminopropyl) carbodiimide hydrochloride (EDC) (Tokyo Chemical Industry, Tokyo, Japan) for structural stabilization following a previously published protocol with minor modifications.<sup>5</sup>

Briefly, freeze-dried collagen (Cell Campus FD-08G, Taki Chemical Co., Ltd., Hyogo, Japan) was dissolved in hydrochloric acid (pH 3.0) and mixed with Dulbecco's phosphate-buffered saline (D-PBS; KAC Co., Ltd., Kyoto, Japan) at 4 °C. The resulting solution was poured into silicone rubber molds (1.0 mm thickness; Ason Corporation, Osaka, Japan) with circular holes (16 mm diameter) and incubated at 25°C to induce fibrillogenesis.

After gelation, the scaffolds were chemically crosslinked by using 1.0% (w/v) EDC dissolved in 99.5% ethanol (Kishida Chemical). Crosslinking was performed by immersing the collagen gel in the EDC solution at a ratio of 100 mg EDC per 7.8 mg of collagen and incubated for 24 hours at room temperature.

After crosslinking, scaffolds were carefully removed from the molds and washed sequentially in 50% ethanol and D-PBS, each for 24 hours under gentle rotational stirring at room temperature. The scaffolds were

then sterilized using  $\gamma$ -irradiation and stored in D-PBS at 4°C until further use.

#### ***Preparation of Porcine Skin-Derived Collagen Scaffold Coated with Acemannan (AceCol Scaffold)***

Fresh porcine skin was obtained from a certified local supplier and processed within 24 hours. After hair removal, the skin was soaked in 70% ethanol for surface sterilization and thoroughly rinsed with normal saline. Collagen was extracted following a previous study.<sup>27</sup> Briefly, the skin was treated with 0.1 M NaOH at a 1:10 (w/v) ratio for 24 hours to remove non-collagenous proteins and lipids. The tissue was washed with ice-cold deionized water until reaching neutral pH, followed by incubation in 0.3 M acetic acid at a 1:15 (w/v) ratio with porcine pepsin (20,000 units/g of skin; Sigma-Aldrich, USA) for 24 hours at 4°C. After centrifugation at 5000 rpm for 20 minutes, the supernatant was collected and precipitated with ice-cold 3 M NaCl at 4°C overnight. The resulting precipitate was centrifuged at 5000 rpm for 30 minutes, dialyzed with deionized water (10x volume), freeze-dried, and stored in a desiccator.

Acemannan was extracted from Aloe vera (*Aloe barbadensis* Miller) leaves as previously described.<sup>22</sup> The outer skin of the leaves was removed, and the inner pulp was washed, homogenized, and centrifuged. The supernatant was precipitated with 100% ethanol at 4°C overnight, followed by collection and lyophilization for use. To fabricate the acemannan–collagen (AceCol) scaffold, freeze-dried porcine collagen was dissolved in 0.1 M acetic acid, while acemannan was dissolved in warm deionized water. The two solutions were mixed at a 1:0.4 (w/w) ratio and homogenized thoroughly.<sup>24</sup> The mixture was then lyophilized to form a scaffold structure. Finally, the scaffold was sterilized using  $\gamma$ -irradiation (Thailand Institute of Nuclear Technology, Nakhon Nayok, Thailand) and stored in a desiccator until further use.

#### ***Characterization Using the Fourier Transform Infrared (FTIR) Spectroscopy***

The FTIR microspectroscopy was employed to investigate the structural characteristics of the collagen-based scaffolds. Samples were embedded in an optimal cutting temperature (OCT) compound using aluminum foil

molds. The compound was allowed to partially solidify until it became opaque and was subsequently positioned horizontally and fully covered with additional OCT. The embedded specimens were rapidly frozen in liquid nitrogen, cryosectioned at –20°C to a thickness of 20  $\mu$ m, and prepared for spectral analysis.

Infrared spectra were acquired using a Bruker Tensor 27 FTIR spectrometer coupled with a Bruker Hyperion 3000 infrared microscope. Measurements were conducted in attenuated total reflectance (ATR) mode using a 15x objective and a 20x ATR lens, along with a high-sensitivity mercury cadmium telluride (MCT) detector. Spectra were recorded over the range of 3400–650  $\text{cm}^{-1}$ , which includes key functional groups such as Amide I, II, and III characteristic of collagen, at a spectral resolution of 4  $\text{cm}^{-1}$  with 64 scans per point. For each scaffold type, samples were prepared from three independent batches. From each batch, three specimens were analyzed, and spectra were collected from three randomly selected areas per specimen. This approach ensured that the spectral data captured both intra-sample and inter-batch variability, thereby enhancing the repeatability and validity of the investigation. The collected data were subsequently analyzed as described in the following section.

#### ***Data Analysis***

OPUS 7.5 software (Bruker Optics Ltd., Ettlingen, Germany) was used for analysis of all obtained spectra. The spectra underwent baseline correction, normalization, and subsequent processing by second derivative transformation to improve the resolution of overlapping peaks, particularly in the Amide I region (1600–1700  $\text{cm}^{-1}$ ), which is sensitive to the triple-helix structure of collagen. Characteristic absorption bands associated with Amide I (C=O stretching), Amide II (N–H bending and C–N stretching), and Amide III (C–N stretching and N–H deformation) were identified and compared between the scaffold groups. Additionally, characteristic peaks in the 1000–1100  $\text{cm}^{-1}$  region were monitored to identify the presence of polysaccharide-specific vibrations (e.g., C–O–C) indicative of acemannan incorporation. Spectra from multiple randomly selected regions of each scaffold sample ( $n = 3$  per group) were averaged to ensure reproducibility and representative



analysis. Comparative assessments between scaffold types focused on shifts in peak positions and changes in relative intensity to evaluate structural differences. Chemical identification and verification of functional groups were performed by comparing the processed spectra against reference data in the OPUS spectral library using the Library Search function.

## Results

### FTIR Spectral Analysis of Fish Scale-derived Collagen Scaffold Crosslinked with EDC

The FTIR spectroscopy is employed to identify functional groups and molecular structures of organic compounds, with each peak corresponding to the vibrational modes of specific chemical bonds. The Fourier Transform Infrared (FTIR) spectrum of collagen derived from fish scales and crosslinked with EDC (n=3 independent samples) revealed specific absorption peaks characteristic of Type I collagen, as illustrated in Figure 1: A notable peak was observed in the range of 3300–3400  $\text{cm}^{-1}$ , corresponding

to the stretching vibrations of O–H and N–H bonds. These absorption peaks are associated with bound water molecules that contain hydroxyl and amino groups within the collagen structure. A prominent peak of Amide I was identified in the range of 1650–1660  $\text{cm}^{-1}$ , representing the C=O stretching vibration of peptide bonds. This peak is a primary indicator of the secondary structure of collagen, particularly its triple-helix configuration. A clear Amide II peak was detected at 1550–1560  $\text{cm}^{-1}$ , associated with N–H bending and C–N stretching, which provides additional structural information about the protein. Amide III was identified by a peak in the range of 1230–1240  $\text{cm}^{-1}$ , which arises from C–N and N–H vibrations. This region is unique for the stability and integrity of the triple-helical structure of collagen. Furthermore, the retention of distinct Amide I, II, and III bands indicates that the EDC crosslinking process did not notably disrupt the native triple-helical structure of collagen. Figure 1 thus serves as the baseline spectrum of the EDC-crosslinked fish collagen scaffold, providing a detailed reference for its molecular integrity.

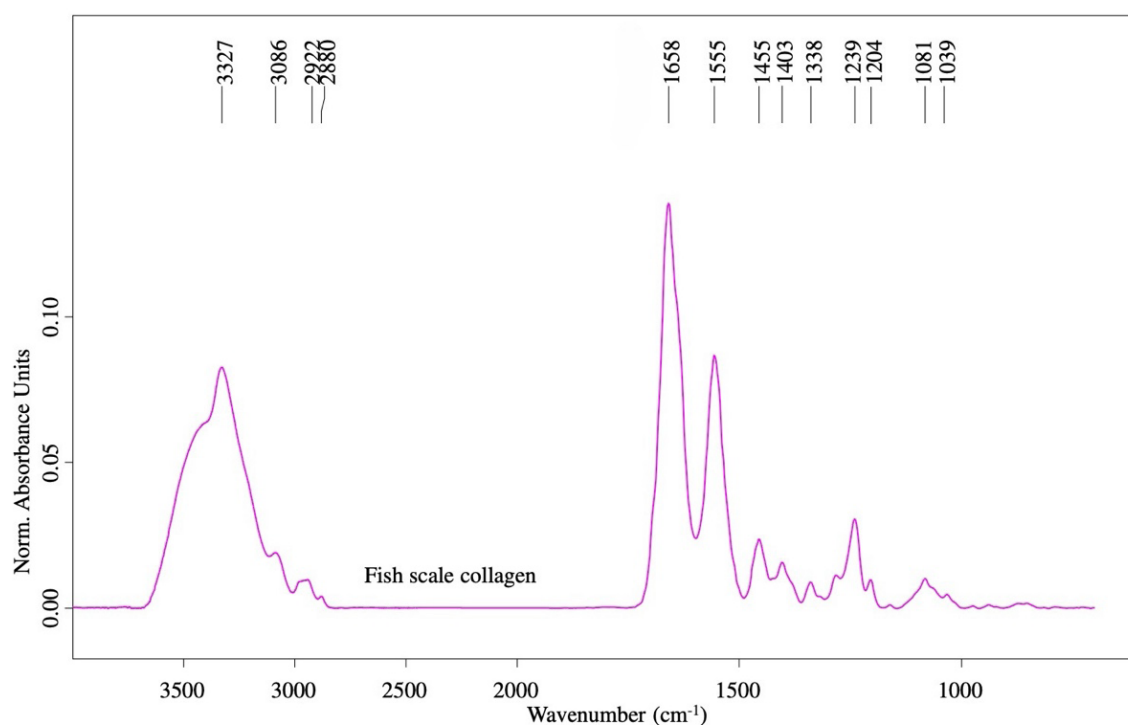


**Figure 1** FTIR spectrum of fish scale-derived collagen scaffold crosslinked with EDC. The spectrum shows the characteristic Amide I (~1650–1660  $\text{cm}^{-1}$ ), Amide II (~1500–1560  $\text{cm}^{-1}$ ), and Amide III (~1230–1240  $\text{cm}^{-1}$ ) bands, confirming the preservation of the triple-helix structure. A broad absorption band at 3300–3400  $\text{cm}^{-1}$  indicates O–H and N–H stretching vibrations associated with hydration and structural stability. This figure serves as the baseline spectral profile of the EDC-crosslinked fish collagen scaffold

### FTIR Spectral Analysis of Porcine Skin-Derived Collagen Scaffold Coated with Acemannan (AceCol Scaffold)

The spectrum of acemannan-coated collagen scaffold (AceCol) (Figure 2, n=3 independent samples) demonstrated several distinct spectral modifications, indicating the integration of polysaccharide-based functional groups into the collagen matrix, compared to the FTIR spectrum of fish scale-derived collagen. The AceCol scaffold exhibited a wider and more distinct absorption peak in the range of 3300–3400  $\text{cm}^{-1}$ , associated with O–H and N–H stretching vibrations. The increased intensity in this region suggests a higher hydroxyl group content, likely attributable to the polysaccharide structure derived from Aloe vera, which is rich in hydroxyl functionalities. Importantly, a new absorption peak appeared at 1737  $\text{cm}^{-1}$ , corresponding to the C=O stretching vibration of acetyl ester groups. This peak serves as a molecular signature of acemannan, confirming the existence of acetyl substitutions in its polysaccharide backbone. The

presence of acemannan in the AceCol spectrum strongly supports its effective deposition onto the collagen surface, as uncoated collagen scaffolds typically lack absorption in this region. Notably, the Amide I (1642  $\text{cm}^{-1}$ ), Amide II (1555  $\text{cm}^{-1}$ ), and Amide III (1239  $\text{cm}^{-1}$ ) bands remained present, suggesting that the acemannan coating did not interfere with the triple-helical structure of the collagen backbone. Additionally, notable spectral changes were observed in the range of 1200–1000  $\text{cm}^{-1}$ , corresponding to C–O and C–O–C stretching vibrations characteristic of sugar ring structures in polysaccharides. These signals were absent in the fish scale-derived collagen, supporting the successful surface modification of acemannan onto the collagen matrix and supporting the hypothesis that the coating process did not disrupt the original collagen framework but instead introduced additional functional groups. Figure 2 therefore provides the baseline spectrum of the acemannan-coated scaffold highlighting unique acemannan-associated features in addition to collagen bands.

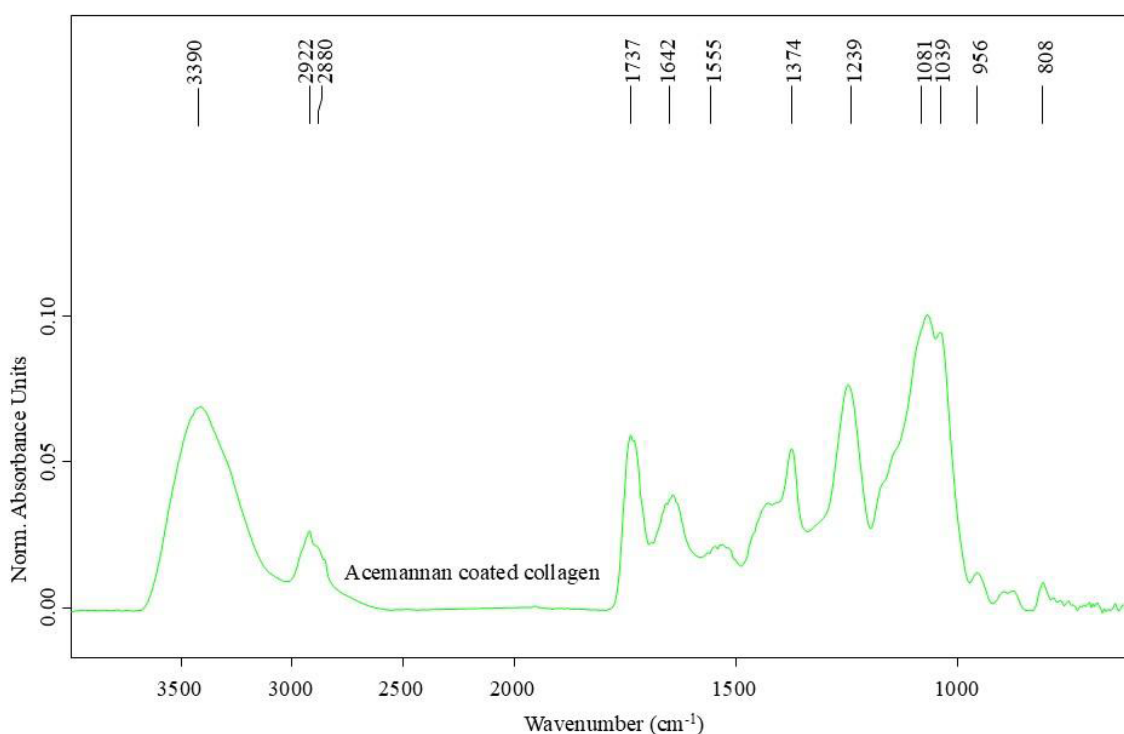


**Figure 2** FTIR spectrum of porcine skin-derived collagen scaffold coated with acemannan (AceCol). In addition to collagen-related amide bands, distinct peaks are observed at 1737  $\text{cm}^{-1}$  (C=O stretching of acetyl ester groups) and 1000–1100  $\text{cm}^{-1}$  (C–O and C–O–C stretching vibrations), representing molecular signatures of acemannan. The intensified absorption at 3300–3400  $\text{cm}^{-1}$  further reflects the hydroxyl-rich polysaccharide structure. This figure provides the baseline spectral profile of the acemannan-coated collagen scaffold, highlighting unique acemannan-associated features

### Comparison of FTIR Spectra for Two Types of Collagen Scaffolds

While Figures 1 and 2 present the baseline spectra of the individual scaffolds, Figure 3 overlays the two spectra to allow direct comparison between the modification strategies. Compared to fish scale collagen (purple line), the acemannan-coated scaffold (green line) exhibited stronger and more complex signals in the hydroxyl (3300–3400  $\text{cm}^{-1}$ ) and polysaccharide fingerprint (1200–1000  $\text{cm}^{-1}$ ) regions, as shown in Figure 3. Both samples

( $n=3$  independent spectra each) retained the major Amide I, II, and III bands, confirming the structural integrity of collagen in both scaffolds. The spectral differences indicate the successful surface modification of collagen with acemannan without disruption of its native conformation. Figure 3 thus provides a comparative overlay that highlights the structural stability of the fish collagen scaffold following EDC crosslinking and the successful incorporation of polysaccharide functional groups in the acemannan-coated scaffold.

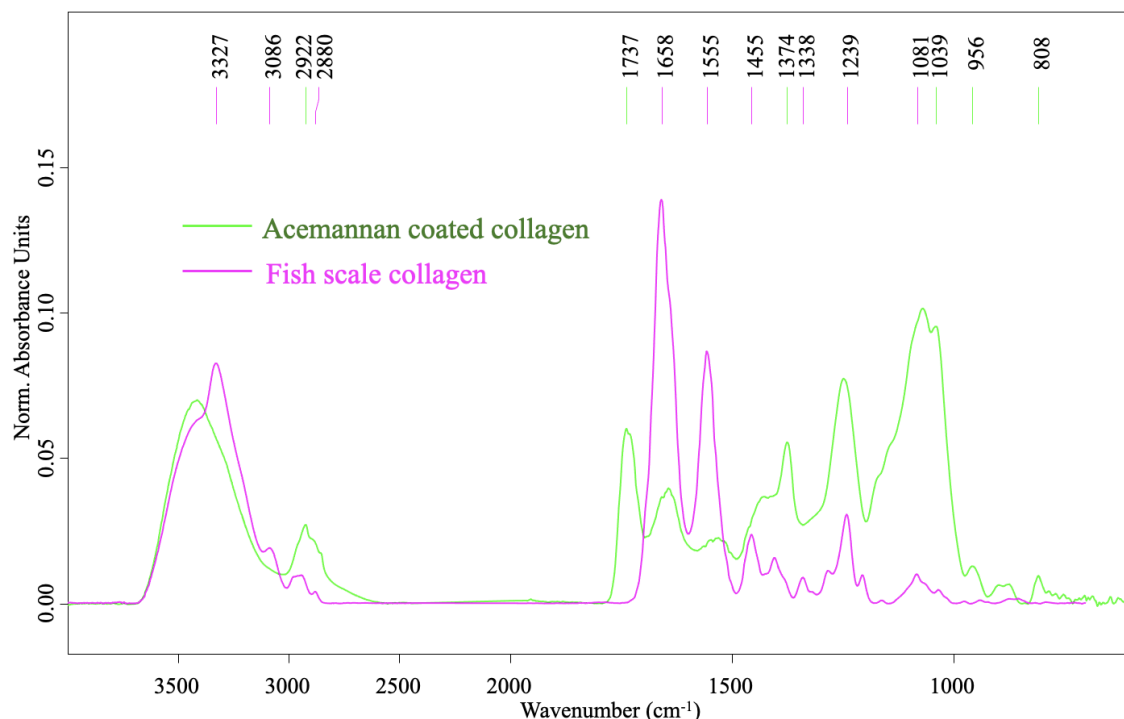


**Figure 3** Overlay of FTIR spectra of fish scale-derived collagen crosslinked with EDC (purple line) and acemannan-coated collagen (green line). The comparison highlights differences in the hydroxyl region (3300–3400  $\text{cm}^{-1}$ ) and polysaccharide fingerprint region (1200–1000  $\text{cm}^{-1}$ ), demonstrating the preservation of collagen's triple-helix structure alongside. The successful incorporation of acemannan functional groups. This figure provides direct comparative analysis of two scaffold modification strategies.

## Discussion

The Fourier Transform Infrared (FTIR) spectroscopy is a widely utilized technique for investigating the structural characteristics of biomaterials. Based on molecular vibrations, FTIR enables the identification of functional groups and secondary structures by detecting unique spectral fingerprints that reflect differences in atomic composition and molecular configuration.<sup>29</sup> This study aimed to characterize and compare the suitability of fish scale-derived collagen scaffolds crosslinked with EDC and porcine skin-derived collagen

scaffolds coated with acemannan for the development of oral mucosal tissue engineering using FTIR. The results validated the hypothesis that FTIR can detect distinct chemical and structural features in these scaffolds. The FTIR analysis of fish scale-derived collagen scaffolds revealed characteristic structural features corresponding to type I collagen, including well-defined peaks at Amide I (~1650–1660  $\text{cm}^{-1}$ ), Amide II (~1550–1560  $\text{cm}^{-1}$ ), and Amide III (~1230–1240  $\text{cm}^{-1}$ ), which are specific features of the triple-

helix structure typical of type I collagen. These peaks serve as key indicators of the secondary structure of protein.<sup>30</sup> In addition, a broad absorption band in the range of 3300–3400  $\text{cm}^{-1}$  was seen, corresponding to the vibrations of O–H and N–H bonds from hydroxyl and amino groups, as well as attached water molecules in the protein matrix.<sup>25</sup> This evidence suggests favorable water retention properties.<sup>8</sup> Previous studies have also reported that the surface hydrophilic groups, particularly O–H and N–H, can promote protein adsorption and integrin-mediated cell attachment, thereby contributing to enhanced cell adhesion.<sup>31</sup> However, FTIR alone cannot provide direct evidence of cellular responses, and future studies incorporating *in vitro* adhesion assays will be required to validate this interpretation. Moreover, these spectral findings align well with previous studies on marine-derived collagen, further supporting the reliability of FTIR in identifying triple-helix structures based on amide band signatures.<sup>32</sup> The retention of all three amide peaks (I, II, and III) after EDC crosslinking suggests that the triple-helix structure remained intact, which is a critical index for assessing the quality of scaffolds intended for oral mucosa tissue engineering.<sup>33</sup> These findings are consistent with several previous studies that recommend EDC as a suitable crosslinker for biomedical applications.<sup>34–37</sup>

In the acemannan-coated collagen scaffolds, increased absorption at 3300–3400  $\text{cm}^{-1}$  and new peaks at 1000–1100  $\text{cm}^{-1}$  indicated the presence of hydroxyl and polysaccharide functional groups. These findings confirm the successful incorporation of acemannan, which likely interacts with collagen through hydrogen bonding and electrostatic interactions. Importantly, the secondary structure of collagen remained unaffected, and all amide peaks were preserved ( $n=3$  independent spectra).

While the principal Amide I, II, and III bands were preserved in both scaffolds, variations in their relative intensities were noted. In the acemannan-coated collagen scaffold, the Amide III band was more prominent relative to Amide I and II, while fish scale collagen exhibited a more balanced intensity pattern. This increased intensity of the Amide III signal, associated with C–N stretching and N–H bending, indicates preferred interactions between

acemannan and amino groups in collagen via hydrogen bonding and electrostatic interactions. These spectrum modifications indicate local environmental changes surrounding the collagen molecules without compromising the triple-helix structure, therefore supporting the notion that surface functionalization rather than backbone disruption occurred. In comparison to the collagen scaffold derived from porcine skin and coated with acemannan, an increase in absorption at 3300–3400  $\text{cm}^{-1}$  suggests the presence of abundant hydroxyl (–OH) groups in the acemannan structure.<sup>22</sup> Furthermore, notable changes were detected in the range of 1000–1100  $\text{cm}^{-1}$ , corresponding to the stretching vibrations of C–O and C–O–C bonds, which are characteristic of polysaccharides.<sup>25</sup> These changes indicate the presence of acemannan on the collagen surface. The detection of these polysaccharide-associated peaks provides qualitative evidence of successful acemannan coating; however, FTIR alone cannot be used to quantify the amount of coating, as peak intensity may vary with sample thickness, baseline correction, and local molecular environment. To determine coating levels more precisely, complementary methods such as thermogravimetric analysis (TGA), X-ray photoelectron spectroscopy (XPS), or biochemical assays would be required in future studies. This observation is consistent with other studies<sup>38–39</sup> that reported that acemannan interacts with biomaterials by hydrogen bonding and electrostatic interactions with amino groups in collagen. Importantly, the secondary structure of collagen remained unaffected, with all amide peaks preserved, therefore maintaining its triple-helix integrity, and making it appropriate for biomedical applications. This study also demonstrates that functionalization with acemannan introduces bioactive groups, such as hydroxyl and acetyl groups, which are known to support fibroblast proliferation and collagen production and promote wound healing.<sup>24,40</sup> This surface modification enhances bioactivity without compromising the native collagen structure, offering potential for biomedical applications, particularly for elderly patients with oral mucosal defects.

The FTIR analysis revealed the differences between fish scale-derived collagen and acemannan-coated collagen. The fish scale collagen retained its triple-helix integrity,

while the acemannan-coated collagen scaffold displayed additional functional groups specific to polysaccharides. These findings highlight a notable advantage of acemannan coating that could be applied in future applications for fish scale-derived collagen because, compared to collagen from mammalian sources, marine collagen provides advantages in terms of higher purity and greater ethical acceptability.<sup>12</sup> Coating fish collagen with acemannan may further improve its regenerative and anti-inflammatory properties and warrants further investigation. It should be emphasized that this work represents a pilot study, aiming to demonstrate the potential of FTIR as a primary tool for scaffold characterization. Another limitation of this study is the absence of reference scaffolds, such as uncrosslinked fish collagen or uncoated porcine collagen, which would have allowed more definitive comparisons. Including these controls in future work will help clarify whether the observed spectral features are specifically attributable to EDC crosslinking or acemannan coating. In addition, this study did not include quantitative spectral analysis (e.g., relative peak intensities or band area ratios), which would provide stronger comparative evidence. Future investigations will therefore incorporate such quantitative approaches to complement the present qualitative findings. While the findings indicate the potential of FTIR to distinguish between crosslinked fish collagen and acemannan-coated porcine collagen, relying solely on this single technique imposes limitations, as it cannot fully determine coating quantity, mechanical strength, or *in vivo* stability. The absence of complementary analyses also restricts the depth of interpretation. Therefore, future studies incorporating reference controls and additional techniques such as scanning electron microscopy (SEM), differential scanning calorimetry (DSC), thermogravimetric analysis (TGA), and mechanical testing are required to validate and expand upon these preliminary observations.

## Conclusion

In conclusion, this pilot study demonstrated that FTIR spectroscopy can effectively distinguish the molecular and structural features arising from two scaffold modification strategies. Fish scale-derived collagen

crosslinked with EDC retained its triple helix structure, confirming structural stability, whereas porcine skin-derived collagen coated with acemannan exhibited polysaccharide-related peaks, reflecting enhanced bioactivity. These findings provide preliminary evidence for the feasibility of FTIR in scaffold characterization and highlight the complementary potential of crosslinking for stability and coating for bioactivity. Further *in vitro*, *in vivo*, and clinical investigations, are warranted to validate these observations and guide the development of optimized biomaterials for oral mucosal regeneration in elderly patients.

## Acknowledgement

The authors would like to express their sincere gratitude to Professor Kenji Izumi of the Department of Biomimetics, Niigata University, Japan, for generously supplying the fish scale-derived collagen samples used in this study. We extend our sincere appreciation to the Synchrotron Light Research Institute (SLRI) in Thailand for providing access to the FTIR instrumentation and technical support for spectroscopic analysis. This research was financially supported by the Suranaree University of Technology (SUT), Thailand Science Research and Innovation (TSRI), and the National Science, Research, and Innovation Fund (NSRF) Grant number NRIIS 195680. The authors further confirm that this study did not involve the use of live animals. Fish collagen was obtained from a commercial source, and porcine skin was collected as a food by-product from a local market; therefore, approval from an animal ethics committee was not required.

## References

1. Bozdemir E, Yilmaz HH, Orhan H. Oral mucosal lesions and risk factors in elderly dental patients. *J Dent Res Dent Clin Dent Prospects* 2019;13(1):24-30.
2. Villanueva-Vilchis MD, López-Ríos P, García IM, Gaitán-Cepeda LA. Impact of oral mucosa lesions on the quality of life related to oral health. An etiopathogenic study. *Med Oral Patol Oral Cir Bucal* 2016;21(2):e178-84.
3. Izumi K, Yortchan W, Aizawa Y, Kobayashi R, Hoshikawa E, Ling Y, *et al.* Recent trends and perspectives in reconstruction and regeneration of intra/extra-oral wounds using tissue-engineered oral mucosa equivalents. *Jpn Dent Sci Rev* 2023;59:365-74.
4. Dean J, Hoch C, Wollenberg B, Navidzadeh J, Maheta B, Mandava



- A, *et al.* Advancements in bioengineered and autologous skin grafting techniques for skin reconstruction: a comprehensive review. *Front Bioeng Biotechnol* 2024;12:1461328.
5. Suebsamarn O, Kamimura Y, Suzuki A, Kodama Y, Mizuno R, Osawa Y, *et al.* In-process monitoring of a tissue-engineered oral mucosa fabricated on a micropatterned collagen scaffold: use of optical coherence tomography for quality control. *Heliyon* 2022;8(11):e11468.
6. She J, Liu J, Mu Y, Lv S, Tong J, Liu L, *et al.* Recent advances in collagen-based hydrogels: Materials, preparation and applications. *React Funct Polym* 2025;207:106136.
7. Felician FF, Xia C, Qi W, Xu H. Collagen from Marine Biological Sources and Medical Applications. *Chem Biodivers* 2018; 15(5):e1700557.
8. Amirrah IN, Lokanathan Y, Zulkiflee I, Wee M, Motta A, Fauzi MB. A Comprehensive Review on Collagen Type I Development of Biomaterials for Tissue Engineering: From Biosynthesis to Bioscaffold. *Biomedicines* 2022;10(9):2307.
9. Shoulders MD, Raines RT. Collagen structure and stability. *Annu Rev Biochem* 2009;78:929-58.
10. Gutierrez-Canul CD, Can-Herrera LA, Ramirez-Rivera EJ, Prin-yawiwatkul W, Sauri-Duch E, Moo-Huchin VM, *et al.* A Review of Classical and Rising Approaches the Extraction and Utilization of Marine Collagen. *BioTech (Basel)* 2025;14(2)26.
11. Tang J, Saito T. Biocompatibility of Novel Type I Collagen Purified from Tilapia Fish Scale: An *In Vitro* Comparative Study. *Biomed Res Int* 2015;2015:139476.
12. Jafari H, Lista A, Siekapen MM, Ghaffari-Bohloul P, Nie L, Alimoradi H, *et al.* Fish Collagen: Extraction, Characterization, and Applications for Biomaterials Engineering. *Polymers (Basel)* 2020;12(10):2230.
13. Espinales C, Romero-Peña M, Calderón G, Vergara K, Cáceres PJ, Castillo P. Collagen, protein hydrolysates and chitin from by-products of fish and shellfish: An overview. *Heliyon* 2023;9(4):e14937.
14. Jeevithan E, Bao B, Bu Y, Zhou Y, Zhao Q, Wu W. Type II collagen and gelatin from silvertip shark (*Carcharhinus albimarginatus*) cartilage: isolation, purification, physicochemical and antioxidant properties. *Mar Drugs* 2014;12(7):3852-73.
15. Yamamoto K, Igawa K, Sugimoto K, Yoshizawa Y, Yanagiguchi K, Ikeda T, *et al.* Biological safety of fish (tilapia) collagen. *Biomed Res Int* 2014;2014:630757.
16. Nesreen A. Molecular dynamics simulations of the proline and hydroxyproline of collagen. *Multidiscip tud* 2024;14(1):71-82.
17. Leonard AR, Cumming MH, Ali MA, Cabral JD. Fish Collagen Cross-Linking Strategies to Improve Mechanical and Bioactive Capabilities for Tissue Engineering and Regenerative Medicine. *Adv Funct Mater* 2024;34(45):2405335.
18. Jiang YH, Lou YY, Li TH, Liu BZ, Chen K, Zhang D, *et al.* Cross-linking methods of type I collagen-based scaffolds for cartilage tissue engineering. *Am J Transl Res* 2022;14(2):1146-59.
19. Ullah S, Zainol I. Fabrication and applications of biofunctional collagen biomaterials in tissue engineering. *Int J Biol Macromol* 2025;298:139952.
20. Hamman JH. Composition and applications of Aloe vera leaf gel. *Molecules* 2008;13(8):1599-616.
21. Songsiripradubboon S, Kladkaew S, Trairatvorakul C, Sangvanich P, Soontornvipart K, Banlunara W, *et al.* Stimulation of Dentin Regeneration by Using Acemannan in Teeth with Lipopolysaccharide-induced Pulp Inflammation. *J Endod* 2017;43(7):1097-103.
22. Thant AA, Ruangpornvisuti V, Sangvanich P, Banlunara W, Limcharoen B, Thunyakitpisal P. Characterization of a bioscaffold containing polysaccharide acemannan and native collagen for pulp tissue regeneration. *Int J Biol Macromol* 2023;225:286-97.
23. Trinh HA, Dam VV, Banlunara W, Sangvanich P, Thunyakitpisal P. Acemannan Induced Bone Regeneration in Lateral Sinus Augmentation Based on Cone Beam Computed Tomographic and Histopathological Evaluation. *Case Rep Dent* 2020;2020:1675653.
24. Bai Y, Niu Y, Qin S, Ma G. A New Biomaterial Derived from Aloe vera-Acemannan from Basic Studies to Clinical Application. *Pharmaceutics* 2023;15(7):1913.
25. Movasaghi Z, Rehman S, ur Rehman DI. Fourier transform infrared (FTIR) spectroscopy of biological tissues. *Appl Spectrosc Rev* 2008;43(2):134-79.
26. Tatulian SA. FTIR Analysis of Proteins and Protein-Membrane Interactions. *Methods Mol Biol* 2019;2003:281-325.
27. Nalinanon S, Benjakul S, Visessanguan W, Kishimura H. Use of pepsin for collagen extraction from the skin of bigeye snapper (*Priacanthus tayenus*). *Food Chemistry* 2007;104(2):593-601.
28. Bryan MA, Brauner JW, Anderle G, Flach CR, Brodsky B, Mendelsohn R. FTIR studies of collagen model peptides: complementary experimental and simulation approaches to conformation and unfolding. *J Am Chem Soc* 2007;129(25):7877-84.
29. Gong Y, Chen X, Wu W. Application of fourier transform infrared (FTIR) spectroscopy in sample preparation: Material characterization and mechanism investigation. *Adv Sample Prep* 2024;11:100122.
30. Kong J, Yu S. Fourier transform infrared spectroscopic analysis of protein secondary structures. *Acta Biochim Biophys Sin (Shanghai)* 2007;39(8):549-59.
31. Keselowsky AG, Collard DM, Garcia AJ. Surface chemistry modulates focal adhesion composition and signaling through changes in integrin binding. *Biomaterials* 2004;25(28):5947-5954.
32. Riaz T, Zeeshan R, Zarif F, Ilyas K, Muhammad N, Safi SZ, *et al.* FTIR analysis of natural and synthetic collagen. *Appl Spectrosc Rev* 2018;53(9):703-46.
33. Dong Y, Dai Z. Physicochemical, Structural and Antioxidant Properties of Collagens from the Swim Bladder of Four Fish Species. *Mar Drugs* 2022;20(9):550.
34. Skopinska-Wisniewska J, Tuszyńska M, Olewnik-Kruszkowska E. Comparative Study of Gelatin Hydrogels Modified by Various Cross-Linking Agents. *Materials (Basel)* 2021;14(2):396.

35. Bou-Akl T, Banglmaier R, Miller R, VandeVord P. Effect of crosslinking on the mechanical properties of mineralized and non-mineralized collagen fibers. *J Biomed Mater Res A* 2013;101(9):2507-14.
36. Davidenko N, Schuster CF, Bax DV, Raynal N, Farndale RW, Best SM, *et al.* Control of crosslinking for tailoring collagen-based scaffolds stability and mechanics. *Acta Biomaterialia* 2015;25:131-42.
37. Suzuki A, Kodama Y, Miwa K, Kishimoto K, Hoshikawa E, Haga K, *et al.* Manufacturing micropatterned collagen scaffolds with chemical-crosslinking for development of biomimetic tissue-engineered oral mucosa. *Sci Rep* 2020;10(1):22192.
38. Gonçalves PR, Penha RS, Cardoso JJ, Guimarães AR, Bezerra CWB. Green and Effective: Chitosan Blends with Fish Collagen and Aloe vera Exudate. *J Braz Chem Soc* 2024;36(4):e-20240184.
39. Sularsih S, Mulawarmanti D, Rahmitasari F, Siswodihardjo S. In Silico Analysis of Glycosaminoglycan-Acemannan as a Scaffold Material on Alveolar Bone Healing. *Eur J Dent* 2022;16(3):643-7.
40. Jettanacheawchankit S, Sasithanasate S, Sangvanich P, Banlunara W, Thunyakitpisal P. Acemannan stimulates gingival fibroblast proliferation; expressions of keratinocyte growth factor-1, vascular endothelial growth factor, and type I collagen; and wound healing. *J Pharmacol Sci* 2009;109(4):525-31.

## Original Articles

## Implant Stability in the Era of Digital Dentistry: Comparing Traditional and Technology-Enhanced Surgical Methods

Myo Thiri Win<sup>1</sup>, Sirida Arunjaroenusuk<sup>1</sup>, Atiphan Pimkhaokham<sup>1</sup>, Boosana Kaboosaya<sup>1</sup><sup>1</sup>Department of Oral and Maxillofacial Surgery, Faculty of Dentistry, Chulalongkorn University, Thailand

## Abstract

Implant success is strongly influenced by surgical technique and implant stability throughout the osseointegration process. This retrospective study aimed to compare implant stability in the posterior maxilla using three surgical approaches: freehand, static-guided, and dynamic navigation techniques. Patients who underwent delayed placement of a single Straumann implant between 2015 and 2022 were included. Insertion torque and primary implant stability were recorded at the time of surgery, and secondary stability was assessed approximately three months postoperatively. Additional variables—such as age, sex, healing duration, systemic conditions, implant site, dimensions, type, surface treatment, and adjunctive procedures—were also collected. A paired *t*-test was used to compare primary and secondary stability within each group, while a linear mixed-effects model identified factors associated with changes in implant stability. A total of 49 patients (57 implants) were analyzed. No significant differences were found among groups in terms of baseline characteristics, insertion torque, or primary stability. All groups showed an increase in secondary stability over time. However, the improvement was statistically significant only in the dynamic navigation group ( $9.32 \pm 9.42$  ISQ,  $p < 0.01$ ) and the static-guided group ( $6.26 \pm 8.01$  ISQ,  $p = 0.003$ ). Among the assessed variables, only the primary implant stability was significantly associated with the change in stability. Within the limitations of this study, both dynamic navigation and static-guided surgery demonstrated superior outcomes compared to the conventional freehand technique. These results underscore the clinical value of digital technologies in enhancing surgical accuracy and optimizing implant stability during osseointegration.

**Keywords:** Digital dentistry, Implant stability, Insertion torque, Resonance frequency analysis**Received date:** Jul 7, 2025**Revised date:** Aug 31, 2025**Accepted date:** Sep 15, 2025**Doi:** 10.14456/jdat.2025.25**Correspondence to:**

Boosana Kaboosaya, Department of Oral and Maxillofacial Surgery, Faculty of Dentistry, Chulalongkorn University, Thailand,

Tel: 062-564-4295 Email: Boosana.k@chula.ac.th

## Introduction

Dental implants have become a fundamental component in modern oral rehabilitation, providing long-term functional and aesthetic outcomes for edentulous and partially edentulous patients.<sup>1</sup> Implant stability is a critical factor that directly impacts the long-term survival and

osseointegration of the prosthesis, thereby influencing the efficacy of implant therapy.<sup>2</sup> It is usually divided into two phases: primary stability, which is derived from the initial mechanical anchorage in the bone, and secondary stability which is achieved through bone healing and osseointegration.<sup>3,4</sup>

Placing implants in the posterior maxilla is a particularly complex procedure due to a variety of anatomical and technical limitations. These include restricted access and visibility, frequently reduced inter-arch space, and progressive bone loss following tooth extraction, which is routinely worsened by sinus expansion. Additionally, this region is typically characterized by low-density (type IV) bone, which is composed of a thin cortical shell surrounding porous trabecular bones. This bone is associated with reduced implant success rates.<sup>5</sup> Failure to achieve adequate implant stability, particularly in the posterior, may result in early implant failure, marginal bone loss and prosthetic complications.<sup>6</sup> Although our clinical focus is the posterior maxilla—where Types III–IV bone predominate—the freehand, static-guided, and dynamic navigation approaches are routinely applied across bone Types I–IV, with osteotomy adjustments tailored to local bone quality (e.g., under-preparation in low-density bone; countersinking and avoidance of over-compression in dense cortical bone).

Free-hand implant placement remains one of the most widely practiced surgical procedures due to its clinical adaptability and cost-effectiveness. However, its success is considerably dependent upon the operator's proficiency and comprehension of anatomical structures. This inherent variability has the potential to compromise the precision of implant positioning and impact long-term stability, particularly in anatomically challenging regions.<sup>7</sup> To address these challenges, digital dentistry has implemented a variety of tools to improve precision and outcomes in implant surgery. These consist of static guided surgery and dynamic navigation system. These innovations aim to improve the accuracy of implant positioning, reduce human error and potentially improve both primary and secondary stability outcomes. In particular, these technologies mitigate operator-dependent errors—including entry-point deviation, angulation and depth control issues, and cumulative drill drift—by constraining the drill path (static guides) or providing real-time feedback (dynamic navigation).<sup>8</sup>

In this context, “human error” refers to entry-point, angulation, depth, and drill-diameter deviations; by constraining the drill path (static guides) or providing real-time feedback (dynamic navigation), these systems reduce over-/under-preparation, cortical over-compression, and thermal insult.<sup>9</sup> Several studies have compared the clinical effectiveness of digital instruments to the conventional freehand technique; however, the majority have prioritized surgical accuracy while minimizing operator variability.<sup>7</sup> Nevertheless, there is a lack of comparative data regarding the impact of these procedures on the increase in implant stability during the critical osseointegration period, which is the first three months.

This study aimed to compare the ability of freehand, static-guided, and dynamic navigation techniques in improving implant stability during osseointegration in the posterior maxilla by measuring insertion torque, primary stability, and secondary stability.

## Materials and Methods

This retrospective cohort study was conducted at the Department of Oral and Maxillofacial Surgery, Chulalongkorn University, Bangkok, Thailand. Patient records from January 2014 to December 2023 were reviewed, focusing solely on implant placements in the posterior maxilla. This study was approved by the Human Research Ethics Committee of the Faculty of Dentistry, Chulalongkorn University (HREC-DCU 2022 – 016)

### Subjects

Initially, 62 implant cases were identified. To maintain consistency, one immediate and one early implant placement were excluded. Additionally, cases with abnormal or excessive changes in ISQ values were also excluded as outliers to ensure data reliability. The final analysis included 57 cases of delayed implant placements (Fig. 1). All eligible cases during the study period were included; no a-priori sample-size calculation was performed due to the retrospective design.

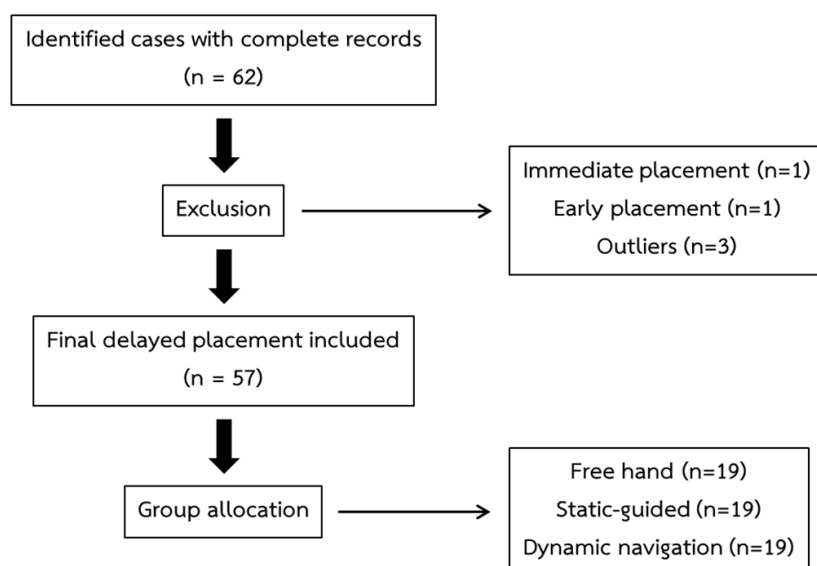


Figure 1 Flowchart of the group allocation

The inclusion criteria and exclusion criteria were as follows:

#### Inclusion criteria:

- Patients aged over 18 to 85 years
- Placement of at least one Straumann dental implant system in the posterior maxilla
- Complete documentation including participant and implant characteristics, surgical techniques, insertion torques, and primary and secondary stability at immediate placement and at follow-up 2-5 months after implant placement

#### Exclusion criteria:

- Implant failure due to trauma or unrelated surgical complications
- Use of medications affecting bone metabolism (e.g. bisphosphonates, etc.)
- History of head and neck radiation therapy
- History of grafting at the intended implant site before the index surgery (e.g., staged GBR or staged sinus floor augmentation)

#### Data collection

Data were extracted from institutional records and categorized as follows:

- 1. Patient-related variables:** age, gender, systemic conditions, implant placement location
- 2. Implant-related variables:** diameter, length, type (bone level and tissue level), surface treatment (SLA or SLActive), and adjunctive procedures (guided bone

regeneration; GBR, osteotomes, simultaneous sinus lift, or none)

**3. Surgical variables:** placement technique (free-hand, static-guided surgery, or dynamic navigation), insertion torque (Ncm). primary and secondary implant stability

#### Outcome measurement

##### 1. Primary outcomes

To compare the increase in implant stability (ISQ values) during the osseointegration period among three surgical techniques (freehand, static-guided, and dynamic navigation) in the posterior maxilla.

ISQ was recorded immediately after implant placement (primary stability) and again during the osseointegration period at approximately 8–20 weeks post-operatively ( $\pm 2$  weeks). The exact follow-up interval (in days) was recorded for each case. ISQ gain was defined as follow-up ISQ minus baseline ISQ.

##### 2. Secondary outcomes:

To evaluate factors associated with changes in implant stability, including:

- Patient-related factors (age, gender, systemic conditions, implant placement location)
- Insertion torque
- Implant dimensions (diameter, length)
- Implant type and surface treatment
- Adjunctive procedures (GBR, osteotomes, simultaneous sinus lift)



### Insertion torque measurements

Insertion torque was recorded at the time of implant placement using either a calibrated torque wrench or a motor-based system, depending on the surgical protocol and clinical accessibility, and was measured in Newton centimeters (Ncm).

### Resonance frequency analysis

Primary and secondary implant stability were assessed using resonance frequency analysis (RFA) and expressed as implant stability quotient (ISQ) values, measured with the Osstell Mentor™ device (Integration Diagnostics Ltd., Sweden) immediately after implant placement and at follow-up.

### Surgical protocols

All patients rinsed with 0.2% chlorhexidine for 30 s, followed by local anesthesia using 2% mepivacaine or 4% articaine with 1:100,000 epinephrine. A crestal incision was made and full-thickness mucoperiosteal flaps were elevated. Osteotomies were prepared under copious irrigation with sequential drills per manufacturer specifications, and implants were placed according to the planned positions, and IT and ISQ were recorded.

In the free-hand group, osteotomy positioning was guided by the surgeon's interpretation of anatomic landmarks and intraoperative measurements referenced to the virtual plan, after which sequential drilling and implant placement were performed to the planned depth and angulation

In the static-guided group, preoperative CBCT DICOM data were imported into coDiagnostiX v9.7 (Dental Wings), STL files from extraoral scans of stone casts (D900L, 3Shape) were merged for prosthetically driven planning, and a 3D-printed soft-tissue-supported surgical guide was fabricated. Prior to surgery, three mini-implants (S-mini ball, Neobiotech) were placed on each edentulous arch as reference/fixation points; the guide was seated and verified with a bite index, three pin holes were drilled, the flap was raised, and the guide was fixed to bone with pins. Osteotomy and implant insertion were then completed using the Straumann Guided Surgery system in a fully guided manner, and IT and ISQ were recorded.

In the dynamic navigation group, CBCT DICOM data were imported into IRIS 100 (EPED Inc.) for planning and real-time navigation. An infrared tracking camera monitored the handpiece and stent; fiducial markers registered patient position to the CBCT. After calibration and accuracy verification, osteotomy preparation and implant placement were performed under real-time navigation with on-screen guidance of drill position and angulation relative to the plan, after which IT and ISQ were recorded.

Implant placement, IT and ISQ measurements were performed by multiple surgeons as part of routine clinical care. Due to the retrospective design, no assessment of intra- or inter-rater reliability (ICC) was conducted.

### Statistical analysis

All statistical analyses were performed using SPSS software (SPSS Statistics for Windows, version 28; IBM). Descriptive statistics were reported as means and standard deviations for continuous variables and as frequencies for categorical variables. Normality of continuous variables was assessed using the Shapiro–Wilk test. Within each technique, change in implant stability was tested with a paired *t*-test (primary vs secondary ISQ). Between-technique inference was based on ISQ gain ( $\Delta$ ISQ = secondary – primary ISQ) using one-way ANOVA.

A linear mixed-effects model was applied to identify factors associated with implant stability change during osseointegration, according to multiple implants placed in individual patients. Fixed effects included patient demographics (age, gender, systemic disease, implant placement location), implant characteristics (diameter, length, implant type, surface treatment), and surgical variables (adjunctive treatment, insertion torque, primary stability). A random intercept was included to control for clustering by patient. Post hoc power for the primary paired ISQ change was estimated (two-sided  $\alpha=0.05$ ) using G\*Power 3.1, and a sensitivity analysis was conducted to determine the minimal detectable effect (MDE). Statistical significance was set at  $P < 0.05$ .

## Results

After excluding outliers, a total of 57 implants in 49 patients (20 males, 29 females; age range 21–85 years, mean  $60.84 \pm 10.49$  years) were analyzed. The study population was equally distributed across the three groups: free-hand ( $n = 19$ ), static-guided ( $n = 19$ ), and dynamic-guided ( $n = 19$ ).

All implants were placed using a delayed protocol, with healing periods ranging from 51–161 days. Table 1 presented the baseline characteristics across the three groups, showing no significant differences in patient demographics, implant characteristics, or surgical variables among the groups.

**Table 1** Baseline data

Variables			Surgical technique		
			Free-hand	Static-guided	Navigation
Patient factors	Age (years)	mean±SD	60.84±5.94	61.05±9.26	60.63±14.87
		P-value		0.99 <sup>a</sup>	
	Gender (n)	Male/ Female	10/7	6/10	4/12
		P-value		0.14 <sup>b</sup>	
	Systemic conditions (n)	Yes/ No	6/13	7/12	7/12
		P-value		0.91 <sup>b</sup>	
Implant factors	Implant placement location (n)	Premolar/ Molar	5/14	11/8	8/11
		P-value		0.14 <sup>b</sup>	
	Healing time (day)	mean±SD	97.11±22.77	99.68±32.80	100.37±31.87
		P-value		0.94 <sup>a</sup>	
	Implant diameter (mm)	mean±SD	4.50±0.44	4.27±0.48	4.35±0.63
		P-value		0.40 <sup>a</sup>	
Surgical factors	Implant length (mm)	mean±SD	9.37±1.17	9.47±1.31	9.47±1.31
		P-value		0.96 <sup>a</sup>	
	Implant system (n)	BL/ BLT/ BLX/ SP/ TE	7/8/0/2/2	14/4/0/1/0	10/8/1/0/0
		P-value		0.15 <sup>b</sup>	
	Surface treatment (n)	SLA/ SLA active	18/1	15/4	18/1
		P-value		0.19 <sup>b</sup>	
Surgical factors	Insertion torque (Ncm)	mean±SD	26.32±9.11	27.11±9.02	24.74±9.93
		P-value		0.73 <sup>a</sup>	
	Primary stability (ISQ)	mean±SD	71.03±7.90	68.03±7.72	65.61±11.21
		P-value		0.19 <sup>a</sup>	

SD=Standard Deviation, BL=bone level implant, BLT=bone level tapered implant, BLX=bone level with aggressive thread design implant, SP=standard plus, TE=Tapered effect, GBR=guided bone regeneration, OS=osteotome, SS=simultaneous sinus lift, ISQ=Implant stability quotient; a One-way ANOVA, b Chi-square test, \* Significant at P-value <0.05, \*\* Significant at P-value <0.01, \*\*\* Significant at P-value <0.001

Figure 2 showed the primary and secondary ISQ values across surgical techniques. All groups exhibited an increase in ISQ during the osseointegration period; however, statistically significant increases were observed only in the dynamic navigation ( $P < 0.001$ ) and static-guided groups ( $P < 0.01$ ), while the free-hand group did not reach significance.

These findings indicated that navigation-assisted and static-guided surgery may enhance implant stability in the posterior maxilla during early healing compared to the conventional free-hand technique. Across techniques,  $\Delta$ ISQ did not differ significantly—free-hand  $4.32 \pm 8.84$ , static-guided  $6.26 \pm 8.01$ , dynamic navigation  $9.32 \pm 9.42$  ( $P = 0.22$ ).

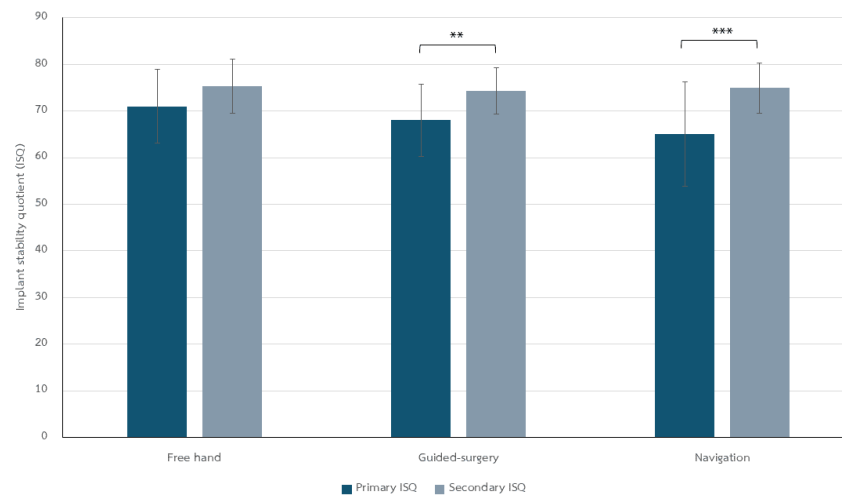


**Figure 2** Primary and secondary implant stability quotient (ISQ) values for free-hand, static-guided, and dynamic navigation techniques

Among the tested variables, only mean primary ISQ was significantly associated with ISQ gain ( $F = 38.73$ ,  $P < 0.001$ ), indicating that implants with higher initial stability tended to exhibit greater ISQ increases during the healing period. Other variables, including age, gender, systemic conditions, implant location, diameter, length, implant type, surface treatment, adjunctive procedures, and insertion torque, were not significantly associated with ISQ gain (all  $P > 0.05$ ).

## Discussion

This study compared the effects of three surgical techniques—free-hand, static-guided, and dynamic navigation, on enhancing implant stability during osseointegration in delayed posterior maxillary placements. While all techniques demonstrated successful outcomes with increased ISQ values over time, significant improvements were observed only in the static-guided and dynamic navigation groups, with the greatest increase observed in dynamic navigation, followed by static guidance. Additionally, primary ISQ emerged as a significant predictor of ISQ gain, indicating that higher initial stability was associated with greater improvements in implant stability during the osseointegration period. In this framework, baseline ISQ primarily reflects primary stability (mechanical interlock at placement), whereas ISQ gain over time reflects secondary stability (biologic integration during healing); thus, technique-related differences are expected to appear more clearly in the change in ISQ than in the baseline value.

The primary stability in dynamic navigation group was found to be lower than the conventional free-hand and static-guided groups. This may be due to the fact that primary stability is largely influenced by quality of the bone and implant design rather than the surgical technique.<sup>3</sup> This finding is consistent with ITI consensus report that although dynamic navigation shows superior accuracy, primary stability may not differ significantly from conventional techniques.<sup>10</sup> Mechanistically, primary stability is governed chiefly by local bone quality/density and implant macrogeometry, while osteotomy adjustments (e.g., under-preparation in softer bone; countersinking in dense cortex) modulate thread engagement.<sup>11-13</sup> Guided approaches do not change intrinsic density, but can standardize entry point, angulation, and depth, reducing over/under-preparation, cortical over-compression, and thermal insult. Dynamic navigation adds real-time trajectory correction that may better preserve trabecular architecture in challenging posterior sites; these features are expected to have a modest effect on primary stability but may favor secondary stability during healing.<sup>8</sup>

The results in our study revealed that implant placement using dynamic navigation yielded significantly higher ISQ gain when compared to the freehand and static guided approaches. This shows that the dynamic navigation group enhanced the precision in implant positioning, leading to more favorable osseointegration.<sup>14,15</sup> Navigation systems allow for real-time adjustments, correct insertion angles, preserve surrounding bone integrity, optimizing

bone-to-implant contact during healing and potentially minimizing micromovements.<sup>16</sup> Accordingly, the greater ISQ gains observed with guided/dynamic techniques are consistent with an effect on secondary stability (osseointegration) rather than on the density-driven primary stability at placement.

There were no statistically significant differences in insertion torque among the three groups. This finding is consistent with the previous studies that insertion torque depends more on local bone density than on the surgical techniques.<sup>10</sup> The dynamic navigation group's mean IT was numerically lower, which could reflect reduced tactile feedback and less bone condensation during osteotomy preparation.<sup>10,17</sup> However, this interpretation remains exploratory given the non-significant difference. This may benefit clinically by reducing the risk of cortical bone damage, particularly in soft bone regions such as the posterior maxilla. Taken together, our data support a model in which bone density primarily determines baseline IT/ISQ, whereas surgical guidance influences the trajectory of stability (ISQ gain) by minimizing procedural trauma and micromotion during the osseointegration period.

Guided and navigation techniques achieved  $\geq 80\%$  post-hoc power for the paired ISQ change, whereas the free-hand analysis did not reach 80% (power  $\approx 0.52$ ; MDE at  $n=19$ :  $d_z \approx 0.68$ ). Accordingly, the smaller effect observed in the free-hand group should be interpreted cautiously given the higher risk of type II error. Despite these insights, this study has limitations. The retrospective design and sample size may limit generalizability, particularly for subgroup analyses. Although implant diameter, length, and insertion torque were controlled, other factors influencing stability, such as variations in bone quality and soft tissue conditions, were not fully assessed. It is important to note that peri-implant bone density provides additional insights into the relationship between bone quality and stability outcomes, emphasizing the necessity of comprehensive bone assessments in future researches. In this routine-care cohort, multiple operators performed ISQ measurements, and no intra-/inter-rater reliability (ICC) was assessed, which may introduce measurement variability. Additionally, the follow-up should investigate long-term outcomes,

such as marginal bone loss, peri-implant bone density changes, and prosthetic success.

Further long-term studies with larger samples are recommended to confirm the benefits of digital surgical techniques on implant stability and peri-implant bone health in delayed posterior maxillary placements. Prospective studies should incorporate standardized duplicate measurements and ICCs to assess rater reliability.

## Conclusion

From this, we can conclude that clinically acceptable implant stability outcomes can be achieved regardless of the surgical techniques. However, dynamic navigation demonstrated greater gains in secondary stability despite initially lower insertion torque, suggesting that its precision in implant positioning may aid favorable bone remodeling and osseointegration, particularly in the posterior maxilla.

## Acknowledgement

The authors wish to thank the Oral and Maxillofacial Surgery and Digital Implant Surgery Research Unit, Faculty of Dentistry, Chulalongkorn University, for clinical support and facility access.

## References

1. Huang YC, Huang YC, Ding SJ. Primary stability of implant placement and loading related to dental implant materials and designs: A literature review. *J Dent Sci* 2023;18(4):1467-76.
2. Alfaraj TA, Al-Madani S, Alqahtani NS, Almohammadi AA, Alqahtani AM, AlQabbani HS, *et al.* Optimizing Osseointegration in Dental Implantology: A Cross-Disciplinary Review of Current and Emerging Strategies. *Cureus* 2023;15(10):e47943.
3. Vollmer Andreas, Babak Saravi, Gernot Lang, Nicolai Adolphs, Derek Hazard, Verena Giers, *et al.* Factors Influencing Primary and Secondary Implant Stability—A Retrospective Cohort Study with 582 Implants in 272 Patients. *Applied Sciences* 2020;10(22):8084.
4. Hiranmayi K Vidy. Factors influencing implant stability. *J Dent Implant* 2018;8:69-76.
5. Pabst AM, Walter C, Ehbauer S, Zwiener I, Ziebart T, Al-Nawas B, *et al.* Analysis of implant-failure predictors in the posterior maxilla: a retrospective study of 1395 implants. *J Craniomaxillofac Surg* 2015;43(3):414-20.
6. AlRowis Raed, Faris Albelaihi, Hamad Alquraini, Saud Almojel,

- Alwaleed Alsudais, Razan Alaqueely. Factors Affecting Dental Implant Failure: A Retrospective Analysis. *Healthcare* 2025;13(12):1356.
7. Yogui FC., Verri FR, Gomes JML, Lemos CAA, Cruz RS EP. Pellizzer. Comparison between computer-guided and freehand dental implant placement surgery: A systematic review and meta-analysis. *Int J Oral Maxillofac Surg* 2021;50(2):242-50.
8. Pimkhaokham A, Jiaranuchart S, Kaboosaya B, Arunjaroenusuk S, Subbalekha K, Mattheos N. Can computer-assisted implant surgery improve clinical outcomes and reduce the frequency and intensity of complications in implant dentistry? A critical review. *Periodontol 2000* 2022;90(1):197-223.
9. Chen ST, Buser D, Sculean A, Belser UC. Complications and treatment errors in implant positioning in the aesthetic zone: Diagnosis and possible solutions. *Periodontol 2000* 2023;92(1):220-34.
10. Tahmaseb A, Wismeijer D, Coucke W, Derksen W. Computer technology applications in surgical implant dentistry: a systematic review. *Int J Oral Maxillofac Implants* 2014;29 Suppl:25-42.
11. Ivanova V, Chenchev I, Zlatev S, Mijiritsky E. Correlation between Primary, Secondary Stability, Bone Density, Percentage of Vital Bone Formation and Implant Size. *Int J Environ Res Public Health* 2021; 18(3):6994.
12. Heimes D, Becker P, Pabst A, Smeets R, Kraus A, Hartmann A, *et al.* How does dental implant macrogeometry affect primary implant stability? A narrative review. *Int J Implant Dent* 2023;9(20).
13. Jamil S. Unlocking implant success: the impact of surgical techniques on primary stability in the posterior maxilla. *Evid Based Dent* 2024; 25(3):125-6.
14. Jorba-García A., A. González-Barnadas, O. Camps-Font, R. Figueiredo, E. Valmaseda-Castellón. Accuracy assessment of dynamic computer-aided implant placement: a systematic review and meta-analysis. *Clin Oral Investig* 2021;25(5):2479-94.
15. Younis Hamza, Chengpeng Lv, Boya Xu, Huixia Zhou, Liangzhi Du, Lifan Liao, *et al.* Accuracy of dynamic navigation compared to static surgical guides and the freehand approach in implant placement: a prospective clinical study. *Head & Face Medicine* 2024;20(1):30.
16. Geng N, Ren J, Zhang C, Zhou T, Feng C, Chen S. Immediate implant placement in the posterior mandibular region was assisted by dynamic real-time navigation: a retrospective study. *BMC Oral Health* 2024;24(1):208.
17. Fernández-Olavarria A, Gutiérrez-Corrales A, González-Martín M, Torres-Lagares D, Torres-Carranza E, Serrera-Figallo MA. Influence of different drilling protocols and bone density on the insertion torque of dental implants. *Med Oral Patol Oral Cir Bucal* 2023;28(4):e385–e94.



## Original Articles

## Manufacturing Method and Build Orientation Influence Alkali-Heat Treated Titanium (Ti-6Al-4V) Dental Implant Surface Characteristics

Tuan Hoang Nguyen<sup>1</sup>, Phetcharat Dhammayannarangsri<sup>2</sup>, Viritpon Srimaneepong<sup>3</sup>,  
Patcharapit Promoppatum<sup>4</sup>, Chalida Nakalekha Limjeerajarus<sup>5,6</sup>, Nuttapol Limjeerajarus<sup>7</sup><sup>1</sup>Graduate Program in Oral Biology, Faculty of Dentistry, Chulalongkorn University, Bangkok, Thailand<sup>2</sup>Department of Dental Biomaterials Science, Graduate School, Faculty of Dentistry, Chulalongkorn University, Bangkok, Thailand<sup>3</sup>Department of Prosthodontics, Faculty of Dentistry, Chulalongkorn University, Bangkok, Thailand<sup>4</sup>Center for Lightweight Materials, Design, and Manufacturing, Department of Mechanical Engineering, Faculty of Engineering, King Mongkut's University of Technology Thonburi (KMUTT), Bangkok, Thailand<sup>5</sup>Center of Excellence for Dental Stem Cell Biology, Faculty of Dentistry, Chulalongkorn University, Bangkok, Thailand<sup>6</sup>Department of Physiology, Faculty of Dentistry, Chulalongkorn University, Bangkok, Thailand<sup>7</sup>Office of Academic Affairs, Faculty of Dentistry, Chulalongkorn University, Bangkok, Thailand

## Abstract

This study examined the impact of alkali-heat treatment on the surface properties of Ti-6Al-4V titanium implants fabricated by conventional machining and laser powder bed fusion (LPBF) additive manufacturing with horizontal and vertical build orientations. Disc-shaped specimens were produced, immersed in 10 M NaOH at 90 °C for 24 hours, and heat-treated at 600 °C. Scanning electron microscopy revealed uniform nanostructures, such as nanospikes and crevices, across all treated groups while preserving the original microtopography. Energy-dispersive X-ray spectroscopy and X-ray diffraction confirmed the formation of a sodium titanate layer, indicated by increased sodium and oxygen content and a new diffraction peak at 48.3°. Surface roughness analysis showed that LPBF samples had significantly higher roughness than machined ones ( $p < 0.0001$ ), with horizontally printed specimens rougher than vertically printed counterparts ( $p < 0.05$ ). Importantly, the treatment did not significantly alter the initial roughness in any group ( $p > 0.1$ ). These findings demonstrate that alkali-heat treatment effectively creates bioactive nanostructures and modifies the surface chemistry of titanium implants without compromising their roughness or microtopography. Moreover, build orientation influences surface characteristics, highlighting the importance of optimizing manufacturing parameters. Overall, combining LPBF fabrication with alkali-heat treatment may enhance the bioactivity of complex titanium implants for dental applications.

**Keywords:** Alkali-heat treatment, Dental implants, Laser powder bed fusion (LPBF), Surface modification, Ti-6Al-4V

Received date: Jul 7, 2025

Revised date: Sep 5, 2025

Accepted date: Sep 15, 2025

Doi: 10.14456/jdat.2025.26

## Correspondence to:

Nuttapol Limjeerajarus, Office of Academic Affairs, Faculty of Dentistry, Chulalongkorn University, Henri Dunant Rd., Bangkok, 10330, Thailand. Email: Nuttapol.l@chula.ac.th

## Introduction

Dental implants have become the standard treatment for replacing missing teeth, with titanium implants widely

used due to their excellent biocompatibility and mechanical properties, enabling effective osseointegration with bone.<sup>1,2</sup>

However, titanium and its alloys, particularly Ti-6Al-4V, are inherently bioinert, which can limit direct bone bonding.<sup>3</sup> The physico-chemical properties of biomaterials used for fabricating implants, including surface microtopography, chemical composition, and wettability, significantly influence the host cellular activity, which in turn affects treatment outcomes.<sup>4</sup> Hence to enhance the bioactivity of implant surfaces, a variety of surface modification techniques have been developed, such as alkali-heat treatment, sandblasting, acid etching, anodization, and plasma spraying.<sup>5,6</sup>

Of these, surface modification using sodium hydroxide (NaOH) has been shown to improve the bioactivity of titanium implants, due to the formation of a highly bioactive sodium titanate layer.<sup>7</sup> In particular, this layer enhances hydrophilicity, roughness, and cell compatibility of the implant surface.<sup>4,8</sup> The outcomes of such alkali treatment with sodium hydroxide (NaOH) depend on several factors, including the concentration and temperature, treatment duration, and the initial surface microtopography.<sup>8,9</sup> Studies on conventionally machined titanium implants have demonstrated that alkali-heat treatment can influence the behavior of host cell types, including macrophages, gingival fibroblasts, osteocytes, and periodontal ligament cells, prompting them to exhibit functions suited to their surroundings.<sup>8,10-15</sup>

Moreover, different implant production methods result in varying mechanical and physical properties.<sup>16,17</sup> While most titanium implants have been produced using subtractive manufacturing, additive manufacturing (AM), particularly laser powder bed fusion (LPBF), has recently gained attention for fabricating patient-specific titanium implants with optimal mechanical strength and biocompatibility.<sup>18,19</sup> This technique, also called three-dimensional (3D) printing, is a computer-controlled process that translates 3D structural information into parts by melting materials layer by layer.<sup>20</sup> The LPBF method allows precise control over several manufacturing parameters impacting implant properties, such as the laser power, scanning speed, scanning pattern, powder layer thickness, and building orientation.<sup>21,22</sup> Additionally, the building orientation in LPBF can influence the physical and mechanical properties of the implant, including surface roughness, wettability, and free energy, all of which can modulate cell responses.<sup>16,23,24</sup>

In addition to enhancing bioactivity, surface modification techniques such as chemical and electrochemical methods have been applied to 3D-printed titanium implants to remove the unmelted particles, particularly in porous scaffolds.<sup>25</sup> However, there have been no previous studies comparing alkali-heat treatment effects across machining and LPBF orientations.

Hence in the present study, two different production methods, additive, laser powder bed fusion (LPBF) and subtractive manufacturing to treat Ti-6Al-4V discs were evaluated. The LPBF specimens were printed in two different building directions: horizontal (0°) and vertical (90°). Half of the samples from each group underwent alkali-heat treatment, which involved immersion in a 10 M NaOH solution at 90°C for 24 hours, followed by heat treatment at 600°C for 1 hour. The remainder of the sample was used as negative controls.

The current study aims to evaluate the effects of alkali-heat treatment on surface topography, physical properties, and chemical composition of additively manufactured titanium implants with different building orientations. We therefore hypothesized that such treatment and manufacturing parameters would significantly alter the properties of the materials, providing valuable insights into the relationship between production methods and surface modification outcomes.

## Materials and methods

### Sample Size Calculations

For surface characterization, three samples per group were analyzed by the Scanning Electron Microscopy (SEM) and the Energy Dispersive X-ray Spectroscopy (EDS), while one sample per group was used for X-ray Diffraction (XRD). The sample size for roughness analysis was determined using G\*Power with a significance level of 0.05, a power of 0.80, and an effect size of 2.11 from prior research<sup>16</sup>, yielding a calculated minimum of two samples. To allow for a 10% margin of error, three specimens per experimental group were included for roughness measurements.

### Preparation of Titanium Specimens

The disc-shaped titanium samples (10 mm diameter, 2 mm thickness) were fabricated via machining and laser powder bed fusion (LPBF). LPBF specimens were built in

horizontal (0°) and vertical (90°) orientations. A 3D model created in ANSYS Spaceclaim was prepared in Materialise Magics Print and printed from Ti-6Al-4V ELI powder (15–45 µm; AP&C, Canada) using a TruPrint 1000 machine (Trumpf, Germany). Process parameters included 100 W laser power, 1200 mm/s scanning speed, 80 µm hatch spacing, 20 µm layer thickness, and 30 µm laser spot diameter in an argon atmosphere (≤100 ppm oxygen). Printed specimens were removed by wire-cut EDM. Machined specimens were cut from Ti-6Al-4V ELI rods and sequentially polished with 400–1200 grit silicon carbide paper. All samples were ultrasonically cleaned with deionized water, acetone, ethanol, and DI water.

Surface modification involved immersion in 10 M NaOH at 90 °C for 24 hours, rinsing, air drying, and sintering at 600 °C for 1 hour.<sup>10–12</sup> Six experimental groups were prepared: non-treated machined (M), non-treated horizontally printed (H), non-treated vertically printed (V), treated machined (TM), treated horizontally printed (TH), and treated vertically printed (TV) specimens.

#### Scanning Electron Microscope and Energy Dispersive X-ray Spectroscopy

The surface topography and chemical composition of the six groups of titanium samples were evaluated using a scanning electron microscope (SEM) equipped with an energy-dispersive X-ray spectroscopy (EDS) (Quanta 250, FEI, USA). Prior to analysis, the prepared samples were stored in a desiccator overnight. SEM and EDS analyses were performed in high vacuum mode with an acceleration voltage of 20 kV. For SEM imaging, magnifications of 1,000×, 10,000×, and 50,000× were used to observe surface features. The SEM working distance ranged from 7.7 to 10 mm, and the spot size was set to 3.0. EDS analysis was conducted to determine the weight percentages (wt%) of elements present on the specimen surfaces at 1,000× magnification. The EDS working distance and spot size were set to 10 mm and 5.6, respectively.

#### X-ray Diffraction Analysis

X-ray diffraction (XRD) was conducted to identify the chemical composition and crystal structure of titanium samples produced by two different methods, with and without alkali-heat treatment. The analysis was performed at room temperature using a diffractometer (D8 Discover,

Bruker, Germany) with Cu K $\alpha$  radiation. Data was continuously collected over a  $2\theta$  range of 10° to 80° at a scan rate of 0.02° per second. The resulting diffraction data was analyzed using OriginPro (version 2025, OriginLab Corporation, Northampton, MA, USA).

#### Roughness Analysis

Surface roughness parameters, such as the arithmetic mean height (Ra), average roughness over an area (Sa), and 3D roughness profile were evaluated for six groups of titanium specimens. Each group consisted of three samples, and three locations were measured per sample. The assessments were conducted with 10x lens using an optical profilometer ( Alicona InfiniteFocus SL, Austria). Scanning was performed using the ALICONA Laboratory Measurement Module 5.4, and the results were analyzed with ALICONA MeasureSuite software ( Alicona, Austria).

#### Data Analysis

The weight percentages (wt%) of elements obtained from EDS analysis and surface roughness data (Sa and Ra) from the six experimental groups were analyzed. Normality was confirmed using the Shapiro-Wilk test. Since the data were normally distributed, a one-way ANOVA was performed to compare the six groups, followed by Tukey's post hoc test for pairwise comparisons. All data were reported as mean±SD. Statistical significance was set at  $p < 0.05$ . Data analysis was performed using GraphPad Prism (version 10.3.1, GraphPad Software, Boston, USA).

## Results

### Surface Topography of Differently Produced and Modified Titanium Specimens

The surface topography of titanium specimens, produced by different methods and modified via alkali-heat treatment, was examined using a scanning electron microscopy (SEM). In both vertically and horizontally printed LPBF samples, spherical particles were observed (Fig. 1C1, E1), with the vertically printed specimens showing a denser particle distribution. In contrast, the machined samples (Fig. 1A1) exhibited relatively smooth surfaces marked by polishing-induced scratches. At higher magnifications (10,000× and 50,000×), the unmodified specimens (Fig. 1A2, C2, E2, A3, C3, E3) displayed relatively smooth surfaces. After alkali-heat treatment, all modified groups at 1,000× (Fig.

1B1, D1, F1) showed uneven surface deposition while still retaining visible features of the original microtopography. At 10,000 $\times$  magnification (Fig. 1B2, D2, F2), irregularly distributed cracks and nanocrevices were observed. At 50,000 $\times$  (Fig. 1B3, D3, F3), the modified surfaces revealed numerous nanospikes with a porous surface texture.

### Surface Chemistry of Differently Produced and Modified Titanium Specimens

Energy-dispersive X-ray spectroscopy (EDS) characterized the titanium surfaces quantitatively (Table 1). Within both the non-treated and treated groups, most elements did not differ significantly between manufacturing methods. Untreated machined, horizontally, and vertically printed samples contained over 80 wt% titanium, with minor aluminum, vanadium, oxygen, and carbon evenly distributed. However, the aluminum and oxygen levels in the untreated vertical specimens were significantly different from those in the other two untreated groups. The analysis revealed statistically significant differences in chemical composition between treated and untreated groups, except for the proportion of carbon. Specifically, alkali-heat treatment significantly reduced titanium content to 46–48 wt%, increased oxygen to 39–42 wt%, and introduced sodium (5.12–5.82 wt%), suggesting sodium titanate formation. In the treated groups, the vertically printed samples exhibited the highest oxygen content, while the machined samples had the lowest. These results demonstrate that alkali-heat treatment alters surface chemistry by decreasing the proportion of metallic elements and enriching oxygen and sodium.

X-ray diffraction (XRD) was employed to further examine the chemical composition and crystalline structure of the titanium samples (Fig. 2). All groups exhibited strong diffraction peaks corresponding to the hexagonal close-packed ( $\alpha$ -phase) titanium (PDF 04-004-9156), with prominent peaks near 35.5°, 38.6°, 40.5°, 53.4°, and 63.6°. A weaker peak around 39.5°, associated with the body-centered cubic ( $\beta$ -phase) titanium (PDF 04-019-6427), was observed in both machined and treated machined specimens, indicating the presence of  $\alpha$ - $\beta$  titanium alloys. Following alkali-heat treatment, a new low-intensity diffraction peak emerged in all treated groups, notably at 48.3°, which did not correspond to either the  $\alpha$ - or  $\beta$ -Ti phases.

### Surface Roughness of Differently Produced and Modified Titanium Specimens

Three-dimensional surface profiles (Fig. 3A–F), obtained using an optical profilometer, qualitatively illustrate the topography of the specimens. These profiles were further evaluated to determine surface roughness parameters, including arithmetic mean height ( $R_a$ ) and area roughness ( $S_a$ ). Quantitative roughness analysis is shown in Fig. 3G, H. Machined and treated machined surfaces exhibited the lowest  $R_a$  and  $S_a$  values, indicating smoother topographies. In contrast, horizontally and vertically printed surfaces showed significantly higher roughness, with horizontally printed samples exhibiting the highest  $R_a$  and  $S_a$  values, followed by vertically printed ones. Notably, alkali-heat treatment did not significantly alter the surface roughness across any of the groups.

**Table 1** Chemical Composition of Different Titanium Surfaces

Treatment	Groups	Element (wt%) (Mean $\pm$ SD)					
		Titanium (Ti)	Aluminum (Al)	Vanadium (V)	Oxygen (O)	Carbon (C)	Sodium (Na)
Untreated	M	81.35 $\pm$ 0.16 <sup>A</sup>	5.50 $\pm$ 0.09 <sup>A</sup>	3.05 $\pm$ 0.08 <sup>A</sup>	6.03 $\pm$ 0.38 <sup>A</sup>	4.07 $\pm$ 0.22 <sup>AB</sup>	0 $\pm$ 0 <sup>A</sup>
	H	81.26 $\pm$ 0.84 <sup>A</sup>	5.69 $\pm$ 0.25 <sup>A</sup>	2.96 $\pm$ 0.12 <sup>A</sup>	6.03 $\pm$ 0.40 <sup>A</sup>	4.06 $\pm$ 0.55 <sup>AB</sup>	0 $\pm$ 0 <sup>A</sup>
	V	80.83 $\pm$ 0.38 <sup>A</sup>	4.80 $\pm$ 0.03 <sup>B</sup>	3.20 $\pm$ 0.07 <sup>A</sup>	7.59 $\pm$ 0.28 <sup>B</sup>	3.58 $\pm$ 0.06 <sup>B</sup>	0 $\pm$ 0 <sup>A</sup>
Treated	TM	48.45 $\pm$ 1.53 <sup>B</sup>	1.06 $\pm$ 0.28 <sup>C</sup>	1.06 $\pm$ 0.17 <sup>B</sup>	39.31 $\pm$ 0.79 <sup>C</sup>	5.00 $\pm$ 0.62 <sup>A</sup>	5.12 $\pm$ 0.62 <sup>B</sup>
	TH	46.79 $\pm$ 2.02 <sup>B</sup>	0.68 $\pm$ 0.13 <sup>C</sup>	0.86 $\pm$ 0.06 <sup>B</sup>	40.73 $\pm$ 0.75 <sup>CD</sup>	5.13 $\pm$ 0.61 <sup>A</sup>	5.82 $\pm$ 0.85 <sup>B</sup>
	TV	46.30 $\pm$ 0.61 <sup>B</sup>	0.70 $\pm$ 0.06 <sup>C</sup>	0.86 $\pm$ 0.02 <sup>B</sup>	41.72 $\pm$ 0.17 <sup>D</sup>	5.03 $\pm$ 0.26 <sup>A</sup>	5.40 $\pm$ 0.28 <sup>B</sup>

**Legend.** M (Machined); H (Horizontally Printed); V (Vertically Printed); TM (Treated Machined); TH (Treated Horizontally Printed); TV (Treated Vertically Printed). Different superscript capital letters within the same column indicate significant differences between the six titanium surfaces (one-way ANOVA with Tukey's post hoc test,  $p < 0.05$ ).



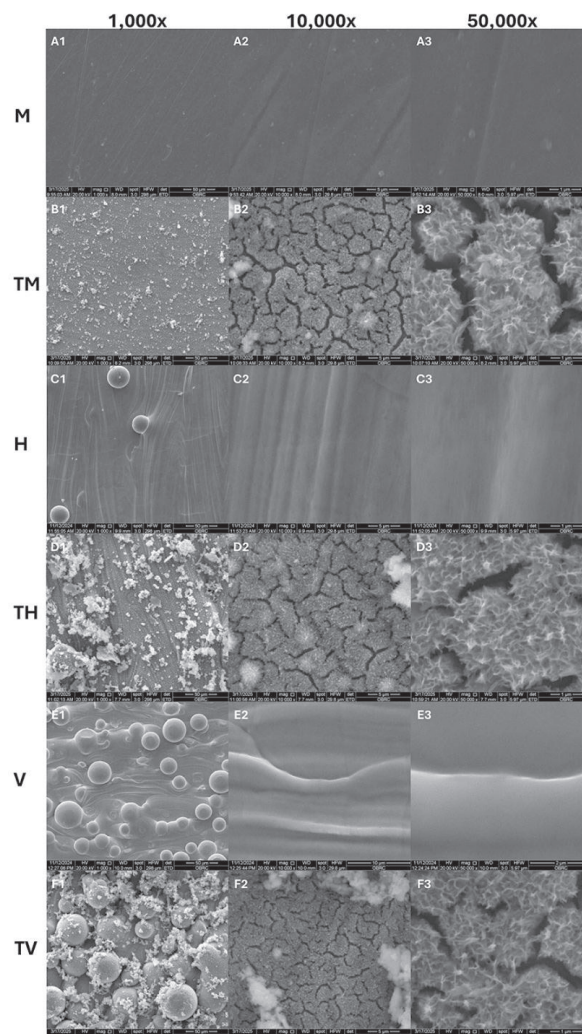


**Figure 1** Scanning Electron Micrographs of Different Titanium Surfaces at 1,000x, 10,000x, and 50,000x Magnifications (A1–A3) Untreated machined (M) specimens show smooth surfaces with polishing marks. (C1–C3) Horizontally printed (H) specimens exhibit globular particles with uniform distribution. (E1–E3) Vertically printed (V) specimens show denser particle accumulation. (B1, D1, F1) Alkali-heat-treated surfaces (TM, TH, TV) display surface deposits while retaining microtopography. (B2, D2, F2) At 10,000x, scattered cracks and nanoscale crevices are visible. (B3, D3, F3) At 50,000x, nanospikes and porous morphology appear.

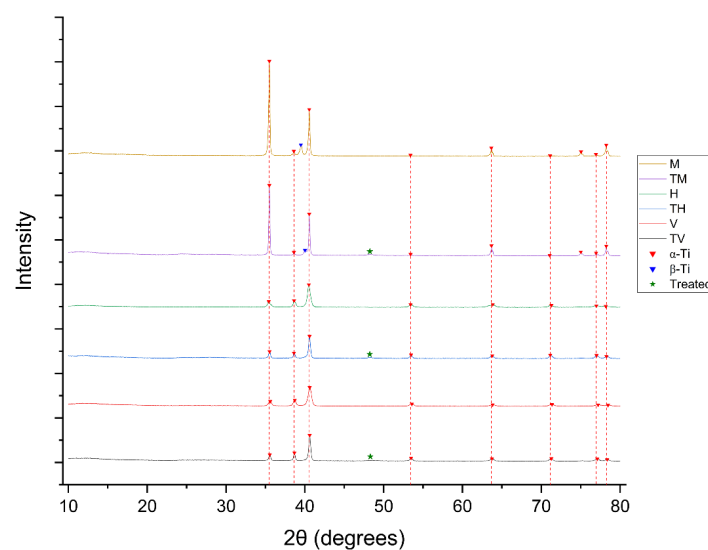


**Figure 2** XRD Patterns of Different Titanium Surfaces  
M, Machined; TM, Treated Machined; H, Horizontally Printed; TH, Treated Horizontally Printed; V, Vertically Printed; TV, Treated Vertically Printed.  
Red Triangle: Peaks corresponding to  $\alpha$ -phase titanium; Blue Triangle: Peaks corresponding to  $\beta$ -phase



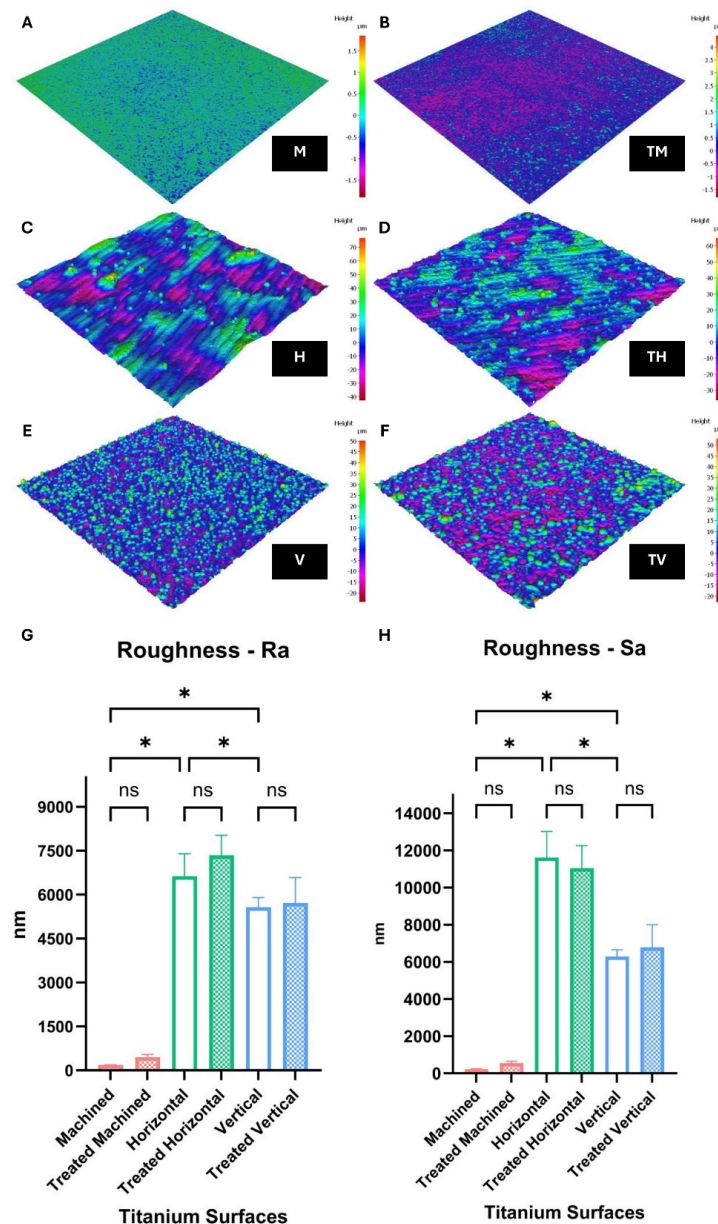


**Figure 3** 3D Roughness Profile and Roughness Parameters Analysis  
(A-F) 3D Roughness Profiles of different titanium surfaces  
M, Machined; TM, Treated Machined; H, Horizontally Printed; TH, Treated Horizontally Printed; V, Vertically Printed; TV, Treated Vertically Printed. (G) Mean arithmetic mean height (Ra); (H) Mean area roughness (Sa) of different titanium surfaces. Data are presented as means±standard deviation (SD). The asterisks indicate the statistical significance ( $p < 0.05$ ; Tukey's honest significant difference [HSD] test).

## Discussion

This study aimed to assess how alkali-heat treatment affects the surface characteristics of Ti-6Al-4V specimens produced by different manufacturing methods including subtractive (machined) and additive (LPBF with horizontal and vertical orientations). The findings show that both the production method and the surface modification technique significantly influence surface morphology, chemistry, and roughness of the titanium implant.

SEM imaging revealed clear distinctions in surface topography between production methods. As expected, machined specimens exhibited smooth surfaces with polishing marks, while LPBF-produced specimens showed prominent spherical particles, more densely distributed in vertically printed samples. The presence and distribution of partially melted powder remnants described in the present study are commonly observed

in LPBF-manufactured titanium surfaces with different building directions.<sup>16,17</sup> Following alkali-heat treatment, all groups displayed significant morphological changes, including nanospikes and nanocrevices distributed unevenly across the surface, which align with previous observations of sodium titanate nanostructure formation.<sup>8,11</sup> Furthermore, the nanotopography created by alkali-heat treatment has been shown to influence osseointegration. Previous studies using the same treatment on machined samples have shown that the resulting titanium surfaces can promote the formation of an osteocyte lacunar–canalicular network and enhance peri-implant osseointegration.<sup>10,14</sup> In this study, SEM images revealed similar nanostructures on both machined and LPBF specimens, suggesting comparable properties. However, further *in vitro* and *in vivo* investigations are needed to confirm these findings. Interestingly, the LPBF-manufactured samples retained much of their original microtopography after alkali-heat treatment, while the machined surfaces became noticeably more textured. This suggests that the treatment has a more pronounced effect on the nanotopography of titanium surfaces.

EDS analysis confirmed a substantial shift in surface composition after alkali-heat treatment. Untreated specimens consisted primarily of titanium, aluminum, and vanadium, consistent with Ti-6Al-4V alloy composition. Notably, a high proportion of carbon was detected across all groups, likely indicating surface contamination from handling, the environment, or the sample preparation process, which has also been reported in a previous titanium surface study.<sup>26</sup> Since the contamination was present across all groups at comparable levels, it should not affect the relative comparisons or overall interpretations of elemental changes after alkali-heat treatment. Post-treatment, there was a marked increase in oxygen and the appearance of sodium, indicating successful formation of a sodium titanate layer, a key objective of this study. These results are consistent with earlier studies reporting the transformation of titanium surfaces through NaOH treatment into bioactive titanate layers.<sup>7,11,27</sup> The higher oxygen content after alkali-heat treatment reflects the formation of a thicker TiO<sub>2</sub> layer that could increase surface wettability and facilitate osteoblast attachment.<sup>28</sup> The sodium detected on the surface originates from sodium titanate, which can undergo ion exchange

with protons under physiological conditions, generating Ti-OH groups that promote apatite nucleation.<sup>7,29</sup> This bioactive apatite layer has been shown to mediate strong bone bonding, consistent with prior *in vitro* and *in vivo* studies demonstrating improved osseointegration of alkali heat-treated titanium implants.<sup>10,12,30,31</sup>

XRD analysis further supported the observed compositional changes. Untreated samples exhibited dominant peaks corresponding to the  $\alpha$ -Ti phase, with minor  $\beta$ -phase peaks, consistent with previous studies.<sup>16,32</sup> In Ti-6Al-4V, the  $\alpha$ -phase provides strength and corrosion resistance, while the  $\beta$ -phase contributes ductility.<sup>33</sup> In this study,  $\beta$ -phase peaks were observed only in the machined specimens, while LPBF-produced samples exhibited predominantly  $\alpha$ -phase, could be due to the rapid cooling suppressing  $\beta$ -phase retention.<sup>34</sup> Since these phases mainly influence the mechanical properties of the alloy, their distribution may affect implant stability, whereas biological performance is more directly related to surface chemistry and topography. Following alkali-heat treatment, all groups displayed a new diffraction peak around 48.3°, likely associated with the formation of sodium titanate. The presence of this peak across all treated groups, regardless of manufacturing method, indicates that the alkali-heat process reliably induces a chemical phase transformation. However, the relatively low intensity and the appearance of only a single sodium titanate peak suggest that further investigation is necessary to confirm the extent and crystallinity of the newly formed phase.

Surface roughness analysis revealed that LPBF specimens, particularly those printed in the horizontal orientation, had significantly higher Ra and Sa values than machined specimens, both before and after treatment. This aligns with prior findings where LPBF processes inherently produce rougher surfaces due to powder sintering characteristics and layer-by-layer fabrication.<sup>16,24,35</sup> However, some studies have reported that vertically printed specimens typically demonstrate greater surface roughness than those printed horizontally, which contrasts with the findings of the present study.<sup>16,32</sup> This discrepancy may be explained by differences in measurement instruments and magnifications. Our analysis was performed using an optical profilometer with a 10x

lens and a scan area of 2 × 2 mm. In contrast, Celles *et al* used a laser confocal microscope at 428× magnification and reported vertically printed samples to be rougher.<sup>16</sup> Similarly, Huang *et al.* employed both a contact profilometer and atomic force microscopy (scan areas of 500 µm × 500 µm and 5 µm × 5 µm, respectively) and found higher roughness in vertical specimens.<sup>26</sup> To the best of our knowledge, our study is the first to report horizontal orientation producing a rougher surface. This may be due to larger scan areas capturing greater disparities between peaks and valleys, or to limitations of the measurement technique, in which densely packed particles could prevent full detection of the deepest points on the surface.

Contrary to some expectations based on previous literature<sup>8,12</sup>, alkali-heat treatment did not significantly alter the surface roughness in any of the experimental groups. This may be attributed to the already high baseline roughness of the LPBF specimens, which could have masked subtle changes, or to limitations in the resolution of the measurement equipment, which may not effectively capture nanoscale modifications.

A key limitation of this study is its exclusive focus on the chemical composition and physical surface properties of titanium implants. While these characteristics provide valuable insights into material performance, they do not capture the biological interactions critical to clinical outcomes. Therefore, future research should include both *in vitro* and *in vivo* studies to evaluate cellular responses and determine the clinical relevance of the different production methods and surface treatments.

## Conclusion

This study shows that both the manufacturing method and alkali-heat treatment influence the surface properties of Ti-6Al-4V implants. While the elemental composition remained consistent, the manufacturing method led to distinct differences in surface topography. Machined specimens exhibited an  $\alpha$ - $\beta$  phase, whereas LPBF specimens showed an  $\alpha$  phase. Surface roughness was also higher in LPBF implants compared with machined ones, with horizontal LPBF rougher than vertical. Alkali-heat treatment effectively modified the surface chemistry by forming a sodium titanate layer without significantly

changing roughness. Overall, these findings indicate that optimizing processing and surface modification can tailor surface properties to potentially enhance bioactivity, although further biological validation is needed.

## Acknowledgement

This project was supported by the National Research Council of Thailand and the Faculty of Dentistry Chulalongkorn Dental Research Grant. The authors gratefully acknowledge Assist. Prof. Dr. Soranun Chantarangsu for reviewing the statistical analysis methodology, and K Dental Laboratory for providing the furnace used in the heat treatment process.

## References

1. Gupta R, Gupta N, Weber DK. Dental Implants. StatPearls. Treasure Island (FL)2024.
2. Zhang K, Zhang B, Huang C, Gao S, Li B, Cao R, *et al.* Biocompatibility and antibacterial properties of pure titanium surfaces coated with yttrium-doped hydroxyapatite. *J Mech Behav Biomed Mater* 2019; 100:103363.
3. Van Noort R. Titanium: the implant material of today. *J Mater Sci* 1987;22:3801-11.
4. Feller L, Jadwat Y, Khammissa RA, Meyerov R, Schechter I, Lemmer J. Cellular responses evoked by different surface characteristics of intraosseous titanium implants. *Biomed Res Int* 2015;2015:171945.
5. Inchingolo AM, Malcangi G, Ferrante L, Del Vecchio G, Viapiano F, Inchingolo AD, *et al.* Surface Coatings of Dental Implants: A Review. *J Funct Biomater* 2023;14(5):287.
6. Mandracci P, Mussano F, Rivolo P, Carossa S. Surface treatments and functional coatings for biocompatibility improvement and bacterial adhesion reduction in dental implantology. *Coatings* 2016;6(1):7.
7. Kokubo T, Yamaguchi S. Bioactive titanate layers formed on titanium and its alloys by simple chemical and heat treatments. *Open Biomed Eng J* 2015;9:29-41.
8. Kato E, Sakurai K, Yamada M. Periodontal-like gingival connective tissue attachment on titanium surface with nano-ordered spikes and pores created by alkali-heat treatment. *Dent Mater* 2015;31(5):e116-30.
9. Pattanayak DK, Fukuda A, Matsushita T, Takemoto M, Fujibayashi S, Sasaki K, *et al.* Bioactive Ti metal analogous to human cancellous bone: Fabrication by selective laser melting and chemical treatments. *Acta Biomater* 2011;7(3):1398-406.
10. He X, Yamada M, Watanabe J, Pengyu Q, Chen J, Egusa H. Titanium nanotopography enhances mechano-response of osteocyte three-dimensional network toward osteoblast activation. *Biomater Adv* 2024;163:213939.
11. Yamada M, Kimura T, Nakamura N, Watanabe J, Kartikasari N, He X, *et al.* Titanium Nanosurface with a Biomimetic Physical

Microenvironment to Induce Endogenous Regeneration of the Periodontium. *ACS Appl Mater Interfaces* 2022;14(24):27703-19.

12. Kartikasari N, Yamada M, Watanabe J, Tiskratok W, He X, Kamano Y, *et al.* Titanium surface with nanospikes tunes macrophage polarization to produce inhibitory factors for osteoclastogenesis through nanotopographic cues. *Acta Biomater* 2022;137:316-30.

13. Kartikasari N, Yamada M, Watanabe J, Tiskratok W, He X, Egusa H. Titania nanospikes activate macrophage phagocytosis by ligand-independent contact stimulation. *Sci Rep* 2022;12(1):12250.

14. He X, Yamada M, Watanabe J, Tiskratok W, Ishibashi M, Kitaura H, *et al.* Titanium nanotopography induces osteocyte lacunar-canalicular networks to strengthen osseointegration. *Acta Biomater* 2022;151:613-27.

15. Yamada M, Kato E, Yamamoto A, Sakurai K. A titanium surface with nano-ordered spikes and pores enhances human dermal fibroblastic extracellular matrix production and integration of collagen fibers. *Biomed Mater* 2016;11(1):015010.

16. Celles CAS, Teixeira ABV, da Costa Valente ML, Sangali M, Rodrigues JFQ, Caram R, *et al.* Effect of post-processing and variation of the building angle of Ti-6Al-4 V disks obtained by selective laser melting: A comparison of physical, chemical and mechanical properties to machined disks. *Mater Today Commun* 2024;39:108700.

17. Lee UL, Yun S, Lee H, Cao HL, Woo SH, Jeong YH, *et al.* Osseointegration of 3D-printed titanium implants with surface and structure modifications. *Dent Mater* 2022;38(10):1648-60.

18. Nyberg EL, Farris AL, Hung BP, Dias M, Garcia JR, Dorafshar AH, *et al.* 3D-Printing Technologies for Craniofacial Rehabilitation, Reconstruction, and Regeneration. *Ann Biomed Eng* 2017;45(1):45-57.

19. Steinbacher DM. Three-Dimensional Analysis and Surgical Planning in Craniomaxillofacial Surgery. *J Oral Maxillofac Surg* 2015;73(12 Suppl):S40-56.

20. Carter LN, Martin C, Withers PJ, Attallah MM. The influence of the laser scan strategy on grain structure and cracking behaviour in SLM powder-bed fabricated nickel superalloy. *J Alloys Compd* 2014;615:338-47.

21. Elambasseril J, Rogers J, Wallbrink C, Munk D, Leary M, Qian M. Laser powder bed fusion additive manufacturing (LPBF-AM): the influence of design features and LPBF variables on surface topography and effect on fatigue properties. *Critical reviews in solid state and materials sciences* 2023;48(1):132-68.

22. Lin WS, Starr TL, Harris BT, Zandinejad A, Morton D. Additive manufacturing technology (direct metal laser sintering) as a novel approach to fabricate functionally graded titanium implants: preliminary investigation of fabrication parameters. *Int J Oral Maxillofac Implants* 2013;28(6):1490-5.

23. Calazans Neto JV, Reis ACD, Valente M. Influence of building direction on physical and mechanical properties of titanium implants: A systematic review. *Heliyon* 2024;10(9):e30108.

24. Weissmann V, Drescher P, Seitz H, Hansmann H, Bader R, Seyfarth A, *et al.* Effects of Build Orientation on Surface Morphology and Bone Cell Activity of Additively Manufactured Ti6Al4V Specimens. *Materials (Basel)* 2018;11(6):915.

25. Liu W, Li W, Wang H, Bian H, Zhang K. Surface modification of porous titanium and titanium alloy implants manufactured by selective laser melting: A review. *Advanced Engineering Materials* 2023;25(21):2300765.

26. Huang LZ, Truong VK, Murdoch BJ, Elbourne A, Caruso RA. Inherent variation in surface roughness of Selective Laser Melting (SLM) printed titanium caused by build angle changes the mechanomicrobiocidal effectiveness of nanostructures. *Journal of Colloid and Interface Science* 2025:137866.

27. Luo Y, Jiang Y, Zhu J, Tu J, Jiao S. Surface treatment functionalization of sodium hydroxide onto 3D printed porous Ti6Al4V for improved biological activities and osteogenic potencies. *J Mater Res Technol* 2020;9(6):13661-70.

28. Mizutani T, Tsuchiya S, Honda M, Montenegro Raudales JL, Kuroda K, Miyamoto H, *et al.* Alkali-treated titanium dioxide promotes formation of proteoglycan layer and altered calcification and immunotolerance capacity in bone marrow stem cell. *Biochem Biophys Rep* 2023;36:101569.

29. Kokubo T, Yamaguchi S. Novel bioactive titanate layers formed on Ti metal and its alloys by chemical treatments. *Materials* 2009; 3(1):48-63.

30. Lei H, Zhou Z, Liu J, Cao H, Wu L, Song P, *et al.* Structural Optimization of 3D-Printed Porous Titanium Implants Promotes Bone Regeneration for Enhanced Biological Fixation. *ACS Applied Materials & Interfaces* 2025;17(12):18059-73.

31. da Costa Valente ML, Uehara LM, Lisboa Batalha R, Bolfarini C, Trevisan RLB, Fernandes RR, *et al.* Current Perspectives on Additive Manufacturing and Titanium Surface Nanotopography in Bone Formation. *J Biomed Mater Res B Appl Biomater* 2025;113(3):e35554.

32. Sarker A, Tran N, Rifai A, Brandt M, Tran PA, Leary M, *et al.* Rational design of additively manufactured Ti6Al4V implants to control Staphylococcus aureus biofilm formation. *Materialia* 2019;5:100250.

33. Bieler TR, Trevino RM, Zeng L. Alloys: Titanium. In: Bassani F, Liedl GL, Wyder P, editors. Encyclopedia of Condensed Matter Physics. Oxford: Elsevier; 2005. p. 65-76.

34. Arputharaj JD, Nafisi S, Dareh Baghi A, Ghomashchi R. Continuous cooling transformation of L-PBF Ti64. *J Alloys Compd* 2025;1021:179700.

35. Wysocki B, Maj P, Sitek R, Buhagiar J, Kurzydowski KJ, Swieszkowski W. Laser and electron beam additive manufacturing methods of fabricating titanium bone implants. *Applied Sciences* 2017;7(7):657.



## Original Articles

# Biodentine™ and MAC28 Inhibit Lipopolysaccharides-Induced Pulpal Inflammation in Human Dental Pulp Cells

Witsuta Pongphaladisai<sup>1</sup>, Sitthikorn Kunawarote<sup>1</sup>, Guang Liang<sup>2</sup>, Siriporn C. Chattipakorn<sup>3,4,5</sup>, Savitri Vaseenon<sup>1</sup>

<sup>1</sup>Department of Restorative Dentistry and Periodontology, Faculty of Dentistry, Chiang Mai University, Chiang Mai, Thailand

<sup>2</sup>Chemical Biology Research Center, School of Pharmaceutical Sciences, Wenzhou Medical University, Wenzhou, Zhejiang, China

<sup>3</sup>Neurophysiology Unit, Cardiac Electrophysiology Research and Training Center, Faculty of Medicine, Chiang Mai University, Chiang Mai, Thailand

<sup>4</sup>Center of Excellence in Cardiac Electrophysiology Research, Chiang Mai University, Chiang Mai, Thailand

<sup>5</sup>Department of Oral Biology and Diagnostic Sciences, Faculty of Dentistry, Chiang Mai University, Chiang Mai, Thailand

## Abstract

Our previous results demonstrated that pretreatment with monocarbonyl analogue of curcumin compound 28 (MAC28) in lipopolysaccharides (LPS)-treated human dental pulp cells (HDPCs) could suppress inflammation. However, the pharmacological action of MAC28 co-incubated with LPS in HDPCs remained unclear. Furthermore, the impact of MAC28 in combination with Biodentine™ in LPS-treated HDPCs was still unclear. This study aimed to examine the cell viability and anti-inflammatory effects of Biodentine™ and MAC28 in LPS-treated HDPCs. HDPCs were assigned to five groups: (1) control, (2) LPS, (3) LPS + MAC28, (4) LPS + Biodentine™, and (5) LPS + MAC28 + Biodentine™. The concentration of LPS and MAC28 used in this study were 20 µg/mL and 10 µM, respectively. The Biodentine™ extract was mixed with Alpha modification of Minimum Essential Medium Eagle ( $\alpha$ -MEM) at a 1:16 dilution ratio for cell treatments. Cell viability was assessed using the Alamar Blue assay. The expressions of toll-like receptor-4 (TLR-4), myeloid differentiation factor-2 (MD-2), tumor necrosis factor-alpha (TNF- $\alpha$ ), and interleukin-6 (IL-6) mRNA were analyzed by qRT-PCR. Data was analyzed using one-way ANOVA with LSD post hoc tests at a 95% confidence interval. The results demonstrated that LPS treatment did not significantly affect HDPC viability compared with the control ( $p > 0.05$ ). Similarly, co-treatment with MAC28, Biodentine™, or both combined did not affect cell viability ( $p > 0.05$  vs. control), indicating no cytotoxicity under the experimental conditions. LPS significantly upregulated TLR-4, MD-2, TNF- $\alpha$ , and IL-6 mRNAs when compared with the control ( $p < 0.05$ ). However, LPS-induced HDPCs co-incubated with MAC28, Biodentine™, or their combination significantly reduced the expressions of TLR-4, MD-2, and TNF- $\alpha$  mRNAs ( $p < 0.05$ ), while the expression of IL-6 mRNA levels remained unchanged when compared with the LPS group ( $p > 0.05$ ). MAC28 and Biodentine™ exhibited anti-inflammatory effects without cytotoxicity in LPS-treated HDPCs, supporting their potential as adjunctive agents for the treatment of pulpitis.

**Keywords:** Biodentine™, Dental pulp, Inflammation, Lipopolysaccharides, Pulpitis

**Received date:** Jul 7, 2025

**Revised date:** Sep 15, 2025

**Accepted date:** Sep 18, 2025

**Doi:** 10.14456/jdat.2025.27

### Correspondence to:

Savitri Vaseenon, Department of Restorative Dentistry and Periodontology, Faculty of Dentistry, Chiang Mai University, Suthep Road, Muang District, Chiang Mai, 50200, Thailand. Tel: 053-944-457 Email: savitri.v@cmu.ac.th



## Introduction

Dental caries-induced pulpitis is among the most common oral diseases worldwide.<sup>1</sup> Toll-like receptor-4 (TLR-4) has received significant attention as it is involved in the inflammatory process of the dental pulp at the cellular level.<sup>2</sup> Myeloid differentiation factor-2 (MD-2) is a protein essential for the activation of TLR-4 signaling, which plays a critical role in inflammation across various tissues.<sup>3,4</sup> Several studies have demonstrated that the TLR-4/MD-2 complex is present on cell surfaces, including the membranes of dental pulp cells.<sup>5,6</sup> Lipopolysaccharide (LPS) is one of the most important molecules initiating TLR-4/MD-2 signaling. It binds to hydrophobic MD-2, thereby triggering inflammation.<sup>4,7</sup> Therefore, blocking TLR-4

signaling via MD-2 inhibitors represents a potential therapeutic strategy for the treatment of pulpitis (Fig. 1).<sup>8</sup>

The monocarbonyl analogue of curcumin compound 28 (MAC28), a curcumin-derived compound that functions as an MD-2 inhibitor, has been shown to block TLR-4 signaling in LPS-treated macrophages by directly binding to MD-2.<sup>9</sup> Our previous results demonstrated that pretreatment with MAC28 in LPS-treated human dental pulp cells (HDPCs) effectively inhibited inflammation (Fig. 1).<sup>8</sup> However, the pharmacological effects of MAC28 when co-incubated with LPS in HDPCs remain unclear. In addition, evidence regarding the pharmacodynamic effects of MAC28 in combination with Biodentine™ in LPS-stimulated HDPCs is still lacking.

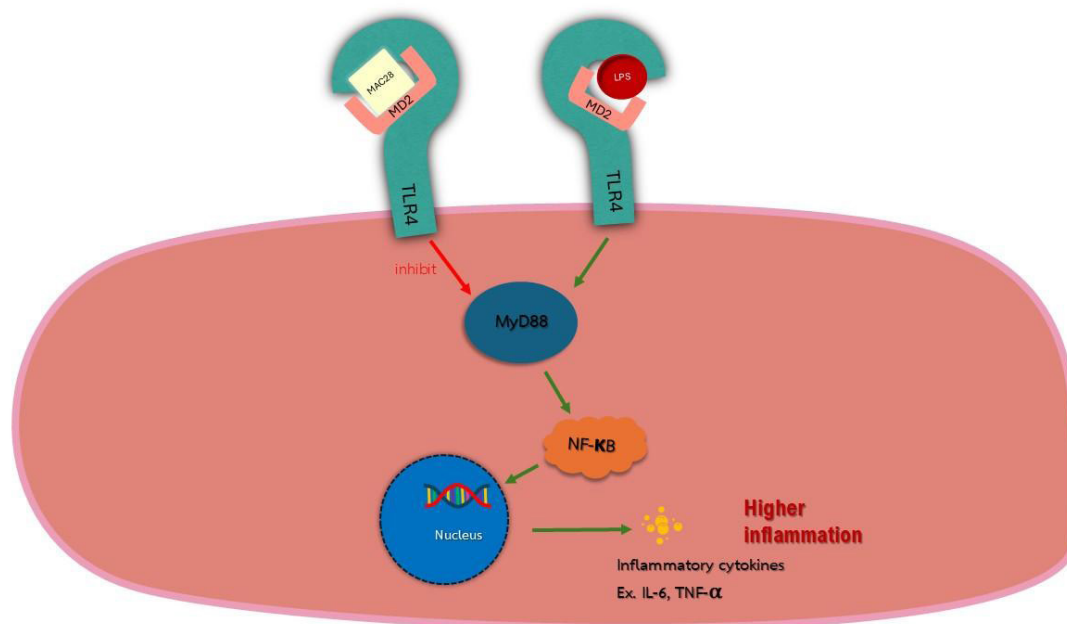


**Figure 1** The relationship between LPS, MD-2, TLR-4, and MAC28. IL-6, interleukin-6; LPS, lipopolysaccharides; MAC28, monocarbonyl analogue of curcumin compound 28; MD-2, myeloid differentiation factor-2; MyD88, Myeloid differentiation primary response 88; NF-κB, nuclear factor kappa-light-chain-enhancer of activated B cells; TLR-4, toll-like receptor-4; TNF-α, tumor necrosis factor-alpha

This study aimed to investigate the cell viability and anti-inflammatory effects of Biodentine™ and MAC28 in LPS-stimulated HDPCs. It was hypothesized that both materials would reduce inflammation in LPS-stimulated HDPCs and that their combination would synergistically inhibit the inflammatory response.

## Materials and methods

### Dental pulp tissue collection and dental pulp cell culture

This study was performed following approval from the Human Experimentation Committee, Faculty of Dentistry, Chiang Mai University, Thailand (ethical approval number: 53/2022). After informed consent was obtained

from all participants, healthy dental pulp tissues were collected from individuals aged 18-21 years who were scheduled for the surgical removal or extraction of impacted teeth. Following tooth extraction, dental pulp tissues were aseptically removed from teeth and collected for cell culture as previously described.<sup>10</sup> The HDPCs were cultured in Alpha modification of Minimum Essential Medium Eagle ( $\alpha$ -MEM) (Sigma-Aldrich, St Louis, MO, USA) containing 10% fetal bovine serum (FBS) (Gibco, USA), 100 U/mL of penicillin, 100  $\mu$ g/mL streptomycin (Gibco, USA), and 100  $\mu$ mol/L of L-ascorbic acid at 37°C in an atmosphere of 5% CO<sub>2</sub>. The medium was renewed every other day. HDPCs from passages two to five were used in the experiment.

### The study design

HDPCs were divided into five groups,  $n = 3$ /group, as follows: 1) control group: cells were maintained in culture medium containing 0.0001% dimethyl sulfoxide (DMSO); 2) LPS group: cells were maintained in culture medium containing 20  $\mu$ g/mL LPS; 3) LPS + MAC28 group: cells were maintained in culture medium containing 20  $\mu$ g/mL LPS and 10  $\mu$ M MAC28; 4) LPS + Biodentine™ group: cells were maintained in culture medium containing 20  $\mu$ g/mL LPS and Biodentine™ extract; and 5) LPS + MAC28 + Biodentine™ group: cells were maintained in culture medium containing 20  $\mu$ g/mL LPS, 10  $\mu$ M MAC28, and Biodentine™ extract. After 24 hours of treatment, cell viability and inflammation were analyzed.

### Preparation of LPS, MAC28, and Biodentine™

A concentration of 20  $\mu$ g/mL LPS, 10  $\mu$ M MAC28, and Biodentine™ extract was used in this study, in accordance with previous studies.<sup>8-10</sup> LPS from *Escherichia coli* (O111:B4; #0000110081) was purchased from Sigma-Aldrich. MAC28 was provided by Wenzhou Medical University, Zhejiang, China. A 1 M stock solution of MAC28 (molecular weight = 469.53) was prepared in 100% DMSO according to previous reports.<sup>8</sup> The absolute concentration of 10  $\mu$ M MAC28 in culture medium was used for cell treatment.<sup>8,9</sup> Since the absolute concentration of DMSO diluted in culture medium consisting of MAC28 was 0.0001%, 0.0001% DMSO was also included in the control group, LPS group,

and Biodentine™ group. Biodentine™ extract was prepared following a previously described method.<sup>10-12</sup> The Biodentine™ extract was diluted in culture medium at a ratio of 1:16 for cell treatments.

### Determination of cell viability

To determine the viability of HDPCs in culture medium containing LPS, MAC28, and Biodentine™, HDPCs were divided into eight groups ( $n = 3$ /group), as follows: 1) control group; 2) LPS group; 3) MAC28 group; 4) Biodentine™ group; 5) MAC28 + Biodentine™ group; 6) LPS + MAC28 group; 7) LPS + Biodentine™ group; and 8) LPS + MAC28 + Biodentine™ group. After seeding 10,000 HDPCs per well in 96-well plates for 24 hours, cell treatments were performed as previously mentioned. In each assigned group, the cell treatment was performed in triplicate. At the end of the 24-hour experiment, cell viability was examined by an Alamar Blue assay as described by Weekate *et al.*<sup>10</sup> In brief, 10% AlamarBlue® was added to each well and incubated for four hours at 37°C. The absorbance reading was set at 570-600 nm using a multi-well scanning spectrophotometer (Tecan Group Ltd., Männedorf, canton of Zürich, Switzerland). HDPCs in the control group were interpreted as 100% viable.

### Determination of inflammation by quantitative real-time polymerase chain reaction (qRT-PCR)

To examine the inflammatory markers, HDPCs were seeded in 6-well plates at a density of  $2.5 \times 10^5$  cells/well. The HDPCs were assigned to five groups as previously stated in the study design. In each assigned group, the cell treatment was performed in triplicate. After 24 hours of treatment, qRT-PCR was conducted using the RNeasy Mini Kit (QIAGEN). Subsequently, cDNA was synthesized using PCRBIOSYSTEMS cDNA UltraScript kit according to the manufacturer's instructions. qRT-PCR was conducted using the SYBR Green-based method. The primer pairs for TLR-4, MD-2, tumor necrosis factor-alpha (TNF- $\alpha$ ), interleukin-6 (IL-6), and GAPDH used in this study are presented in Table 1. The relative changes in gene expression were normalized with GAPDH and quantified using the  $2^{-\Delta\Delta CT}$  method.<sup>13</sup>

**Table 1** List of primer pairs used for qRT-PCR analysis<sup>8</sup>

mRNA	Primer sequences (5' to 3')
TLR-4	Forward: CAA CAA AGG TGG GAA TGC TT Reverse: TGC CAT TGA AAG CAA CTC TG
MD-2	Forward: TTC CAC CCT GTT TTC TTC CA Reverse: AAT CGT CAT CAG ATC CTC GG
TNF- $\alpha$	Forward: GCT GCA CTT TGG AGT GAT CG Reverse: CTT ACC TAC AAC ATG GGC TAC AG
IL-6	Forward: ATG AAC TCC TTC TCC ACA AGC GC Reverse: GAA GAG CCC TCA GGC TGG ACT G
GAPDH	Forward: ACC ACA GTC CAT GCC ATC AC Reverse: TCC ACC ACC CTG TTG CTG TA

Abbreviations: GAPDH, glyceraldehyde-3-phosphate dehydrogenase; IL-6, interleukin 6; MD-2, myeloid differentiation factor-2; qRT-PCR, quantitative real-time polymerase chain reaction; TLR-4, toll-like receptor-4; TNF- $\alpha$ , tumor necrosis factor-alpha.

## Statistical analysis

The statistical analysis was performed based on  $n = 3/\text{group}$  for all experiments. The results were expressed as mean  $\pm$  standard deviation (SD). One-way ANOVA followed by post hoc LSD tests were conducted for group comparison. All statistical analyses were carried out using GraphPad Prism 10 (version 10.2.1) software for macOS. A 95% confidence level for statistical significance was applied in this study ( $p < 0.05$ ).

## Results

### Effects of LPS, MAC28, and Biodentine™ on HDPC viability

At the 24-hour incubation period, 20  $\mu\text{g}/\text{mL}$  LPS did not influence HDPC viability when compared with the control group (Fig. 2,  $p > 0.05$ ). In addition, HDPCs co-incubated with 10  $\mu\text{M}$  MAC28, Biodentine™ extract, and the combination of MAC28 and Biodentine™ for 24 hours also showed comparable cell viability compared with the control group (Fig. 2,  $p > 0.05$ ). Furthermore, LPS-induced HDPCs co-incubated with either MAC28, Biodentine™, or both combined for 24 hours showed no reduction in viability, as the percentages of the viable HDPCs were similar to those in the control (Fig. 2,  $p > 0.05$ ).

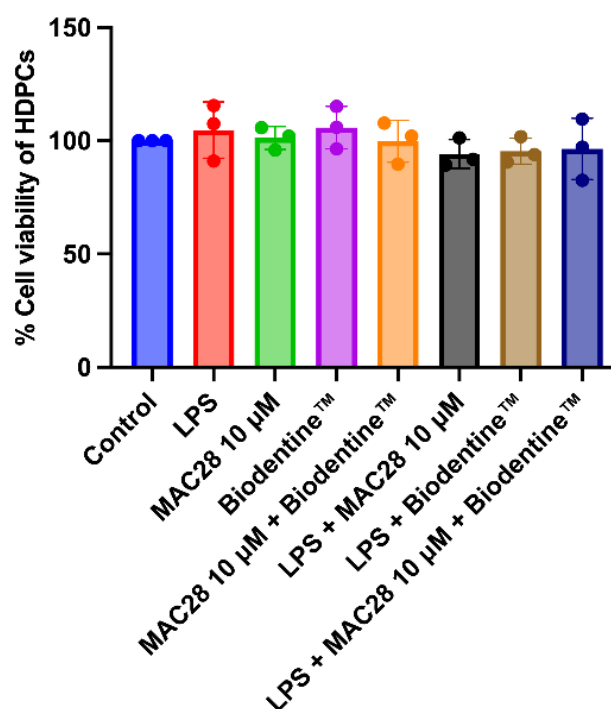


**Figure 2** Cell viability (% control) in LPS-treated HDPCs exposed to MAC28, Biodentine™, and their combination for 24 h ( $n = 3/\text{group}$ ). \*  $p < 0.05$ . Statistical analyses were performed by One-way ANOVA. HDPCs, human dental pulp cells; LPS, lipopolysaccharides; MAC28, monocarbonyl analogue of curcumin compound 28

## Effects of MAC28, Biodentine™, and both combined on the LPS-induced inflammation in HDPCs

Treatment with 20 µg/mL LPS for 24 hours significantly induced inflammation as the levels of TLR-4, MD-2, TNF- $\alpha$ , and IL-6 mRNAs were upregulated when compared with the controls (Fig. 3A-D,  $p < 0.05$ ). Co-incubation of either 10 µM MAC28, Biodentine™ extract, or the combination of

MAC28 and Biodentine™ significantly reduced the levels of TLR-4, MD-2, and TNF- $\alpha$  mRNAs compared with the LPS group (Fig. 3A-C,  $p < 0.05$ ). However, the expression of IL-6 mRNA remained unchanged in LPS-induced HDPCs treated with the MAC28, Biodentine™, or combined conditions (Fig. 3D,  $p > 0.05$ ).

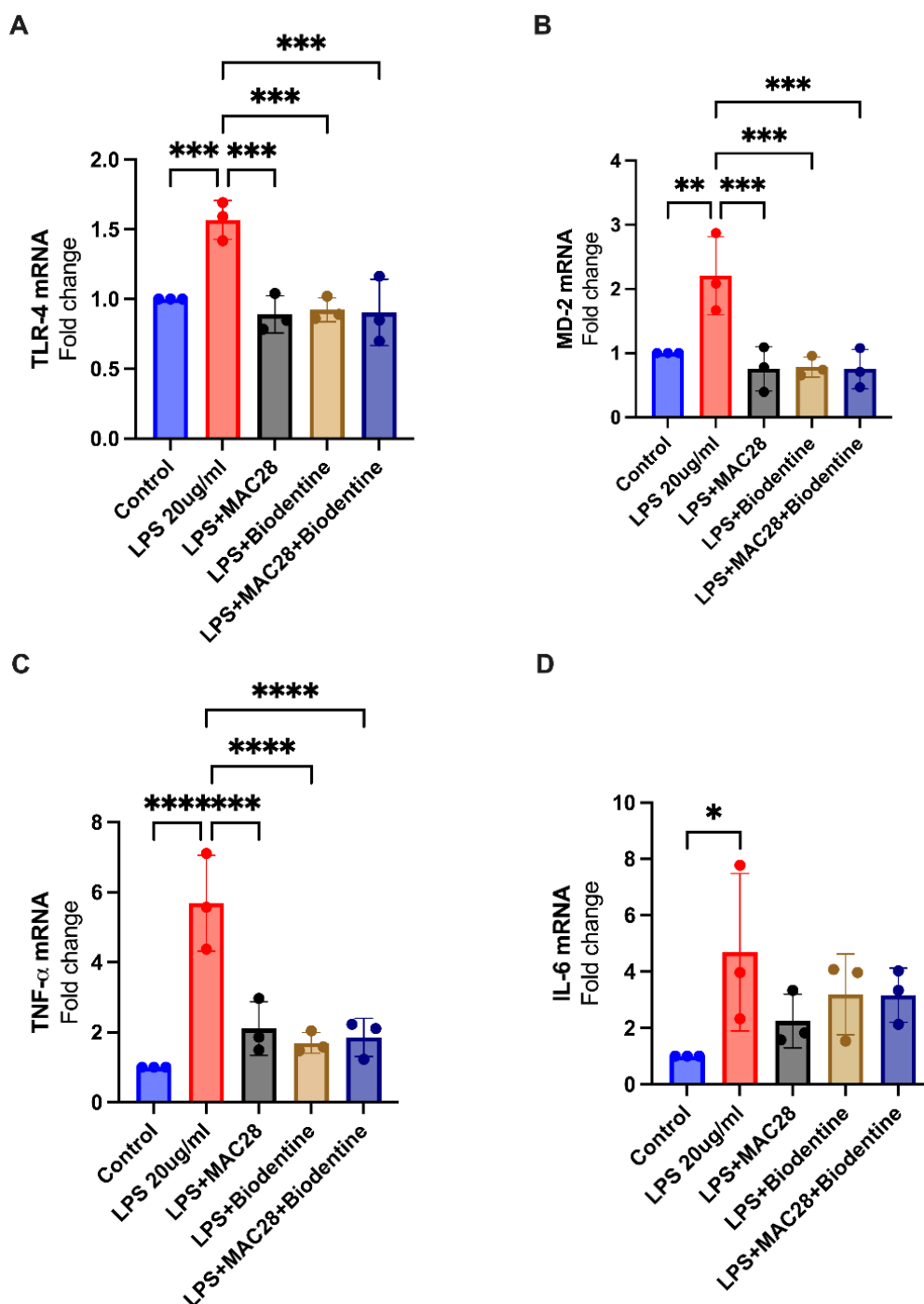


**Figure 3** Inflammatory profiles of LPS-treated HDPCs: A) Expression of TLR-4 mRNA ( $n = 3/\text{group}$ ), B) Expression of MD-2 mRNA ( $n = 3/\text{group}$ ), C) Expression of TNF- $\alpha$  mRNA ( $n = 3/\text{group}$ ), and D) Expression of IL-6 mRNA ( $n = 3/\text{group}$ ). \*  $p < 0.05$ , \*\*  $p < 0.01$ , \*\*\*  $p < 0.001$ , \*\*\*\*  $p < 0.0001$ . IL-6, interleukin-6; LPS, lipopolysaccharides; MAC28, monocarbonyl analogue of curcumin compound 28; MD-2, myeloid differentiation factor-2; TLR-4, toll-like receptor-4; TNF- $\alpha$ , tumor necrosis factor-alpha

## Discussion

The major findings from this study were: 1) 20 µg/mL LPS, 10 µM MAC28, Biodentine™ extract, and their combinations had no effect on HDPC viability at 24 hours; 2) LPS induced inflammation in HDPCs by upregulating TLR-4, MD-2, TNF- $\alpha$ , and IL-6 mRNAs; and 3) MAC28, Biodentine™, and their combination suppressed inflammation in LPS-treated HDPCs, but no synergistic anti-inflammatory effect was observed between MAC28 and Biodentine™. Therefore, the hypothesis that these materials reduce inflammation in LPS-treated HDPCs were partially accepted; however, their combination did not synergistically inhibit the inflammatory response.

A previous study demonstrated that 0.1 – 100 µg/mL LPS did not alter cell viability at 24 hours and induced cell proliferation in the dental pulp stem cells of young and aged rats.<sup>14</sup> Furthermore, our previous findings showed that 20 µg/mL LPS did not reduce HDPC viability at 24 hours.<sup>8,10,15</sup> In this study, it was confirmed that 24-hour exposure to 20 µg/mL LPS did not significantly affect the viability of HDPCs. In addition, these current results were in accordance with our previous study that 10 µM MAC28 did not compromise HDPC viability.<sup>8</sup> It was also reported that Biodentine™ extract applied in this study did not compromise HDPC viability, which agreed with a previous report that tested Biodentine™ extract at 10-25% dilution for 24-72 hours and discovered no impairment of HDPC viability.<sup>16,17</sup> Combining 20 µg/mL LPS with either 10 µM MAC28, Biodentine™ extract, or both combined did not impair HDPC viability either. These findings suggest that all the treatment conditions did not adversely affect HDPC viability.

LPS derived from *Escherichia coli* is one of the most commonly studied endotoxins and is widely used to model dental pulp cell inflammation due to its ability to induce proinflammatory cytokine production.<sup>18</sup> According to previous studies, LPS activates the TLR-4/myeloid differentiation primary response 88 (MyD88)/nuclear factor- $\kappa$ B (NF- $\kappa$ B) signaling pathway, leading to the secretion of pro-inflammatory cytokines such as TNF- $\alpha$  and IL-6.<sup>4,16-19</sup> TLR-4, which recognizes LPS, requires

MD-2 as a cofactor for effective signal transduction (Fig. 1).<sup>4,22</sup> Results from our previous study and findings from this study confirm that LPS upregulates TNF- $\alpha$  and IL-6 mRNAs with concomitant increases in TLR-4 and MD-2 mRNAs.<sup>8</sup> Therefore, the application of 20 µg/mL LPS for 24 h is suitable for inflammation induction in HDPCs without compromising cell viability.

Following the LPS treatment, our results revealed that MAC28, Biodentine™, and their combination reversed the LPS-induced inflammation in HDPCs as TLR-4, MD-2, and TNF- $\alpha$  mRNAs decreased. However, no synergistic effect was observed between MAC28 and Biodentine™, as the lowered TLR-4, MD-2, and TNF- $\alpha$  mRNA levels were not significantly lower than either MAC28 or Biodentine™ alone in LPS-induced HDPCs. The absence of an additional benefit with co-application can be explained by several biological factors. First, both MAC28 and Biodentine™ likely converge on the same signaling complex (TLR-4/MD-2/NF- $\kappa$ B), therefore, further suppression by combining these materials provides no additional effect. Second, a concentration mismatch is possible, as only one concentration of each material was tested. Third, the two materials may exhibit potential antagonism, which could hinder any additive effect when co-incubated. Finally, some mediators, such as IL-6, can be regulated through TLR-4-independent pathways, which may sustain their expression despite upstream suppression.<sup>23</sup> Further studies are needed to confirm these speculations. In line with this, our previous study reported that a 2-h pretreatment of MAC28 prior to LPS stimulation reduced TNF- $\alpha$  and IL-6 mRNA and protein expression through downregulation of TLR-4/MD-2.<sup>8</sup> The present findings extend this by confirming that MAC28 co-incubated with LPS also suppressed inflammation via the TLR-4/MD-2 signaling pathway. Although none of the treatments tested reduced IL-6 mRNA compared with the LPS group, which is consistent with our earlier observation that, although MAC28 pretreatment inhibited inflammatory cytokines, IL-6 mRNA and protein levels did not return to control levels.<sup>8</sup> Taken together, these findings suggest that persistent IL-6 expression during co-treatment may be maintained



through TLR-4-independent pathways,<sup>23</sup> thereby explaining the lack of additional anti-inflammatory benefit when MAC28 and Biodentine™ were combined.

Biodentine™ has been shown to possess anti-inflammatory and immunomodulatory properties in cells harvested from periapical lesions. It inhibited the production of TNF- $\alpha$  and IL-6, while enhancing the secretion of anti-inflammatory cytokines in granulocytes and other inflammatory cells from periapical lesions. Interestingly, the non-cytotoxic concentration of conditioned Biodentine™ medium that lowered IL-6 lay between 12.5%-25%.<sup>17</sup> In our study, the Biodentine™ extract was diluted at a ratio of 1:16, which corresponds to approximately 6.25% of the original extract. A 1:16 extract was intentionally selected to align with established HDPC protocols and to ensure cytocompatibility as confirmed in previous studies,<sup>10-12</sup> thereby providing a reliable concentration for assessing biological effects without confounding artifacts from higher extract concentrations. However, as discussed earlier, further studies are needed to verify the time course and determine the optimal concentration of Biodentine™ extract in the *in vitro* pulpitis model.

Both MAC28 and Biodentine™ reduced selected LPS-responsive genes (TLR-4, MD-2, TNF- $\alpha$ ) at 24 hours without compromising HDPC viability, supporting the biological plausibility of attenuating early innate immune signals that are relevant to vital pulp therapy (VPT), hemostasis, and postoperative comfort. For regenerative or reparative procedures, early immunomodulation could help establish a more permissive microenvironment; however, these *in vitro* gene-level findings do not yet demonstrate clinical benefit, sealing performance, or effects on osteo/odontogenic differentiation. Co-application was biologically compatible but did not exceed the effects of either material alone at 24 hours. More studies are therefore required before concluding that the combination of MAC28 and Biodentine™ offers no advantage over Biodentine™ alone in clinical practice. Future VPT-related studies should confirm cytokine protein levels, assess the dose-response relationship of MAC28 and Biodentine™, evaluate extended time courses to determine cytokine kinetics, and investigate osteo/odontogenic differentiation and mineralization

in both *in vitro* and *in vivo* models before any clinical inferences can be made.

## Conclusion

Within the limitations of this study, MAC28 and Biodentine™ reduced inflammation without affecting HDPC viability; however, their combination did not demonstrate a synergistic effect. These findings suggest that MAC28 could serve as an alternative to Biodentine™ by targeting the modulation of selected LPS-responsive genes in HDPCs.

## Acknowledgment

MAC28 was kindly provided by Wenzhou Medical University, Zhejiang, China.

## Funding

The research grant for this project was supported by the Faculty of Dentistry Research Funding, Chiang Mai University, Chiang Mai, Thailand.

## Conflicts of interest

The authors declare no conflicts of interest.

## Reference

- Cooper PR, Takahashi Y, Graham LW, Simon S, Imazato S, Smith AJ. Inflammation-regeneration interplay in the dentine-pulp complex. *J Dent* 2010;38(9):687-97.
- Veerayutthwilai O, Byers MR, Pham TT, Darveau RP, Dale BA. Differential regulation of immune responses by odontoblasts. *Oral Microbiol Immunol* 2007;22(1):5-13.
- Raetz CR, Whitfield C. Lipopolysaccharide endotoxins. *Annu Rev Biochem* 2002;71:635-700.
- Nagai Y, Akashi S, Nagafuku M, Ogata M, Iwakura Y, Akira S, *et al.* Essential role of MD-2 in LPS responsiveness and TLR4 distribution. *Nat Immunol* 2002;3(7):667-72.
- Kang JY, Lee JO. Structural biology of the Toll-like receptor family. *Annu Rev Biochem* 2011;80:917-41.
- Park BS, Lee JO. Recognition of lipopolysaccharide pattern by TLR4 complexes. *Exp Mol Med* 2013;45(12):e66.
- Rallabhandi P, Bell J, Boukhvalova MS, Medvedev A, Lorenz E, Arditi M, *et al.* Analysis of TLR4 polymorphic variants: new insights into TLR4/MD-2/CD14 stoichiometry, structure, and signaling. *J Immunol* 2006;177(1):322-32.
- Vaseenon S, Srisuwan T, Liang G, Chattipakorn N, Chattipakorn SC. Myeloid differentiation factor 2 inhibitors exert protective effects on lipopolysaccharides-treated human dental pulp cells via suppression of toll-like receptor 4-mediated signaling. *J Dent Sci* 2024;19(1):220-30.

9. Zhang Y, Liu Z, Wu J, Bai B, Chen H, Xiao Z, *et al.* New MD2 inhibitors derived from curcumin with improved anti-inflammatory activity. *Eur J Med Chem* 2018;148:291-305.
10. Weekate K, Chuenjitkuntaworn B, Chuveera P, Vaseenon S, Chompu-Inwai P, Ittichaicharoen J, *et al.* Alterations of mitochondrial dynamics, inflammation and mineralization potential of lipopolysaccharide-induced human dental pulp cells after exposure to N-acetyl cysteine, Biodentine or ProRoot MTA. *Int Endod J* 2021;54(6):951-65.
11. Saiyasilp S, Vaseenon S, Srisuwan T, Chuveera P. Effects of D-galactose induction on aging characteristics of the human dental pulp cell culture model: An *in vitro* study. *Eur Endod J* 2025;10(2):142-150.
12. Alborzy L, Hashemikamangar SS, Hodjat M, Chiniforush N, Behniafar B. Impact of diode laser irradiation along with Biodentine on dental pulp stem cell proliferation and pluripotent gene expression. *Sci Rep* 2025;15(1):24955.
13. Livak KJ, Schmittgen TD. Analysis of relative gene expression data using real-time quantitative PCR and the 2(-Delta Delta C(T)) Method. *Methods* 2001;25(4):402-8.
14. Ning T, Shao J, Zhang X, Luo X, Huang X, Wu H, *et al.* Ageing affects the proliferation and mineralization of rat dental pulp stem cells under inflammatory conditions. *Int Endod J* 2020;53(1):72-83.
15. Vaseenon S, Srisuwan T, Chattipakorn N, Chattipakorn SC. Lipopolysaccharides and hydrogen peroxide induce contrasting pathological conditions in dental pulpal cells. *Int Endod J* 2023;56(2):179-92.
16. Schuster L, Sielker S, Kleinheinz J, Dammaschke T. Effect of light-cured pulp capping materials on human dental pulp cells *in vitro*. *Int Endod J* 2025;58(7):1060-72.
17. Erakovic M, Duka M, Bekic M, Tomic S, Ismaili B, Vucevic D, *et al.* Anti-inflammatory and immunomodulatory effects of Biodentine on human periapical lesion cells in culture. *Int Endod J* 2020;53(10):1398-412.
18. Meredith TC, Aggarwal P, Mamat U, Lindner B, Woodard RW. Redefining the requisite lipopolysaccharide structure in Escherichia coli. *ACS Chem Biol* 2006;1(1):33-42.
19. Pan S, Peng L, Yi Q, Qi W, Yang H, Wang H, *et al.* Ginsenoside Rh2 alleviates LPS-induced inflammatory responses by binding to TLR4/MD-2 and blocking TLR4 dimerization. *Int J Mol Sci* 2024;25(17):9546.
20. Takeuchi O, Akira S. Pattern recognition receptors and inflammation. *Cell* 2010;140(6):805-20.
21. Zanoni I, Ostuni R, Marek LR, Barresi S, Barbalat R, Barton GM, *et al.* CD14 controls the LPS-induced endocytosis of Toll-like receptor 4. *Cell* 2011;147(4):868-80.
22. Visintin A, Mazzoni A, Spitzer JA, Segal DM. Secreted MD-2 is a large polymeric protein that efficiently confers lipopolysaccharide sensitivity to Toll-like receptor 4. *Proc Natl Acad Sci U S A* 2001;98(21):12156-61.
23. Tanaka T, Narazaki M, Kishimoto T. IL-6 in inflammation, immunity, and disease. *Cold Spring Harb Perspect Biol* 2014;6(10):a016295.

## Original Articles

Effect of Lemongrass Essential Oil on *Candida albicans*-infected Raw 264.7 Macrophages: An *In Vitro* StudyMyat Thiri<sup>1</sup>, Matsayapan Pudla<sup>2</sup>, Suwan Choonharuangdej<sup>2</sup><sup>1</sup>Oral biology and integrative biomedical science program, Faculty of Dentistry, Mahidol University, Bangkok, Thailand<sup>2</sup>Department of Oral Microbiology, Faculty of Dentistry, Mahidol University, Bangkok, Thailand

## Abstract

Macrophages are key components of the innate immune system by eliminating pathogens through phagocytosis. Their activity can be influenced by various agents including plant-derived essential oil. Lemongrass essential oil (LG-EO) exhibits potent antifungal properties, however, its immunomodulatory effects on macrophage function remain unclear. This study aimed to evaluate the effect of LG-EO on the phagocytic activity of RAW 264.7 macrophages infected with *C. albicans*. The cytotoxicity of LG-EO was assessed using the MTT reduction method. Three concentrations--0.003% (1/20 MIC), 0.006% (1/10 MIC), and 0.03% (1/2 MIC) (v/v)--were selected to evaluate their effects on the phagocytosis of *C. albicans*-infected RAW 264.7 cells. Infected macrophages were treated with various concentrations of LG-EO for four, six, and eight hours, after which surviving fungal cells were quantified using a cultivation method. LG-EO exhibited dose-dependent cytotoxicity, with fewer than 5% of RAW 264.7 cells surviving at concentrations  $\geq$  0.03% (v/v). In the untreated control, fungal recovery (log<sub>10</sub> CFU/mL) was 2.08 (1.84-2.08), 2.48 (2.42-2.52), and 2.56 (1.93-2.66) after four, six, and eight hours of incubation, respectively. Treatment with 0.003% and 0.006% LG-EO showed no significant enhancement in phagocytosis, with fungal counts comparable or slightly higher than controls. In contrast, 0.03% LG-EO reduced fungal recovery to 1.48 (1.39-1.54), 1.7 (1.59-1.85), and 1.7 (1.5-1.83) at the respective time points, likely due to its cytotoxicity rather than enhanced phagocytic activity. At sub-cytotoxic concentrations, LG-EO did not significantly modulate the phagocytic activity of *C. albicans*-infected RAW 264.7 macrophages. These findings imply that LG-EO has limited immunomodulatory effects on macrophage mediated fungal clearance.

**Keywords:** *Candida albicans*, Cytotoxicity, Lemongrass essential oil (LG-EO), RAW 264.7 macrophages**Received date:** Jul 15, 2025**Revised date:** Sep 23, 2025**Accepted date:** Sep 24, 2025**Doi:** 10.14456/jdat.2025.28**Correspondence to:**

Suwan Choonharuangdej, Department of Oral Microbiology, Faculty of Dentistry, Mahidol University, 6 Yothi Road, Ratchatawi, Bangkok 10400 Thailand. Phone: 02-200-7805 Fax: 02-200-7804 E-mail: suwan.cho@mahidol.ac.th

## Introduction

Lemongrass essential oil (LG-EO), a natural extract from *Cymbopogon citratus*, has been investigated for various medicinal properties, particularly its antimicrobial activity. LG-EO has demonstrated potent antifungal effects, especially against *Candida albicans*, an opportunistic

pathogen that primarily causes superficial or invasive candidiasis in immunocompromised individuals.<sup>1-4</sup> Citral, a key active compound in LG-EO, plays a crucial role in inhibiting the growth of planktonic yeast cells and their biofilm counterparts by targeting the fungal cell wall,

inhibiting enzymes essential for fungal growth, and suppressing hyphal formation.<sup>5-7</sup> Consequently, LG-EO has been incorporated or applied as a coating on the surfaces of dental materials, including tissue conditioners, denture acrylic resin, and silicone elastomers, to reduce the risk of fungal infections.<sup>8-11</sup> However, other medicinal properties of LG-EO—particularly its effects on immune responses—have not yet been extensively investigated.

The innate immune response is the first line of defense in the immune system, activated upon exposure to microorganisms, particularly pathogens. Phagocytes such as macrophages, neutrophils, and dendritic cells play a major role in pathogen clearance and immune signaling. The clearance of *C. albicans* involves phagocytosis by macrophages, infiltrating monocytes, and neutrophils.<sup>12</sup> However, the hyphal form of the fungus produces candidalysin, a hypha-associated cytolytic peptide toxin that damage the membrane of immune cells and enables the fungus to escape from host defense mechanism.<sup>13</sup> Consequently, this study aimed to investigate the effect of LG-EO on macrophage phagocytosis of *C. albicans*. The findings may contribute valuable data for further studies on the role of LG-EO in modulating immune responses.

## Materials and methods

### Chemical reagents

LG-EO was purchased from Thai-China Flavours and Fragrances Industry Co., Ltd. (TCFF), Thailand. Dulbecco's Modified Eagle Medium (DMEM) and Triton X-100 were purchased from Sigma-Aldrich, USA, whereas L-glutamine, and fetal bovine serum (FBS) were purchased from Gibco labs, USA, and Cytiva, USA, respectively. Sabouraud dextrose agar and broth were purchased from Becton, Dickinson and company, NJ, USA.

### LG-EO cytotoxicity assessment

RAW 264.7, a murine macrophage cell line, (Department of Oral Microbiology, Faculty of Dentistry, Mahidol University) was cultured in DMEM supplemented with 10% FBS and 1% L-glutamine (complete DMEM, CDMEM). Cells were maintained at 37°C in a humidified incubator (NuAire, Air-jacketed automatic CO<sub>2</sub> incubator,

Model NU-5810E) with 5% CO<sub>2</sub> and subcultured every two days. RAW 264.7 cells (1.75×10<sup>5</sup> cells) were seeded into each well of a 96-well plate and incubated for 24 hours under the conditions described above. The cells were then treated with various concentrations of LG-EO—2%, 1%, 0.5%, 0.25%, 0.125%, 0.06%, 0.03%, 0.015%, 0.007%, and 0.003% (v/v) in CDMEM. After 18 hours of LG-EO exposure, cell viability was assessed using the MTT assay. Briefly, MTT solution [3-(4,5-dimethylthiazol-2-yl)-2,5-Diphenyltetrazolium Bromide] was added to each well and incubated for two hours before the enzymatic reaction product was measured at 590 nm using microplate reader (BioTek ELx800, BioTek Instruments. Inc., USA). RAW 264.7 cells cultured in CDMEM without treatment and those treated with 1.0% Triton X-100 were used as negative and positive controls, respectively. Macrophage viability was calculated as follows.

$$\% \text{ Cell viability} = \frac{(\text{Mean OD of treated cells})}{(\text{Mean OD of control})} \times 100$$

### Effect of LG-EO on *Candida albicans*-infected macrophages

*C. albicans* ATCC 10231 (Department of Oral Microbiology, Faculty of Dentistry, Mahidol University) was cultured in Sabouraud dextrose broth and incubated overnight at 37°C. The yeast suspension was confirmed by Gram staining (Figure 1) and adjusted to an optical density (OD) of 1.0 at 600 nm using a cell density meter (WPA CO 8000, Biochrom Ltd., UK). Subsequently, RAW 264.7 cells (5×10<sup>5</sup> cells) were seeded into 6-well plates and incubated overnight under the conditions described above. The cells were then infected with *C. albicans* at a multiplicity of infection (MOI) of 2. After an hour of fungal exposure, various concentrations of LG-EO—0.003%, 0.006%, and 0.03% (v/v)—were added to the cells, followed by incubation under the previously described conditions for four, six, and eight hours. After LG-EO treatment, the cells were harvested, washed three times with phosphate-buffered saline (PBS), and lysed using 0.1% Triton X-100 for 5 min. A 100 µL aliquot of the lysate was then plated onto Sabouraud dextrose agar and incubated at 37°C for 48 hours. Fungal survival was quantified and expressed as Log<sub>10</sub> colony-forming units per millimeter (CFU/mL). RAW 264.7 cells cultured in CDMEM

were used as the negative control, while *C. albicans*-infected macrophages without treatment served as baseline for the phagocytic process.

All experiments were performed in triplicate for three different time periods.

### Statistical analysis

Statistical analysis was performed using descriptive statistics, the Shapiro-Wilk test to assess data normality, and the Kruskal-Wallis test to evaluate differences between groups. A *P* value of <0.05 was considered statistically significant.

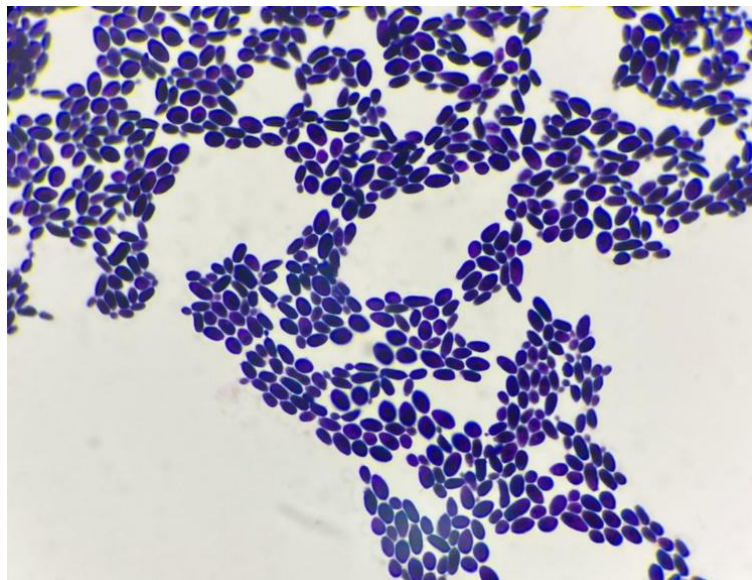


**Figure 1** Gram staining of *Candida albicans* suspension prepared for evaluating phagocytosis by RAW 264.7 cells (1000x)

## Results

### LG-EO cytotoxicity assessment

The viability of RAW 264.7 cells treated with various concentrations of LG-EO—2%, 1%, 0.5%, 0.125%, 0.06%, 0.03%, and 0.015% (v/v)—was significantly reduced, ranging from 15.5%±8.5% to 4.65%±0.7%, compared to untreated

cells (control), which exhibited 100% viability. In contrast, cell viability was 81%±10.5% and 51%±5% when the cells were treated with 0.003% and 0.007% (v/v) LG-EO, respectively, as shown in Figure 2.

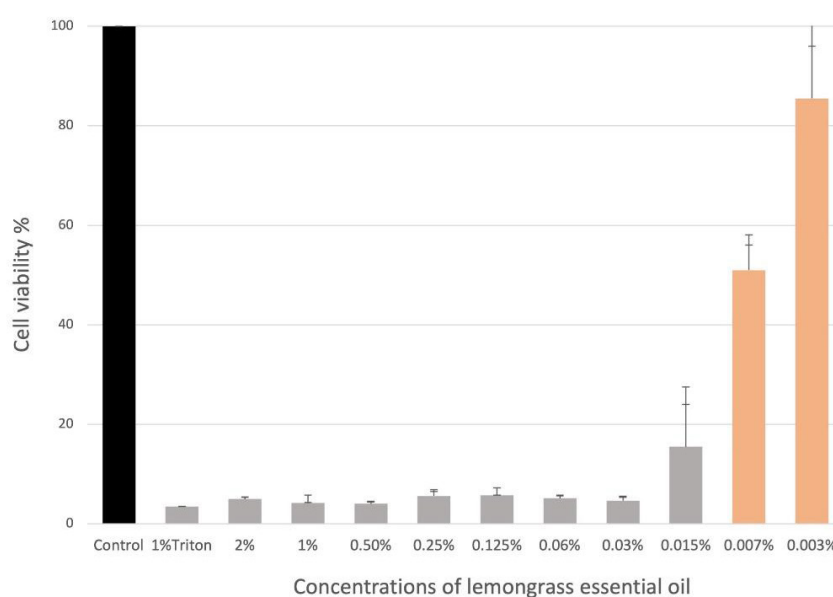


**Figure 2** Cytotoxic effect of lemongrass essential oil (LG-EO) on RAW 264.7 cells. Data are expressed as the percentage of viable cells (mean ± SEM) (n = 9 per group)



### Effect of LG-EO on *Candida albicans*-infected macrophages

Three concentrations of LG-EO—0.003%, 0.006%, and 0.03% (v/v)—were tested to evaluate their effects on the phagocytosis of *C. albicans*-infected RAW 264.7 cells. In the untreated control group, the number of *C. albicans* recovered from macrophages was expressed as the median of log<sub>10</sub> CFU/mL with interquartile range and measured at 2.08 (1.84-2.08), 2.48 (2.42-2.52), and 2.56 (1.93-2.66) after four, six, and eight hours of incubation, respectively. Following treatment with 0.003% LG-EO, fungal recovery was 2.18 (2.02-2.21), 2.28 (2.28-2.33), and 3.1 (2.81-3.16) at

the same time points, while treatment with 0.006% LG-EO resulted in values of 2.26 (2.25-2.48), 2.87 (2.87-2.97), 2.82 (2.59-2.96), respectively. In contrast, treatment with 0.03% LG-EO led to a reduction in fungal recovery, with values of 1.48 (1.39-1.54), 1.7 (1.59-1.85), and 1.7 (1.5-1.83) at four, six, and eight hours, respectively. However, none of the differences observed between LG-EO-treated and untreated groups were statistically significant. The effects of LG-EO on phagocytosis of *C. albicans*-infected RAW 264.7 cells are summarized in Figure 3.

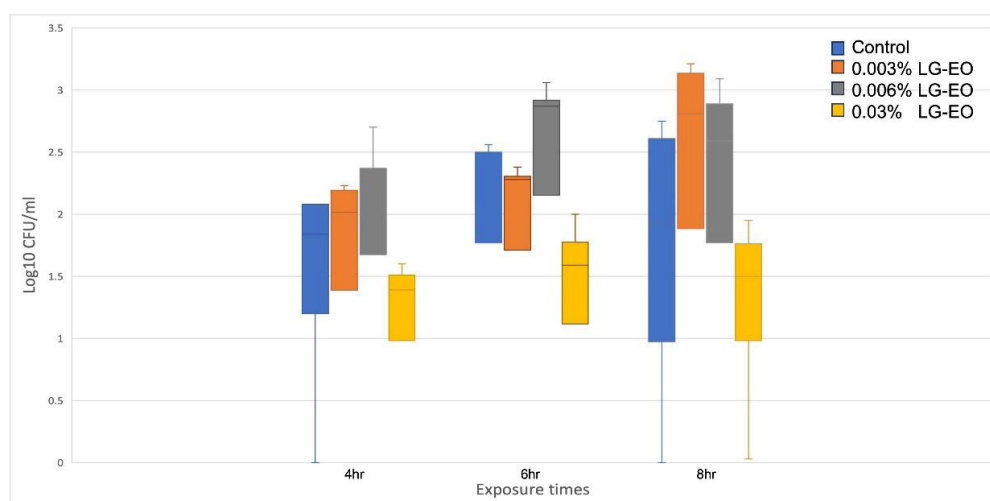


**Figure 3** Effect of lemongrass essential oil (LG-EO) on the phagocytosis of *Candida albicans* by RAW 264.7 macrophages. Data are expressed as the median (log<sub>10</sub> CFU/mL) and interquartile range (n = 9 per group)

## Discussion

LG-EO, which contains citral as its major active component (>70%), has demonstrated potent antifungal activity, with a MIC ranging from 0.04% to 0.06% (v/v)<sup>8,10</sup> It is of interest to evaluate whether LG-EO, at MIC and sub-MIC concentrations, affects the phagocytic activity of RAW 264.7 cells infected with *C. albicans*. Determining the cytotoxicity effect of LG-EO on RAW 264.7 cells is essential, as macrophage viability directly influences their phagocytic function. This study found that RAW 264.7 cells were highly sensitive to LG-EO, with fewer than 5% of the cell surviving after exposure to concentrations  $\geq$  0.03% (v/v). In contrast, approximately 80% of RAW 264.7 cells remained viable when exposed to 0.003% (v/v) LG-EO, which corresponds to a 20-fold dilution of its minimum inhibitory concentration (MIC) against *C. albicans*.<sup>8</sup> These findings differ markedly

from those of a previous study, which reported that RAW 264.7 cells remained viable after exposure to 2.5% (w/v) LG-EO.<sup>14</sup> The discrepancy may be attributed to differences in testing procedures, the batch of LG-EO used, or the cell viability assay employed.<sup>15</sup> Cytotoxicity of LG-EO on RAW 264.7 cells was dose-dependent. Consequently, three concentrations of LG-EO—0.003% (1/20 MIC), 0.006% (1/10 MIC), 0.03% (v/v) (1/2 MIC)—were selected for subsequent evaluation of their effects on phagocytosis of *C. albicans*-infected RAW 264.7 cells.

Macrophages are key components of the innate immune system, serving as a first line defense by rapidly eliminating pathogens through phagocytosis—the process by which macrophages engulf and kill microbes. This study demonstrated that LG-EO at concentrations of 0.003% and

0.006% (v/v) has no significant effect on the killing activity of RAW 246.7 cells against *C. albicans*. These findings are consistent with a previous study, which reported that LG-EO did not directly enhance the killing activity of RAW 246.7 cells against *C. albicans*, likely due to its inhibitory effect on nitric oxide (NO) production.<sup>14</sup> To further clarify the impact of LG-EO on the killing activity of *C. albicans*-infected RAW 264.7 cells, extended incubation times such as 12, 24 and 48 hours should be considered, as the yeast cells are typically destroyed after at least 6 hours of phagocytosis.<sup>16</sup> Moreover, under culture conditions using CDMEM supplemented with FBS, *C. albicans* may transition to its hyphal form, make it more resistant to phagocytic clearance.<sup>17</sup> Since the number of viable and functional macrophages plays a crucial role in phagocytosis against microorganisms, it is important to assess the viability of RAW 264.7 cells after exposure to LG-EO for varying durations (four, six, and eight hours).

Phagocytic endocytosis, or engulfment—the process by which macrophages internalize pathogens—is a critical initial step in their clearance. Therefore, a higher rate of endocytosis generally correlates with more effective pathogen elimination. In this study, treatment with 0.003% and 0.006% (v/v) LG-EO did not significantly affect the endocytosis rate of RAW 264.7 cells infected with *C. albicans*, compared to untreated *C. albicans*-infected cells. This may be due to limitations of the cultivation method used to assess surviving fungi, which does not directly reflect the endocytosis process. Interestingly, the fungus-infected RAW 264.7 cells treated with these LG-EO concentrations appeared to exhibit increased endocytosis, as suggested by the higher numbers of surviving fungi in the raw CFU/mL data. To verify this observation, further experiment should be conducted using LG-EO treatment durations of 0.5, one, two, and three hours, followed by the quantification of internalized fungi using fluorescent-labeled or stained *Candida* cells, rather than relying solely on cultivation assay. Consequently, further studies using shorter exposure times and alternative methods for assessing phagocytosis—such as fluorescent labeling—are warranted to clarify the impact of LG-EO on the early stages of fungal uptake and clearance.

## Conclusion

This study demonstrated that RAW 264.7 macrophages were highly sensitive to LG-EO, with significant cytotoxicity observed at concentrations above 0.03% (v/v). At sub-cytotoxic concentrations [0.003% and 0.006% (v/v)], LG-EO did not significantly enhance the phagocytic or killing activity of macrophages against *C. albicans*. These findings suggest that, despite its strong direct antifungal effects, LG-EO does not promote macrophage-mediated antifungal immunity at concentrations that are non-toxic to innate immune cells.

## Acknowledgements

The authors express their sincere gratitude to the Faculty of Dentistry, Mahidol University, particularly the Departments of Oral Microbiology and Oral biology and integrative biomedical science program (International program), Faculty of Dentistry, Mahidol University, for their generous support in providing materials, reagents, and instruments essential to this study.

## Funding

Neither governmental nor non-governmental organizations provided funding to this project.

## References

1. Baumgardner DJ. Oral fungal microbiota: To thrush and beyond. *J Patient Cent Res Rev* 2019;28;6(4):252–61.
2. Sahu SR, Bose S, Singh M, Kumari P, Dutta A, Utkalaja BG, *et al*. Vaccines against candidiasis: Status, challenges and emerging opportunity. *Front Cell Infect Microbiol* 2022;18:12:1002406.
3. Talapko J, Juzbasic M, Matijevic T, Pustijanac E, Bakic S, Kotris I, *et al*. *Candida albicans*- The Virulence Factors and Clinical Manifestations of Infection. *J Fungi (Basel)* 2021;22;7(2):79.
4. Chen CY, Cheng A, Tien FM, Lee PC, Tien HF, Sheng WH, *et al*. Chronic disseminated candidiasis manifesting as hepatosplenic abscesses among patients with hematological malignancies. *BMC Infect Dis* 2019;19:635.
5. Mukarram M, Choudhary S, Khan MA, Poltronier P, Khan MMA, Ali J, *et al*. Lemongrass essential oil components with antimicrobial and anticancer activities. *Antioxidants (Basel)* 2021;22:11(1):20.
6. Paiva LFDE, Teixeira-Loyola ABA, Schnaider TB, Souza ACDE, Lima LMZ, Dias DR. Association of the essential oil of *Cymbopogon citratus* (DC) Stapf with nystatin against oral cavity yeasts. *An Acad Bras Cienc* 2022;94(1):e20200681.

7. Miranda-Cadena K, Marcos-Arias C, Perez-Rodriguez A, Cabello-Beitia I, Mateo E, Sevilano E, *et al.* *In vitro* and *in vivo* anti-*Candida* activity of citral in combination with fluconazole. *J Oral Microbiol* 2022;14(1):2045813.
8. Amornvit P, Choonharuangdej S, Srithavaj T. Lemongrass-incorporated tissue conditioner against *Candida albicans* culture. *J Clin Diagn Res* 2014;8(7):ZC50-2.
9. Choonharuangdej S, Srithavaj T, Chantanawilas P. Lemongrass-incorporated tissue conditioner with adjustable inhibitory effect against *Candida albicans*: An *in vitro* study. *Int J Prosthodont* 2022;35(3):338–42.
10. Choonharuangdej S, Srithavaj T, Thummawanit S. Fungicidal and inhibitory efficacy of cinnamon and lemongrass essential oils on *Candida albicans* biofilm established on acrylic resin: An *in vitro* study. *J Prosthet Dent* 2021;125(4):707.e1-707.e6.
11. Mat-Rani S, Chotprasert N, Srimaneekarn N, Choonharuangdej S. Fungicidal effect of lemongrass essential oil on *Candida albicans* biofilm pre-established on maxillofacial silicone specimens. *J Int Soc Prev Community Dent* 2021;11(5):525–30.
12. Rudkin FM, Bain JM, Walls C, Lewis LE, Gow NAR, Erwig LP. Altered dynamics of *Candida albicans* phagocytosis by macrophages and PMNs when both phagocyte subsets are present. *mBio* 2013; 4(6):e00810-13.
13. Konig A, Hube B, Kasper L. The dual function of the fungal toxin candidalysin during *Candida albicans*-macrophage interaction and virulence. *Toxins (Basel)* 2020;12(8):469.
14. Wisidsri N, Thungmungmee S, Khobjai W. Nitric oxide inhibitory and cytotoxic activities of spice essential oils. *CMU J Nat Sci* 2019; 18(3):373-92.
15. Madorran E, Ambroz M, Knez J, Sobocan M. An overview of the current state of cell viability assessment methods using OECD classification. *Int J Mol Sci* 2025;26(1):220.
16. Zhang Y, Tang C, Zhang Z, Li S, Zhao Y, Weng L, *et al.* Deletion of the ATP2 gene in *Candida albicans* blocks its escape from macrophage clearance. *Front Cell Infect Microbiol* 2021; 16:11:643121.
17. Chen H, Zhou X, Ren B, Cheng L. The regulation of hyphae growth in *Candida albicans*. *Virulence* 2020; 11(1):337–348.

ชื่อผู้แต่ง	เล่ม/หน้า	ชื่อผู้แต่ง	เล่ม/หน้า
<b>ก</b>		<b>ม</b>	
กฤษณ์ ขวัญเงิน	2/62	แมนสรวง วงศ์อภัย	2/99
กันยา บุญธรรม	3/175	<b>ร</b>	
เกศกัญญา สัพพะเลข	3/175	รตนอร จูห้อง	2/99
<b>จ</b>		รติชนก นันทนีย์	3/185
จินตนาภรณ์ สิริพิพัฒน์	2/107	รัชชา รักศักดิ์มนุษย์	2/107
<b>ช</b>		รินรดา ภิรมย์ภักดี	3/185
ชุตินา ไตรรัตน์วรกุล	3/185	<b>ล</b>	
<b>ญ</b>		लगน มุททาพงศ์	2/62
ญาดา อนันต์วัฒน์	2/107	ลิลินดา ศรีสุนทรไท	2/107
<b>ด</b>		<b>ว</b>	
เดชา ทำดี	2/99	วรรณพงษ์ ชลนภาสถิตย์	1/40
<b>ท</b>		<b>ศ</b>	
ทรงชัย ฐิตโสเมกุล	1/40	ศศิพิมล จันทร์รัตน์	2/107
ทัศนยา ฤทธิกุล	2/99	<b>ส</b>	
ทิพวรรณ ธราวิพัฒนานนท์	3/185	สัญญา เรื่องสิทธิ์	2/54
<b>ธ</b>		สุกรีข พูลสุข	2/107
ธนะภูมิ รัตนานุพงศ์	2/84	สุกัญญา เขียววิวัฒน์	1/40
ธนาภรณ์ มหาสุชัยกุล	1/30	สุชยา ดำรงค์ศรี	3/185
<b>ผ</b>		สุพาณี บุรณธรรม	1/30
ผกาภรณ์ พันธุ์ดี พิศาลธุรกิจ	3/175	สุภัทสร ฉันทภากร	3/175
<b>พ</b>		<b>อ</b>	
พนรัตน์ ขอดแก้ว	2/62	อรรถพล ยงวิกุล	2/54
พรกวี เจริญลาภ	3/185	อังสุมา สุขเมธโชติเมธา	2/107
พลินี เดชสมบูรณ์รัตน์	3/175	อัมพาภรณ์ นิธิประทีป	2/107
พิมพ์ไฉ่ ลิ้มสมวงศ์	2/99	อานนท์ วรยิ่งยง	2/84
พิรัตน์ การเที่ยง	2/107	อุษา จึงพัฒนาวดี	2/99
<b>ภ</b>			
ภทิตา ภูริเดช	3/175		
ภวิกา เสริมศักดิ์	2/84		
ภัทราภรณ์ หัสติเสวี	3/175		

NAME	ISSUE/PAGE	NAME	ISSUE/PAGE
<b>A</b>		<b>M</b>	
Akkapol Banlue	3/119	Mansuang Wongsapai	2/99
Ampaporn Nithipratheep	2/107	Matsayapan Pudla	4/274
Angsuma Sumethchotimetha	2/107	Myat Thiri	4/274
Arnond Vorayingyong	2/84	Myo Thiri Win	4/249
Atapol Yongvikul	2/54	<b>N</b>	
Atiphan Pimkhaokham	4/249	Natnisha Arkarapattarawong	4/207
<b>B</b>		Nattapon Rotpenpian	3/141, 3/164
Boosana Kaboosaya	4/249	Nattawit Promma	2/92
<b>C</b>		Nuttapol Limjeerajarus	4/257
Chaiwat Maneenut	4/224	<b>O</b>	
Chalida Nakalekha Limjeerajarus	4/257	Orakarn Kanwiwatthanakun	4/238
Chookiat Wachiralarpphaithoon	4/194	<b>P</b>	
Chutima Trairatvorakul	3/185	Pagaporn Pantuwadee Pisarnaturakit	3/175
<b>D</b>		Palinee Detsomboonrat	3/175
Decha Tamdee	2/99	Panarat Kodkeaw	2/62
<b>G</b>		Panicha Sroithong	4/216
Guang Liang	4/266	Parintorn Sutthiprapa	4/207
<b>I</b>		Pasika Meenamphant	3/153
Issara Wongpraparatanana	3/153	Pasutha Thunyakitoisal	4/238
<b>J</b>		Patcharapit Promoppatum	4/257
Jintanaporn Siripipat	2/107	Patita Bhuridej	3/175
<b>K</b>		Patraporn Hasadisevee	3/175
Kanokporn Teerakiatkamjorn	3/141, 3/164	Pavika Searmsak	2/84
Kanya Boontham	3/175	Phetcharat Dhammayannarangi	4/257
Keskanya Subbalekha	3/175, 4/207	Pimpilai Limsomwong	2/99
Kopkrit Hataiareerug	3/153	Pirat Karntiang	2/107
Krit Khwanngern	2/62	Pongthep Somsriphang	4/194
Kunlarut Kongwanich	1/12	Pornkawe Charoenlarp	3/185
<b>L</b>		Puthita Leewisutthikul	4/207
Lapon Mutthapong	2/62		
Lilinda Srisoontornthai	2/107		



NAME	ISSUE/PAGE	NAME	ISSUE/PAGE
<b>R</b>		<b>T</b>	
Rangsima Sakoolnamarka	3/153	Tanaporn Mahasurachaikul	1/30
Ratanaon Juhong	2/99	Tanyaporn Treyasorasai	1/1
Ratcha Rakskmanut	2/107	Thanaphum Osathanon	4/216
Ratichanok Nantanee	3/185	Thanapoom Rattananupong	2/84
Ratsa Sripirom	4/238	Thatsana Ritthikul	2/99
Rinrada Pirompak	3/185	Thipawan Tharapiwattananon	3/185
<b>S</b>		Thitirat Tungtorsakul	4/207
Sappasith Panya	4/207	Tuan Hoang Nguyen	4/257
Sasipimon Chanrat	2/107	<b>U</b>	
Savitri Vaseenon	4/266	Usa Chuengpattanawadee	2/99
Sirida Arunjarosuk	4/249	Utaisar Chunmanus	4/238
Sirima Petdachai	1/20	Uthai Uma	2/75, 3/132
Siripim Prukpaiboon	2/92	<b>V</b>	
Siriporn C. Chattipakorn	4/266	Vannaporn Chuenchompoonut	1/20
Sirivimol Srisawasdi	1/1	Viritpon Srimaneepong	4/257
Sitthikorn Kunawarote	4/266	<b>W</b>	
Songchai Thitasomakul	1/40	Waleerat Sukarawan	4/216
Sookwasa Hirunmekavanich	4/224	Wannapong Chonnapasatid	1/40
Suchaya Pornprasertsuk-Damrongsri	3/185	Wanthip Plooksawasdi	3/164
Sukanya Tianviwat	1/40	Wikanda Khemaleelakul	2/92
Sukrit Jaiklaew	3/119	Witsuta Pongphaladisai	4/266
Sukrit Poonsuk	2/107	<b>Y</b>	
Sunya Ruangsitt	2/54	Yada Anantawat	2/107
Supanee Buranadham	1/30	Yosaphon Songphum	1/20
Supassara Chanpakorn	3/175		
Suwan Choonharuangdej	4/274		
Suwit Wimonchit	1/12		